Cite this article
Dean ETR (2023)
Point loads on the surface of a transversely isotropic linear elastic half-space.
Geotechnical Research **10(2)**: 78–99,
https://doi.org/10.1680/jgere.22.00063

Research Article
Paper 2200063
Received 01/12/2022; Accepted 21/03/2023
First published online 27/03/2023

Geotechnical Research

ice Publishing

Point loads on the surface of a transversely isotropic linear elastic half-space

Edward Timothy Richard Dean PhD, MBA
Geotechnical Consultant, Caribbean Geotechnical Design SLU, L'Escala, Spain (Orcid:0000-0002-0234-2261) (richard.dean@caribgeo.com)

General solutions for the displacements, strains and changes in stress in a transversely isotropic linear elastic (TILE) half-space subject to a point load were published in 1998. They represent a massive advance on the nineteenth-century solutions by Boussinesq, Cerruti and others, which were for fully isotropic linear elastic half-spaces. The 1998 solutions were for loads at a general depth below the surface and were criticised for being difficult. The present paper deduces more accessible expressions for the special case of loads that are on the surface. This allows one clarification and one potential error in the original equations to be identified and avoided. With support from existing data of geological materials, agreement is found with a previous claim that a limit proposed in 1970 on one of the shear moduli for a TILE material is invalid. Corrected equations derived herein can be the basis of calculating ground stresses and movements due to linear responses to distributed surface loads, behaviours of flexible foundations and stiffnesses for rigid surface footings.

Keywords: cross-anisotropy/ground movements/linear elasticity/point load/settlement/stress/transverse isotropy/UN SDG 9: Industry, innovation and infrastructure/UN SDG 11: Sustainable cities and communities

Notation

Principal stress and principal strain are taken positive in compression. 'Vertical' means parallel to the axis of material symmetry (the z-direction), and horizontal means at 90° to the axis. Displacements are assumed to be small enough that second-order effects due to the associated small changes of geometry can be neglected. Symbols for stress refer to changes of effective stress but do not carry the traditional prime marker. Total stresses and constant-volume parameters are identified by superscript u. The ± and ∓ signs are such that the upper sign is for subscript $i = 1$ and the lower is for $i = 2$.

A_{ij}	constrained modulus, Liao and Wang (1998) notation
a, b	miscellaneous parameters defined where used
C_{ab}	(with letter subscripts) dimensionless compliance factor characterising the surface displacement in direction a due to a point load in direction b
C_{ij}	(with integer subscripts) constrained modulus, some sources in the literature
d	Infinitesimal
E_h, E_v	Young's moduli in the horizontal and vertical directions, respectively
G	shear modulus (un-subscripted for a fully isotropic linear elastic (FILE) material, subscripted for a transversely isotropic linear elastic (TILE) material)
k	Liao and Wang (1998) factor with dimensions of inverse modulus
K'	dimensionless factor
m_i	two ($i = 1, 2$) of Liao and Wang (1998) dimensionless factors
P	point load
q	dimensionless ratio A_{11}/A_{33}
R	actual distance from the origin to a point
R_i, R_i^*	modified distances
r, θ, z	cylindrical coordinates
S	dimensionless parameter involved in solving the characteristic equation
T	one of Liao and Wang (1998) factors with dimensions of inverse modulus
U	displacement at a general point in the half-space
u	change in pore pressure
u_a	(with letter subscript) surface displacement in direction a
u_i	($i = 1, 2, 3$) three of Liao and Wang (1998) dimensionless factors that multiply the z-coordinate
W	strain energy, computed as work done starting from an initial stress of zero
x, y, z	Cartesian coordinates, z in the direction of the axis of material symmetry
γ_{ij}	small engineering shear strain in a plane containing the directions of the i and j axes
Δ, Δ_1, Δ_2	determinant and two of the factors in the determinant of the TILE compliance matrix

ε	dimensionless infinitesimal
ε_r, ε_θ, ε_z	small radial, circumferential and vertical normal strains, respectively
λ_i	dimensionless factor
μ	Poisson's ratio (un-subscripted for an FILE material, subscripted for a TILE material)
σ	change in normal stress
τ	change in shear stress

Subscripts

ax	axial
h	relating to a lateral direction
hh	for shearing in a horizontal (z = constant) plane
i	integer index
ij	integer indices indicating directions; (123) = ($r\theta z$) for a cylindrical coordinate system, (123) = (xyz) for a Cartesian coordinate system
q	deviatoric
r, θ, z	associated with radial, circumferential and vertical directions, respectively
rad	radial in the triaxial cell
v	relating to the direction of material symmetry (taken to be vertical)
vh	for shearing in a vertical plane (one containing a line parallel to the z-axis)
vol	volumetric
x, y, z	associated with Cartesian directions x, y and z

Superscripts

u	total stress, for undrained (constant-volume) condition
u2	the parameter with superscript u is squared

Introduction

Geomaterials, including soils and rocks, are known to be anisotropic in their small-strain elastic responses. Casagrande and Carillo (1944) made the distinction between induced anisotropy, which is generated by strain history and so is a feature of plasticity, and inherent anisotropy, associated with soil formation processes. Transverse isotropy, also called cross-anisotropy, is when there is an axis of rotational material symmetry in the material behaviour (e.g. Atkinson, 1975; Barden, 1963; Gibson, 1974; Graham and Houlsby, 1983; Simpson, 2017). Gazetas (1981) argued that transverse isotropy can be important in calculating the elastic settlements of footings.

Anisotropy can affect all aspects of soil behaviour (Carter, 2023), but the present paper focuses solely on small-strain responses that are conventionally termed 'elastic', for serviceability states at loads much lower than those expected to induce ultimate limits such as bearing capacity failure (e.g. Das, 2009).

Calculations for a transversely isotropic linear elastic (TILE) material are significantly more complicated than those for a fully isotropic linear elastic (FILE) half-space. Liao and Wang (1998) appear to have been the first to propose a general solution for stresses and displacements in a TILE half-space subject to three orthogonal point loads. Their solution method used a Hankel transform. They identified previous solutions for vertical loading, noting that some previous solutions were either partial or contained errors. They used notation that is easy to relate to subsequent work in geotechnical engineering by Lings *et al*. (2000) and others.

The solutions by Liao and Wang (1998) for three orthogonal loads, together with advances in soil testing for TILE properties, have the potential to improve significantly the accuracy of geotechnical calculations for settlements and more general ground motions. They may be integrated, analytically or numerically, to find displacements and stresses due to distributed loads or to loads on rigid footings, just as solutions by Boussinesq (1878), Cerruti (1884–1885) and others are used in this way for FILE materials (Davis and Selvadurai, 1996; Holl, 1941; Newmark, 1935). The methodology by Liao and Wang (1998) has also been applied to buried loads (Wang and Liao, 2002), piles (Wang, 2003; Wang and Pan, 2004; Wang *et al*., 2008) and strip loads (Wang, 2005).

Anyaegbunam (2014) reviewed previous work including solutions for vertical loading by Gerrard and Wardle (1973) and Liao and Wang (1998), but used similar notation to Mitchell (1900), which seems less easy to relate to modern work. An upper limit on shear modulus was proposed by Raymond (1970) on the basis of the use by Barden (1963) of the solution by Mitchell (1900) for point vertical loading. Anyaegbunam (2014) argued that this limit is theoretically invalid. This finding is supported by data examined in the present paper.

Marmo *et al*. (2020) presented an updated review, including Liao and Wang (1998), and proposed a completely different analysis based on a theorem by Almansi (1899). Their results were presented in terms of a differential operator weighted by a quasi-potentials or their derivatives. They require further processing to obtain relationships to notation in geomechanics. They presented fascinating graphics of the stresses due to lateral load on the surface of an E-glass/epoxy TILE half-space.

Dean (2019) explored some of published data on the transverse isotropy of soils. Measurement procedures and data for geomaterials tested in modified triaxial, hollow cylinder and other devices were described by Kuwano (1999), Sadek *et al*. (2007), Fioravante *et al*. (2013), Ratananikom *et al*. (2013), Wang *et al*. (2019), Liu *et al*. (2020), Shi *et al*. (2021), Gu *et al*. (2022), Zuo *et al*. (2022) and others. The present paper is illustrated using data by Wang (2002a, 2002b) for geological materials found at depths of up to several kilometres. These depths can be relevant to geophysical interpretation (e.g. Kearey *et al*., 2002, 2009), deep mining and deep waste and other facilities. Tectonic processes may move materials to or from the surface over geological timescales.

Constitutive properties: a brief review

Notation

Figure 1 shows Cartesian (x, y, z) and cylindrical coordinates (r, θ, z) and the sign conventions for directions of changes in stress that are positive in this paper. The origin is on the surface of the half-space, at the point at which loads are applied. The z-axis points downwards into the half-space. The surface is at $z = 0$. The z-axis is also the axis of material symmetry. $R = (r^2 + z^2)^{1/2}$ is the shortest distance from the origin to a point at (r, θ, z).

Strain is assumed to be sufficiently small that second-order effects can be neglected. Except in the discussion of strain energy, stress symbols such as σ_{zz} refer to changes in stress from an initial state at which strain is taken to be zero. Principal stresses and principal strains are taken positive in compression. Following Lings (2001), symbols superscripted 'u' (such as σ_{zz}^{u}) are used only for total stress and for constant-volume, undrained conditions. Symbols without such a superscript are for effective, drained conditions but can be regarded as general where convenient.

Constitutive equations for TILE materials

The present paper uses the notation by Lings *et al*. (2000), but with occasional exceptions. The relation between normal strains ε and changes in effective normal stresses σ in cylindrical coordinates with the axis of symmetry in the vertical, z-direction is expressed as

1. $$\begin{bmatrix} \varepsilon_{rr} \\ \varepsilon_{\theta\theta} \\ \varepsilon_{zz} \end{bmatrix} = \begin{bmatrix} \frac{1}{E_h} & -\frac{\mu_{hh}}{E_h} & -\frac{\mu_{vh}}{E_v} \\ -\frac{\mu_{hh}}{E_h} & \frac{1}{E_h} & -\frac{\mu_{vh}}{E_v} \\ -\frac{\mu_{vh}}{E_v} & -\frac{\mu_{vh}}{E_v} & \frac{1}{E_v} \end{bmatrix} \begin{bmatrix} \sigma_{rr} \\ \sigma_{\theta\theta} \\ \sigma_{zz} \end{bmatrix}$$

E_h and E_v are non-negative normal moduli and are equal for the special case of an FILE material. Poisson's ratios μ_{hh} and μ_{vh} are equal for an FILE material. Lings *et al*. (2000) and others use μ_{hv}/E_h instead of the equivalent μ_{vh}/E_v in the third row. However, the reciprocity relations by Onsager (1931) imply that the matrix is symmetric, and the present paper follows Gibson (1974) and others by incorporating the symmetry automatically in the notation. For shear strains and changes of shear stresses

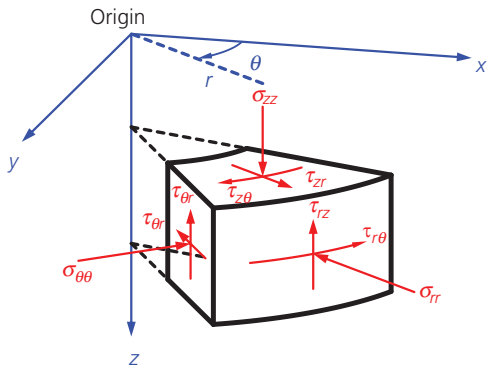

Figure 1. Cartesian and cylindrical coordinate frames and directions for positive stresses. The origin is the point of loading. The flat horizontal surface of the half-space is at $z = 0$. The z-axis is the axis of material symmetry

2. $$\gamma_{zr} = \frac{\tau_{zr}}{G_{vh}}$$

3. $$\gamma_{z\theta} = \frac{\tau_{z\theta}}{G_{vh}}$$

4. $$\gamma_{r\theta} = \frac{\tau_{r\theta}}{G_{hh}}$$

The two non-negative shear moduli G_{hh} and G_{vh} are equal for FILE materials. A combination of tensor rules and material symmetry about the z-axis gives

5. $$G_{hh} = \frac{E_h}{2(1 + \mu_{hh})}$$

This reduces to a familiar relation for FILE materials (e.g. Davis and Selvadurai, 1996). For general TILE materials, there is no analogous relation for G_{vh}.

Some authors express the compliance equations in a 6 × 6 matrix in which the 3 × 3 matrix of Equation 1 is a part and the shear equations in Equations 2–4 are also represented. The determinant of the 6 × 6 matrix is $\Delta/(G_{vh}^2 G_{hh})$, where $\Delta = \Delta_1 \Delta_2 / E_v$ is the determinant of the 3 × 3 matrix and

6. $$\Delta_1 = \frac{1 + \mu_{hh}}{E_h} = \frac{1}{2G_{hh}}$$

7. $$\Delta_2 = \frac{1 - \mu_{hh}}{E_h} - \frac{2\mu_{vh}^2}{E_v}$$

The inverse of the 3 × 3 matrix is

8. $$\begin{bmatrix} \sigma_{rr} \\ \sigma_{\theta\theta} \\ \sigma_{zz} \end{bmatrix} = \frac{E_v}{\Delta_1 \Delta_2} \begin{bmatrix} \frac{1}{E_h E_v} - \frac{\mu_{vh}^2}{E_v^2} & \frac{\mu_{hh}}{E_h E_v} + \frac{\mu_{vh}^2}{E_v^2} & \frac{\mu_{vh}(1 + \mu_{hh})}{E_h E_v} \\ \frac{\mu_{hh}}{E_h E_v} + \frac{\mu_{vh}^2}{E_v^2} & \frac{1}{E_h E_v} - \frac{\mu_{vh}^2}{E_v^2} & \frac{\mu_{vh}(1 + \mu_{hh})}{E_h E_v} \\ \frac{\mu_{vh}(1 + \mu_{hh})}{E_h E_v} & \frac{\mu_{vh}(1 + \mu_{hh})}{E_h E_v} & \frac{1 - \mu_{hh}^2}{E_h^2} \end{bmatrix} \begin{bmatrix} \varepsilon_{rr} \\ \varepsilon_{\theta\theta} \\ \varepsilon_{zz} \end{bmatrix}$$

Liao and Wang (1998) presented the point load solutions that are the basis of proposals in the present paper. They used A_{ij} for the 6 × 6 matrix of constrained moduli. The above is represented as

$$9.\quad \begin{bmatrix} \sigma_{rr} \\ \sigma_{\theta\theta} \\ \sigma_{zz} \end{bmatrix} = \begin{bmatrix} A_{11} & A_{12} & A_{13} \\ A_{12} & A_{11} & A_{13} \\ A_{13} & A_{13} & A_{33} \end{bmatrix} \begin{bmatrix} \varepsilon_{rr} \\ \varepsilon_{\theta\theta} \\ \varepsilon_{zz} \end{bmatrix}$$

with $A_{12} = A_{11} - 2A_{66}$. The shear moduli are $A_{44} = A_{55} = G_{\mathrm{vh}}$ and $A_{66} = G_{\mathrm{hh}}$. All other A_{ij} are zero. Some authors use C_{ij} instead of A_{ij}.

Strain energy per unit volume

Gibson (1974) proposed that the strain energy of a material must be non-negative and zero only when the stress is zero. This is consistent with conventional continuum mechanics (e.g. Spencer, 1980). For infinitesimal strains and if a TILE material modelling a soil under static conditions was initially under zero stress, the strain energy W per unit volume is the work done on a unit volume to reach the current state of stress, so that

$$10.\quad W = \frac{1}{2}\left(\sum \sigma_i \varepsilon_i + \frac{\tau_{zr}^2}{G_{\mathrm{vh}}} + \frac{\tau_{z\theta}^2}{G_{\mathrm{vh}}} + \frac{\tau_{r\theta}^2}{G_{\mathrm{hh}}}\right)$$

where in this equation the stress symbols refer to stresses that are zero when the strain is zero. The sum is for $i = zz$, rr and $\theta\theta$. Using Equation 1 gives

$$11.\quad \frac{1}{2}\sum \sigma_i \varepsilon_i = \frac{\Delta_1^*}{4}\left(\sigma_{rr} + \sigma_{\theta\theta} - \frac{2\mu_{\mathrm{vh}}}{\Delta_1^* E_{\mathrm{v}}}\sigma_{zz}\right)^2 + \frac{\Delta_1}{4}(\sigma_{rr} - \sigma_{\theta\theta})^2 + \frac{\Delta_2}{2\Delta_1^* E_{\mathrm{v}}}\sigma_{zz}^2$$

with

$$12.\quad \Delta_1^* = \frac{1 - \mu_{\mathrm{hh}}}{E_{\mathrm{h}}}$$

giving

$$13.\quad \Delta_2 = \Delta_1^* - \frac{2\mu_{\mathrm{vh}}^2}{E_{\mathrm{v}}}$$

Using Equation 8 to substitute for the changes of stress in terms of the strains gives

$$14.\quad \frac{1}{2}\sum \sigma_i \varepsilon_i = \frac{1}{4\Delta_1^*}(\varepsilon_{rr} + \varepsilon_{\theta\theta})^2 + \frac{1}{4\Delta_1}(\varepsilon_{rr} - \varepsilon_{\theta\theta})^2 + \frac{\Delta_1^* E_{\mathrm{v}}}{2\Delta_2}\left[\frac{\mu_{\mathrm{vh}}}{\Delta_1^* E_{\mathrm{v}}}(\varepsilon_{rr} + \varepsilon_{\theta\theta}) + \varepsilon_{zz}\right]^2$$

Recent work in lattice mechanics by Adhikari *et al*. (2020) and others use negative 'equivalent' dynamic Young's moduli that incorporate effects other than stiffness. To be clear, therefore, it can be useful to derive carefully the constraints on 'static' TILE material properties of interest herein. The expressions in parentheses in the preceding equation can be considered to be independent variables whose squares cannot be negative, so the requirement by Gibson (1974) for non-negative strain energy implies that the factors outside the parentheses must be non-negative. The following can then be deduced:

- $\Delta_1^* \geq 0$ to ensure that the first factor in the preceding equation is non-negative
- $\Delta_1 \geq 0$ to ensure that the second factor is non-negative
- $\Delta_2/E_{\mathrm{v}} \geq 0$ is then required to ensure that the third factor is non-negative
- $\Delta_1^* \geq 0$ and $\Delta_1 \geq 0$ taken together imply $-1 \leq \mu_{\mathrm{hh}} \leq 1$ and $E_{\mathrm{h}} \geq 0$
- $\Delta_2/E_{\mathrm{v}} \geq 0$ then implies $\Delta_1^*/E_{\mathrm{v}} \geq 0$, which implies $E_{\mathrm{v}} \geq 0$
- $\Delta_2/E_{\mathrm{v}} \geq 0$ and $E_{\mathrm{v}} \geq 0$ then implies $\Delta_2 \geq 0$,

$\Delta_1 \geq 0$ and $\Delta_2 \geq 0$ are equivalent to limits on Young's moduli and Poisson's ratios attributed to Love (1927), Raymond (1970) and Pickering (1970) and explored further by Lings *et al*. (2000) and Lings (2001). The shear moduli must also be non-negative. Together these limits also ensure that the compliance matrix is positively definite, giving stable material behaviour.

Parameters for some geological materials

The present paper looks at data of the seismic anisotropy of sedimentary rocks published by Wang (2002a, 2002b). The data are summarised in Table 1, where the descriptions are geophysical. The 'sands' are classified as soft rocks and may what a geotechnical engineer might call lightly cemented sandstones. The data are presented as constrained moduli C_{ij} (= A_{ij}) and were analysed in various ways. The present paper looks at the data in new ways. Most of the published data are used, excepting where C_{13} was not given or C_{12} was found to be noticeably different from $C_{11} - 2C_{66}$.

Figure 2 shows various aspects of the effective TILE parameters for the tabulated data. Figure 2(a) shows the relation between the effective normal modulus ratio $E_{\mathrm{v}}/E_{\mathrm{h}}$ plotted horizontally against shear modulus ratio $G_{\mathrm{vh}}/G_{\mathrm{hh}}$. Both ratios are 1 for FILE materials, so the spread of values, most less than 1, is an indication of the degree of anisotropy of these soils. For clays, Pegah *et al*. (2021)

Table 1. Data sources and key for data figures

Materials	Symbol in figures	Number of samples	Sample depth: km
Brine-saturated African shales	▫	5	2.3–2.5
Brine-saturated North Sea shales	▫	3	1.6–2.1
Other brine-saturated shales	▫	8	1.4–4.3
Brine-saturated shaly coal	■	1	3.6
Gas-saturated shaly coal	■	1	3.6
Brine-saturated sands	○	8	2.4–4.1
Gas-saturated African sands	○	2	2.4–2.5
Gas-saturated tight sands	○	12	3.6–4.1
Gas-saturated carbonates[a]	◆◆	35	3.3–4.3
Brine-saturated carbonates[a]	◇◇	25	3.5–4.5

[a] Limestone and dolomite
Source: Wang (2002b)

suggested a unique relation of the following form, based on the paper by Mašín and Rott (2014):

$$\frac{E_h}{E_v} = a\left(\frac{G_{hh}}{G_{vh}}\right)^b \quad (15)$$

with $a = 1$ and $b = 1.25$. There is some scatter about this curve for the data of Table 1.

Figures 2(b) and 2(c) show values of Poisson's ratios μ_{hh} and μ_{vh}, plotted against the effective normal modulus ratio. Some authors report considerable difficulty in measuring the latter parameter for clays, partly due to strain dependence. Gibson (1974) showed that μ_{vh} would be 1/2 in an undrained test, and μ_{hh} would equal $1 - \mu_{vh}E_h/E_v$. The latter are plotted against each other in Figure 2(d). This plot confirms that the data of Table 1 were not undrained data (see also Equations 50 and 51 later).

Measures of anisotropy of TILE materials

Figures 2(a)–2(d) indicate that E_v/E_h may be incomplete as an identifier of transverse isotropy. Other proposals include parameters by Thomsen (1986), Tsvankin and Thomsen (1994) and Alkhalifah and Tsvankin (1995) and others, which are focused on geophysical applications and are based on ratios of stress wave velocities.

The five independent material constants of a TILE material are reduced to two for an FILE material, so an unbiased measure of anisotropy needs to involve three components. One possibility might involve two further shear moduli from the geotechnical literature:

$$G_{dtx} = G_{iso} = \frac{E_v}{2(1+\mu_{vh})} \quad (16)$$

$$G_{utx} = G^* = \frac{1}{3}\left[E_v + \frac{(1-2\mu_{vh})^2}{2\Delta_2}\right] \quad (17)$$

Both use drained material parameters and equal G_{hh} for an FILE material. G_{iso} is described by Lings *et al.* (2000) and G^* by Graham and Houlsby (1983). They are one-third of the slopes of a graph of deviator stress against deviator strain in standard drained and undrained triaxial tests, respectively, on a vertically aligned TILE material (see Appendix). Three aspects of anisotropy can then be defined as follows:

$$\text{Normal aspect:} \quad \chi_1 = \frac{E_h - E_v}{E_h + E_v} \quad (18)$$

$$\text{Shear aspect:} \quad \chi_2 = \frac{G_{hh} - G_{vh}}{G_{hh} + G_{vh}} \quad (19)$$

$$\text{Triaxial aspect:} \quad \chi_3 = \frac{G_{utx} - G_{dtx}}{G_{utx} + G_{dtx}} \quad (20)$$

Each would be between −1 and 1. A combined measure might be

$$\chi = \sqrt{\left(\frac{E_h - E_v}{E_h + E_v}\right)^2 + \left(\frac{G_{hh} - G_{vh}}{G_{hh} + G_{vh}}\right)^2 + \left(\frac{G_{utx} - G_{dtx}}{G_{utx} + G_{dtx}}\right)^2} \quad (21)$$

If $\chi = 0$, then the material is an FILE material. Otherwise, the material is anisotropic and may be a TILE material or have more

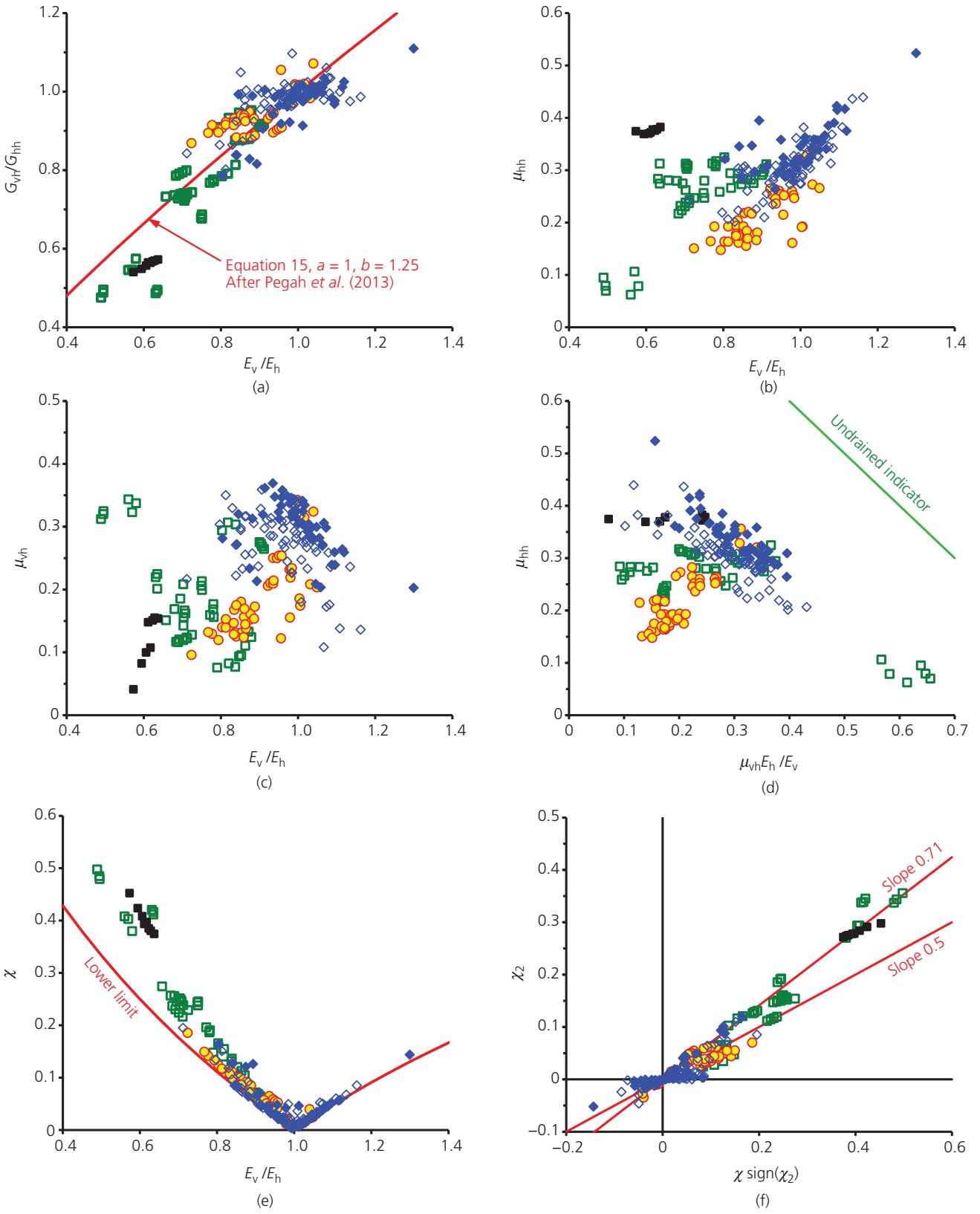

Figure 2. Drained linear elastic properties of some cross-anisotropic geomaterials: (a) modulus ratios; (b–d) Poisson's ratios; (e, f) anisotropy parameters. See Table 1 for data sources and key

complex anisotropy. Larger values of χ would be expected to imply greater inaccuracy if the material is modelled as fully isotropic. The largest possible value is 3.

Figure 2(e) shows χ plotted against E_v/E_h for the data of Table 1. The limit curve corresponds to $\chi_2 = \chi_3 = 0$. The graph indicates that χ correlates approximately but non-linearly with E_v/E_h and that this is 1 when χ is close to zero.

Absolute values of the three aspects might be interpreted as indicators of potential errors associated with assuming that their relevant determining moduli are equal. Figure 2(f) shows χ_2 plotted against χ sign (χ_2). Lines of slopes 0.5 and $1/2^{1/2}$ correspond respectively to $\chi_2^2 = (\chi_1^2 + \chi_3^2)/3$ and $\chi_2^2 = (\chi_1^2 + \chi_3^2)/2$. The graph indicates that the shear aspect is an important part of the overall anisotropy for the data of Table 1.

Liao and Wang (1998) results

Characteristic equation

The solutions by Liao and Wang (1998) for a TILE half-space subject to general point loads are the essential basis of the present paper. Their solutions involve dimensionless variables u_i (i = 1 to 3) and m_i (i = 1–2) that satisfy

22. $$\text{For } i = 1, 2: \quad m_i = \frac{(A_{13} + A_{44})u_i}{A_{33}u_i^2 - A_{44}} = \frac{A_{11} - A_{44}u_i^2}{(A_{13} + A_{44})u_i}$$

23. $$\text{For } i = 3: \quad u_3 = \sqrt{\frac{A_{66}}{A_{44}}} = \sqrt{\frac{G_{hh}}{G_{vh}}}$$

Equation 22 is the 'characteristic equation' for TILE materials. It can be deduced by applying the physical constraints associated with internal equilibrium. It also serves as a definition of the dimensionless parameters m_i. Using the equality between the two expressions for m_i, Liao and Wang (1998) noted that u_1 and u_2 satisfy a quadratic $u_i^4 - su_i^2 + q = 0$ with

24. $$s = \frac{A_{11}A_{33} - A_{13}(A_{13} + 2A_{44})}{A_{33}A_{44}} = u_1^2 + u_2^2$$

25. $$q = \frac{A_{11}}{A_{33}} = u_1^2 u_2^2$$

The solutions for u_i^2, for subscript i = 1 or 2, were deduced as follows:

26. $$u_i^2 = \frac{1}{2}\left(s \pm \sqrt{s^2 - 4q}\right)$$

Liao and Wang (1998) considered three cases, depending on the sign of $s^2 - 4q$. Sheet A4 in the online supplementary material verifies that u_1 and u_2 are either both real and positive for surface loads or else are complex conjugates of each other. The present paper takes the signs in the preceding expression such that $u_1^2 - u_2^2 = \sqrt{s^2 - 4q}$.

Some new results

Using the correspondence between Equations 8 and 9 to substitute for the A_{ij} in the expressions by Liao and Wang (1998) for s and q gives

27. $$s = \frac{2}{1 - \mu_{hh}}\left(\frac{G_{hh}}{G_{vh}} - \mu_{vh}\frac{E_h}{E_v}\right)$$

28. $$q = \frac{2G_{hh}}{1 - \mu_{hh}}\frac{E_h}{E_v}\left(\frac{1}{E_h} - \frac{\mu_{vh}^2}{E_v}\right)$$

Together with Equation 26, these give a way of calculating u_1 and u_2 without needing to invert the compliance matrix. Using the correspondence again, together with the second expression for m_i in the characteristic equation, gives

29. $$\text{For } i = 1, 2: \quad m_i u_i = \frac{\Delta_1 + \Delta_2 - 2\Delta_1\Delta_2 G_{vh}u_i^2}{2\Delta_1(\mu_{vh} + \Delta_2 G_{vh})}$$

This gives a way of calculating m_i without needing to invert the compliance matrix. Using the first expression for m_i in the characteristic equation to compute the product m_1m_2 gives

30. $$m_1 m_2 = \frac{(A_{13} + A_{44})^2}{(A_{33}u_1^2 - A_{44})(A_{33}u_2^2 - A_{44})}u_1 u_2$$

Using Equations 24 and 25 to simplify the denominator gives

31. $$m_1 m_2 = u_1 u_2$$

Liao and Wang (1998) defined a variable k with dimensions of inverse modulus. Its definition may be conveniently re-expressed using a new dimensionless variable k' as follows:

32. $$k = \frac{k'}{A_{44}} = \frac{k'}{G_{vh}}$$

with

33. $$k' = \frac{A_{13} + A_{44}}{A_{33}(u_1^2 - u_2^2)} = \frac{E_h(\mu_{vh} + \Delta_2 G_{vh})}{E_v(1 - \mu_{hh})\sqrt{s^2 - 4q}}$$

where the second expression is deduced using Equations 6–9 and 26. It follows that k' is either wholly real or wholly imaginary. Liao and Wang (1998) also defined four variables T, two of which are related as follows:

$$34. \quad m_1 T_1 = k\frac{u_1 + u_2}{u_2 - u_1} = m_2 T_4$$

Using Equation 31 to simplify the definitions of the other two gives

$$35. \quad T_2 = \frac{k}{m_2}\frac{2u_1(u_2 + m_2)}{(u_2 - u_1)(u_1 + m_1)} = \frac{2k}{u_2 - u_1}$$

$$36. \quad T_3 = \frac{k}{m_1}\frac{2u_2(u_1 + m_1)}{(u_2 - u_1)(u_2 + m_2)} = \frac{2k}{u_2 - u_1}$$

Hence, $T_2 = T_3$. The following new dimensionless variables will be found useful:

$$37. \quad \lambda_1 = \frac{2k'}{u_2 - u_1}(u_1 - m_1) = \lambda_0(u_1 - m_1)$$

$$38. \quad \lambda_2 = \frac{2k'}{u_2 - u_1}(u_2 - m_2) = \lambda_0(u_2 - m_2)$$

with

$$39. \quad \lambda_0 = \frac{2k'}{u_2 - u_1} = \frac{-2k'(u_1 + u_2)}{\sqrt{s^2 - 4q}}$$

λ_1 and λ_2 are real if u_1 and u_2 are real, and complex conjugates otherwise.

Effective properties of some geological materials

Figure 3 shows some of these results for the data of Table 1. Figure 3(a) shows that s is positive for all of these data and in most cases greater than 2. Figure 3(b) shows that $s^2 - 4q$ can be positive or negative for these data. Raymond (1970) proposed that the shear modulus G_{vh} would be limited by a value here denoted as G_R (Lings *et al.*, 2000):

$$40. \quad G_R = \frac{E_v}{2\mu_{vh}(1 + \mu_{hh}) + 2\sqrt{(1 - \mu_{hh}^2)(E_v/E_h - \mu_{vh}^2)}}$$

Anyaegbunam (2014) asserted that this limit is invalid. Using Equations 27 and 28, the criterion $G_{vh} \leq G_R$ is found to be equivalent to insisting that $s^2 - 4q \geq 0$. The data show that this is not satisfied by real materials. The limit by Raymond (1970) is further discussed later in this paper.

Figures 3(c) and 3(d) shows the solutions for u_1 and u_2 for the carbonates of Table 1. In Figure 3(c), the real parts of u_1 and u_2 are plotted on the vertical axis. When $s^2 - 4q > 0$, the real parts are greater for u_1 than for u_2. When $s^2 - 4q < 0$, the real parts are equal because then u_1 and u_2 are complex conjugates. Figure 3(d) shows the imaginary coefficients. The values are zero when $s^2 - 4q > 0$, and equal and opposite when $s^2 - 4q < 0$.

Figures 3(e) and 3(f) show corresponding results for m_1 and m_2. Real values of both m_i and u_i are approximately symmetric about the value of 1, which is the value for FILE materials. This is consistent with the values of s for the carbonates in Figure 3(a) being close to 2.

Surface loading: general cases

Motivation and notation

Surface loading is an application of the equations by Liao and Wang (1998) with practical relevance, since most soils are anisotropic and many calculations in practical engineering are for loaded areas of ground or for rigid footings on or close to the surface. However, those equations occupy a total of over three densely packed pages of their paper. Consequently, a first motivation for exploring them is to find simplifications. A second motivation is that the present author noticed what is believed to be a notational confusion and a typo in one of their equations, and these need to be clarified and avoided.

Regarding simplifications, the equations involve eight different adjusted z-coordinates, eight associated adjusted distance coordinates and eight other distances. Calculation sheet A2 in the online supplementary material shows that these 24 variables reduce to three groups of three for the special case of surface loading. In each group, the subscripts are 1, 2 and 3, with

$$41. \quad z_i = u_i z$$

$$42. \quad R_i = \sqrt{r^2 + z_i^2}$$

$$43. \quad R_i^* = R_i - z_i = \frac{r^2}{R_i + z_i}$$

The factors u_i are 1 for FILE materials, and the parameters then reduce to z, R and $r^2/(R + z)$. These are familiar from solutions by

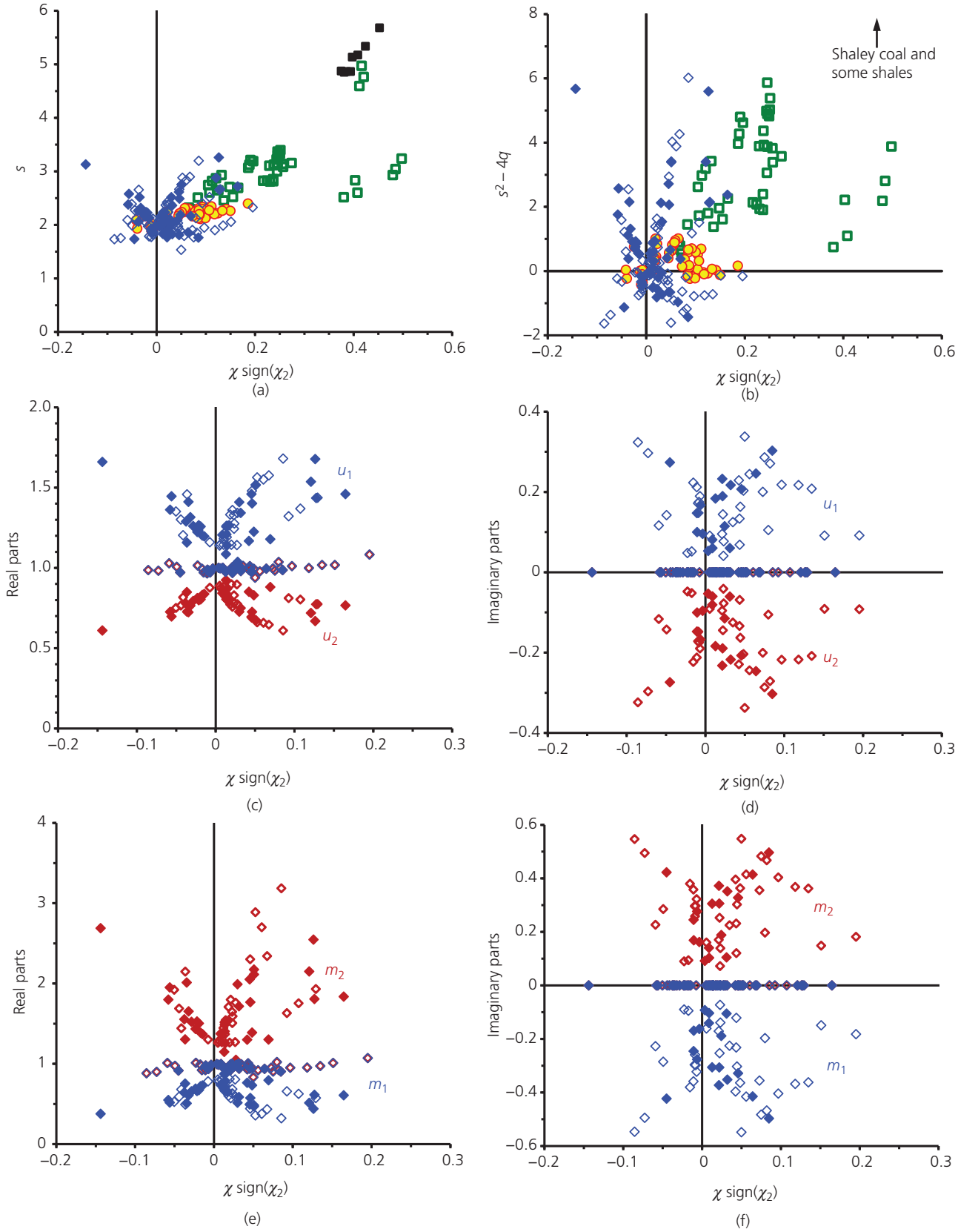

Figure 3. Drained point load properties: (a, b) s and $s^2 - 4q$; (c, d) u_1 and u_1; (e, f) m_1 and m_2. See Table 1 for data sources and key

Boussinesq (1878), Cerruti (1884–1885) and others in the theory of fully isotropic elasticity (e.g. Davis and Selvadurai, 1996).

Regarding the notational confusion and typo, this is explained in the section headed 'Lateral surface loading' and is detailed in the online supplementary material calculation sheets.

Vertical surface loading

Calculations for vertical loading are common in geotechnical practice, and the simplest is for surface loading. The solution by Boussinesq (1878) is the basis for calculations for a surface footing on an FILE material, so a corresponding calculation for a TILE material is naturally of interest.

Liao and Wang (1998) present their results for displacements and stresses in two parts, which are combined to form the complete solution. Combining their Equations 47–49 with Equations 73–75, considering only a vertical point load P_z at the origin of coordinates and applying the simplifications for surface loading gives

$$\text{Radial:}\quad U_r = \frac{P_z}{4\pi}\left[-(m_1T_1 - m_2T_2 + k)\frac{R_1^*}{rR_1} + (m_1T_3 - m_2T_4 + k)\frac{R_2^*}{rR_2}\right] \tag{44}$$

$$\text{Vertical:}\quad U_z = \frac{P_z}{4\pi}\left(-m_1\frac{m_1T_1 - m_2T_2 + k}{R_1} + m_2\frac{m_1T_3 - m_2T_4 + k}{R_2}\right) \tag{45}$$

Using Equations 31–39, these simplify as in (a) in Table 2. Details are provided in sheets B2–B4 in the online supplementary material. Circumferential displacement $U_\theta = 0$ is zero by symmetry.

Table 2. Results for vertical point load at the surface

T2.1	Note	$\lambda_1' = \lambda_2$ and $\lambda_2' = \lambda_1$
	(a) Displacements	
T2.2	Radial	$U_r = \frac{P_z}{4\pi G_{vh}}\sum_{i=1}^{2}\left(-\lambda_i'\frac{R_i^*}{rR_i}\right)$
T2.3	Circumferential	$U_\theta = 0$
T2.4	Vertical	$U_z = \frac{P_z}{4\pi G_{vh}}\sum_{i=1}^{2}\left(\frac{-m_i\lambda_i'}{R_i}\right)$
	(b) Strains	
T2.5		$\varepsilon_{rr} = \frac{P_z}{4\pi G_{vh}}\sum_{i=1}^{2}\left[\lambda_i'\left(\frac{z_i}{R_i^3} - \frac{R_i^*}{r^2R_i}\right)\right]$
T2.6		$\varepsilon_{\theta\theta} = \frac{P_z}{4\pi G_{vh}}\sum_{i=1}^{2}\left[\lambda_i'\frac{R_i^*}{r^2R_i}\right]$
T2.7		$\varepsilon_{zz} = \frac{P_z}{4\pi G_{vh}}\sum_{i=1}^{2}\left[-\lambda_i'm_iu_i\frac{z_i}{R_i^3}\right]$
T2.8		$\gamma_{r\theta} = \gamma_{\theta z} = 0$
T2.9		$\gamma_{rz} = \frac{P_z}{4\pi G_{vh}}\sum_{i=1}^{2}\left[-\frac{\lambda_i'(u_i + m_i)}{R_i^3}\right]$
	(c) Stresses	
T2.10		$\sigma_{rr} = \frac{P_z}{4\pi}\left\{\sum_{i=1}^{2}\left[\lambda_i'u_i(u_i + m_i)\frac{z_i}{R_i^3}\right] + 2\frac{G_{hh}}{G_{vh}}\sum_{i=1}^{2}\left(-\lambda_i'\frac{R_i^*}{r^2R_i}\right)\right\}$
T2.11		$\sigma_{\theta\theta} = \frac{P_z}{4\pi}\left\{\sum_{i=1}^{2}\left[\lambda_i'u_i(u_i + m_i)\frac{z_i}{R_i^3}\right] - 2\frac{G_{hh}}{G_{vh}}\sum_{i=1}^{2}\left[\lambda_i'\left(\frac{z_i}{R_i^3} - \frac{R_i^*}{r^2R_i}\right)\right]\right\}$
T2.12		$\sigma_{zz} = \frac{P_z}{4\pi}\sum_{i=1}^{2}\left[-\frac{\lambda_i'}{u_i}\left(u_i + m_i\right)\frac{z_i}{R_i^3}\right]$
T2.13		$\tau_{r\theta} = \tau_{\theta r} = 0$
T2.14		$\tau_{rz} = \frac{P_z}{4\pi}\sum_{i=1}^{2}\left[-\lambda_i'\left(u_i + m_i\right)\frac{r}{R_i^3}\right]$

Based on the general solutions by Liao and Wang (1998)

Using standard equations for strains in cylindrical coordinates, which Liao and Wang (1998) quoted, gives the equations for strains in (b) in Table 2. Applying the constitutive equations for a TILE material then gives the equations for changes in stress in (b) in Table 2. These are found to be consistent with Equations 50–55 and 76–81 by Liao and Wang (1999). For completeness, sheets F1 and F2 in the online supplementary material confirms that the stresses in (c) in Table 2 also satisfy the standard equilibrium equations in cylindrical coordinates.

Raymond's proposed limit

Raymond (1970) argued that the solution by Mitchell (1900) for vertical point loading, as quoted by Barden (1963), would produce unphysical complex-valued vertical stresses at depths below the load if G_{vh} exceeded G_R. In the equations by Liao and Wang (1998), $r = 0$ implies $R_i = u_i z$, so from the equation for vertical stress in Table 2

$$46.\quad \text{On } r = 0: \quad \sigma_{zz} = \frac{P_z}{4\pi G_{vh} z^2} \sum_{i=1}^{2} \left[-\frac{\lambda_i'}{u_i^2} (u_i + m_i) \right]$$

If λ_i, m_i and u_i are real numbers, the summation is real. Reference to Equations 31–39 shows that if u_1 and u_2 are complex conjugates, each of the two terms in the preceding summation is the complex conjugate of the other, so their sum is real. It can readily be checked that this applies for all the stresses and at all positions in the FILE half-space. Hence, the solutions by Liao and Wang (1998) do not produce complex values of this stress. Raymond's argument does not therefore apply.

As a check, Figure 4 shows the ratio G_{vh}/G_R plotted against the effective normal modulus ratio for the data of Table 1. Figure 4(a) uses the tabulated parameters directly, and Figure 4(b) shows undrained parameters inferred from the drained ones using algebra described later in this paper. The results indicate that Raymond's proposed limit was exceeded in many of the tests. This seems unlikely to be explicable as experimental error. On these theoretical and experimental grounds, in agreement with Anyaegbunam (2014), and unless some other argument is found, it is proposed that the limit on G_{vh} by Raymond (1970) be considered invalid.

Lateral surface loading

Lateral loading is relevant in many geotechnical applications, including when lateral loads from wind, wave and current forces are transmitted into foundations (e.g. Cassidy *et al.*, 2004; Dean, 2009; Randolph and Gourvenec, 2011), or when transport or machine vibrations occur, or seismic events that often involve strong lateral shaking (Kramer, 1996; Srbulov and O'Brien, 2012).

The equations by Liao and Wang (1998) for displacements and stresses use symbols P_r and P_θ described as loads in the radial and circumferential directions, respectively. However, the present author noticed what appeared to be a notational confusion. For a lateral point load applied in some general azimuthal direction θ_P, physical symmetry would indicate that displacements would have reflection symmetry in the plane $\theta = \theta_P$. Vertical and radial displacements would have a symmetry like $\cos(\theta - \theta_P)$, and circumferential displacements like $\sin(\theta - \theta_P)$. However, the

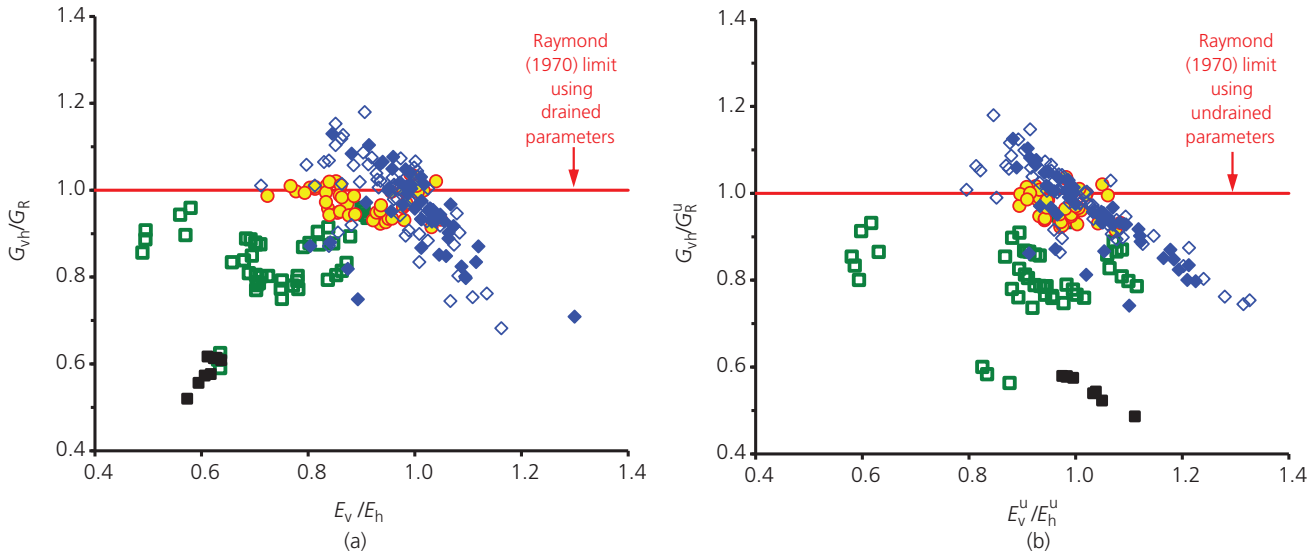

Figure 4. Investigation of the proposed limit by Raymond (1970) on G_{vh} for some sedimentary rocks: (a) drained parameters; (b) constant-volume parameters. See Table 1 for data sources and key

equations by Liao and Wang (1998) indicate that the responses to P_r exhibit symmetries of cos θ and sin θ, respectively, indicating that $\theta_P = 0$. This is considered herein to imply that P_r can be interpreted as a point load P_x in the $+x$ direction. Similarly, P_θ is found to be a point load P_y in the $+y$ direction.

Additionally, a possible typo was noticed in one of the equations for stress. To resolve these issues, the equations by Liao and Wang (1998) for stress for the lateral loading case were ignored. Instead, their equations for displacements were assumed to be correct, and the equations for strains and changes in stress were then calculated explicitly. The results are in Table 3 and were further checked by checking equilibrium. These calculations are included in calculation sheets E1 to G4 in the online supplementary material and are briefly explained in the following.

Liao and Wang (1998) solved the equations by considering two separate analyses whose combination would give the results sought. Combining their Equations 47–49 with Equations 73–75, setting $P_r = P_x$ and $P_z = P_\theta = 0$ and applying the simplifications associated with surface loading gives

Table 3. Results for horizontal point loads at the surface

(a) Displacements		
T3.1	Radial	$U_r = \frac{P_x \cos\theta}{4\pi G_{vh}} \left\{ \left[\sum_{i=1}^{2} \left(-\frac{\lambda_i z_i R_i^*}{m_i r^2 R_i} \right) \right] + \frac{2}{u_3} \frac{R_3^*}{r^2} \right\}$
T3.2	Circumferential	$U_\theta = \frac{P_x \sin\theta}{4\pi G_{vh}} \left\{ \left[\sum_{i=1}^{2} \left(\frac{\lambda_i}{m_i} \frac{R_i^*}{r^2} \right) \right] - \frac{2}{u_3} \frac{z_3 R_3^*}{r^2 R_3} \right\}$
T3.3	Vertical	$U_z = \frac{P_x \cos\theta}{4\pi G_{vh}} \sum_{i=1}^{2} \left(\lambda_i \frac{R_i^*}{r R_i} \right)$
(b) Strains		
T3.4		$\varepsilon_{rr} = \frac{P_x \cos\theta}{4\pi G_{vh}} \left\{ \left[\sum_{i=1}^{2} \left[\frac{\lambda_i}{m_i} \left(\frac{z_i^2}{r R_i^3} - \frac{2 z_i R_i^*}{r^3 R_i} \right) \right] \right] - \frac{2}{u_3} \left(\frac{1}{r R_3} - \frac{2 R_3^*}{r^3} \right) \right\}$
T3.5		$\varepsilon_{\theta\theta} = \frac{P_x \cos\theta}{4\pi G_{vh}} \left\{ \left[\sum_{i=1}^{2} \left(-\frac{\lambda_i}{m_i} \frac{R_i^{*2}}{r^3 R_i} \right) \right] - \frac{2}{u_3} \frac{R_3^{*2}}{r^3 R_3} \right\}$
T3.6		$\varepsilon_{zz} = \frac{P_x \cos\theta}{4\pi G_{vh}} \sum_{i=1}^{2} \left(\frac{\lambda_i u_i r}{R_i^3} \right)$
T3.7		$\gamma_{r\theta} = \frac{P_x \sin\theta}{4\pi G_{vh}} \left\{ \left[\sum_{i=1}^{2} \left[\frac{\lambda_i}{m_i} \left(\frac{2 R_i^{*2}}{r^3 R_i} \right) \right] \right] - \frac{2}{u_3} \left(\frac{3 z_3 R_3^*}{r^3 R_3} - \frac{z_3^2}{r R_3^3} - \frac{R_3^*}{r^3} \right) \right\}$
T3.8		$\gamma_{\theta z} = \frac{P_x \sin\theta}{4\pi G_{vh}} \left\{ \left[\sum_{i=1}^{2} \left[\frac{\lambda_i}{m_i} \left(u_i + m_i \right) \frac{R_i^*}{r^2 R_i} \right] \right] - 2 \left(\frac{z_3}{R_3^3} - \frac{R_3^*}{r^2 R_3} \right) \right\}$
T3.9		$\gamma_{rz} = \frac{P_x \cos\theta}{4\pi G_{vh}} \left\{ \left[\sum_{i=1}^{2} \left[\frac{\lambda_i}{m_i} \left(u_i + m_i \right) \left(\frac{R_i^*}{r^2 R_i} - \frac{z_i}{R_i^3} \right) \right] \right] + 2 \frac{R_3^*}{r^2 R_3} \right\}$
(c) Stresses		
T3.10		$\sigma_{rr} = \frac{P_x \cos\theta}{4\pi} \left\{ \sum_{i=1}^{2} \left[-\frac{\lambda_i}{m_i} u_i \left(u_i + m_i \right) \frac{r}{R_i^3} \right] - \frac{2 G_{hh}}{G_{vh}} \left[\sum_{i=1}^{2} \left(-\frac{\lambda_i}{m_i} \frac{R_i^{*2}}{r^3 R_i} \right) - \frac{2}{u_3} \frac{R_3^{*2}}{r^3 R_3} \right] \right\}$
T3.11		$\sigma_{\theta\theta} = \frac{P_x \cos\theta}{4\pi} \left\{ \sum_{i=1}^{2} \left[-\frac{\lambda_i}{m_i} u_i \left(u_i + m_i \right) \frac{r}{R_i^3} \right] - \frac{2 G_{hh}}{G_{vh}} \left[\sum_{i=1}^{2} \left[\frac{\lambda_i}{m_i} \left(\frac{R_i^{*2}}{r^3 R_i} - \frac{r}{R_i^3} \right) \right] + \frac{2}{u_3} \frac{R_3^{*2}}{r^3 R_3} \right] \right\}$
T3.12		$\sigma_{zz} = \frac{P_x \cos\theta}{4\pi} \sum_{i=1}^{2} \left[\frac{\lambda_i}{m_i u_i} \left(u_i + m_i \right) \frac{r}{R_i^3} \right]$
T3.13		$\tau_{\theta z} = \frac{P_x \sin\theta}{4\pi} \left\{ \sum_{i=1}^{2} \left[\frac{\lambda_i}{m_i} \left(u_i + m_i \right) \frac{R_i^*}{r^2 R_i} \right] + 2 \left(\frac{R_3^*}{r^2 R_3} - \frac{z_3}{R_3^3} \right) \right\}$
T3.14		$\tau_{rz} = \frac{P_x \cos\theta}{4\pi} \left\{ \sum_{i=1}^{2} \left[\frac{\lambda_i}{m_i} \left(u_i + m_i \right) \left(\frac{R_i^*}{r^2 R_i} - \frac{z_i}{R_i^3} \right) \right] + 2 \frac{R_3^*}{r^2 R_3} \right\}$
T3.15		$\tau_{r\theta} = \frac{P_x \sin\theta}{4\pi} \frac{G_{hh}}{G_{vh}} \left[\sum_{i=1}^{2} \left(\frac{\lambda_i}{m_i} \frac{2 R_i^{*2}}{r^3 R_i} \right) + \frac{2}{u_3} \left(\frac{3 z_3 R_3^*}{r^3 R_3} - \frac{R_3^*}{r^3} - \frac{z_3^2}{r R_i^3} \right) \right]$

Deduced from the displacements in the general solutions by Liao and Wang (1998)

$$\text{Radial:}\quad U_r = \frac{P_x \cos\theta}{4\pi}\left[\left(T_2 - T_1 + \frac{k}{m_1}\right)\frac{z_1 R_1^*}{r^2 R_1} + \left(T_3 - T_4 - \frac{k}{m_2}\right)\frac{z_2 R_2^*}{r^2 R_2} + \frac{2}{u_3 A_{44}}\frac{R_3^*}{r^2}\right] \tag{47}$$

$$\text{Circumferential:}\quad U_\theta = \frac{P_x \sin\theta}{4\pi}\left[\left(T_1 - T_2 - \frac{k}{m_1}\right)\frac{R_1^*}{r^2} - \left(T_3 - T_4 - \frac{k}{m_2}\right)\frac{R_2^*}{r^2} - \frac{2}{u_3 A_{44}}\frac{z_3 R_3^*}{r^2 R_3}\right] \tag{48}$$

$$\text{Vertical:}\quad U_z = \frac{P_x \cos\theta}{4\pi}\left\{[m_1(T_1 - T_2) - k]\frac{R_1^*}{rR_1} - [m_2(T_3 - T_4) - k]\frac{R_2^*}{rR_2}\right\} \tag{49}$$

Using Equations 31–39, these simplify as in (a) in Table 3. Details are given in sheets B5–B7 in the online supplementary material. Applying the standard equations for infinitesimal strains in cylindrical coordinates, as quoted by Liao and Wang (1998) and elsewhere, gives the strains in (b) in Table 3. Using material behaviour Equations 1–4 gives the stresses in (c) in Table 3. Details are in sheets C2–C7, D6 and D7 in the online supplementary material.

Except for the shear stress τ_{rz}, the results are found to be consistent with Equations 50–55 and 76–80 by Liao and Wang (1998). The present results would be fully consistent if the first sign on the right of their Equation 79 was changed from plus to minus. Checks on equilibrium are presented in sheets F3–F5 in the online supplementary material. They use the same standard equilibrium equations in cylindrical coordinates as those quoted by Liao and Wang (1998) and elsewhere. They confirm that the equations of Table 3 do satisfy equilibrium. Hence, these equations are judged to be correct.

Special cases 1: constant-volume behaviour

Motivation and notation

The constant-volume condition is considered equivalent to the undrained condition if the soil particles are incompressible and Terzaghi's principle of effective stress applies (Bowles, 1996; Dyvik *et al.*, 1987; Knappett and Craig, 2012). The condition therefore reduces the degrees of freedom available in terms of total stress parameters, and this requires special treatment.

Undrained properties and behaviours of TILE materials were well explored by Gibson (1974), Lings (2001) and others, including empirical proposals for estimating the drained properties from the smaller number of independent undrained parameters (Pegah *et al.*, 2021). For present purposes, following Lings (2001), an undrained parameter is signified by superscript 'u' and a change in the total stress is also denoted by a superscript. With this notation, two key relationships given by Gibson (1974) may be stated as follows:

$$\mu_{\text{vh}}^{\text{u}} = \frac{1}{2} \tag{50}$$

$$\frac{1 - \mu_{\text{hh}}^{\text{u}}}{E_{\text{h}}^{\text{u}}} = \frac{\mu_{\text{vh}}^{\text{u}}}{E_{\text{v}}^{\text{u}}} \tag{51}$$

Reference to Equation 7 reveals that these imply $\Delta_2^{\text{u}} = 0$, which implies that the undrained version of the compliance matrix of Equation 1 is not invertible. The equations by Liao and Wang (1998) use the inverse, so a workaround is developed in the following to enable the equations to be used for undrained conditions.

Calculations for undrained material parameters

As noted earlier, these calculations are well established in the literature. The following can be a useful alternative approach. Changes in pore stress are herein denoted as 'u', and the absence of a subscript on this symbol distinguishes it from displacements and from parameters u_i by Liao and Wang (1998). Terzaghi's principle of effective stress implies that changes σ of effective stress in Equation 1 can be replaced by differences $\sigma^u - u$ (e.g. Knappett and Craig, 2012). When this is done, application of the constant-volume condition $\varepsilon_{rr} + \varepsilon_{\theta\theta} + \varepsilon_{zz} = 0$ gives

$$u = \alpha(\sigma_{rr}^{\text{u}} + \sigma_{\theta\theta}^{\text{u}}) + \beta\sigma_{zz}^{\text{u}} \tag{52}$$

with

$$\alpha = \frac{1}{\gamma}\left(\frac{1 - \mu_{\text{hh}}}{E_{\text{h}}} - \frac{\mu_{\text{vh}}}{E_{\text{v}}}\right) \tag{53}$$

$$\beta = \frac{1}{\gamma}\left(\frac{1 - 2\mu_{\text{vh}}}{E_{\text{v}}}\right) \tag{54}$$

$$\gamma = 2\frac{1 - \mu_{\text{hh}}}{E_{\text{h}}} + \frac{1 - 4\mu_{\text{vh}}}{E_{\text{v}}} = 2\Delta_2 + \frac{(1 - 2\mu_{\text{vh}})^2}{E_{\text{v}}} \tag{55}$$

These imply $2\alpha + \beta = 1$. The condition $\Delta_2 \geq 0$ implies that γ is non-negative. Then, changes in effective stress are given by

$$\begin{bmatrix} \sigma_{rr} \\ \sigma_{\theta\theta} \\ \sigma_{zz} \end{bmatrix} = \begin{bmatrix} 1-\alpha & \alpha & \beta \\ \alpha & 1-\alpha & \beta \\ \beta & \beta & 1-\beta \end{bmatrix} \begin{bmatrix} \sigma^{\mathrm{u}}_{rr} \\ \sigma^{\mathrm{u}}_{\theta\theta} \\ \sigma^{\mathrm{u}}_{zz} \end{bmatrix} \quad 56.$$

Using this to substitute for the changes in effective stress in Equation 1, a new compliance equation is obtained with the drained parameters replaced with undrained ones as follows:

$$\frac{1}{E^{\mathrm{u}}_{\mathrm{h}}} = \frac{1}{E_{\mathrm{h}}} - \alpha^2\gamma \quad 57.$$

$$\frac{\mu^{\mathrm{u}}_{\mathrm{hh}}}{E^{\mathrm{u}}_{\mathrm{h}}} = \frac{\mu_{\mathrm{hh}}}{E_{\mathrm{h}}} + \alpha^2\gamma \quad 58.$$

$$\frac{\mu^{\mathrm{u}}_{\mathrm{vh}}}{E^{\mathrm{u}}_{\mathrm{v}}} = \frac{\mu_{\mathrm{vh}}}{E_{\mathrm{v}}} + \alpha\beta\gamma \quad 59.$$

$$\frac{1}{E^{\mathrm{u}}_{\mathrm{v}}} = \frac{1}{E_{\mathrm{v}}} - \beta^2\gamma = \frac{2\Delta_2}{\gamma E_{\mathrm{v}}} \quad 60.$$

These results are consistent with expressions given by Lings (2001) and others. Equations 57 and 60 ensure that the constant-volume moduli $E^{\mathrm{u}}_{\mathrm{v}}$ and $E^{\mathrm{u}}_{\mathrm{h}}$ are greater than the corresponding drained moduli. Shearing is unaffected by the constant-volume condition, so $G^{\mathrm{u}}_{\mathrm{hh}} = G_{\mathrm{hh}}$ and $G^{\mathrm{u}}_{\mathrm{vh}} = G_{\mathrm{vh}}$, and an undrained version of Equation 5 applies.

Results for undrained material parameters

Figure 5 explores undrained parameters for the TILE data of Table 1. Figure 5(a) shows that the parameter α does not stray far from its value of 1/3 for FILE materials, suggesting that these materials are only weakly anisotropic. Figure 5(b) indicates that there is an approximate correlation between α and the effective anisotropy parameter χ.

Figures 5(c) shows that the undrained normal ratio $E^{\mathrm{u}}_{\mathrm{v}}/E^{\mathrm{u}}_{\mathrm{h}}$ clusters around 1, in contrast to the drained ratio $E_{\mathrm{v}}/E_{\mathrm{h}}$. Gibson (1974) quotes the result '$E_{\mathrm{H}} \leq 4E_{\mathrm{V}}$' by Ferrar (1941) for an incompressible orthotropic elastic medium. Using Equations 6 and 7 with undrained parameters gives

$$\frac{1}{E^{\mathrm{u}}_{\mathrm{h}}} - \frac{\mu^{\mathrm{u2}}_{\mathrm{vh}}}{E^{\mathrm{u}}_{\mathrm{v}}} = \frac{\Delta^{\mathrm{u}}_1 + \Delta^{\mathrm{u}}_2}{2} = \frac{1+\mu^{\mathrm{u}}_{\mathrm{hh}}}{2E^{\mathrm{u}}_{\mathrm{h}}} \quad 61.$$

Hence, the expression on the left is non-negative. Putting $\mu^{\mathrm{u}}_{\mathrm{vh}} = 0.5$ and $E^{\mathrm{u}}_{\mathrm{v}} \geq 0$ then gives the condition for undrained TILE materials by Ferrar (1941). Figure 5(c) confirms that the data of Table 1 satisfy this.

Figure 5(d) shows that $\mu^{\mathrm{u}}_{\mathrm{hh}}$ is more than 1/2 for some of these materials. The data points here form a pattern that is rather similar to that in Figure 5(c). This is because of Gibson (1974) relations, Equations 50 and 51.

Liao and Wang (1998) equations for the undrained condition

Applying Equations 50 and 51 by Gibson (1974) to Equations 27 and 28 gives the undrained values of Liao and Wang (1998) parameters as

$$s^{\mathrm{u}} = 2\left(2\frac{G^{\mathrm{u}}_{\mathrm{hh}}}{G^{\mathrm{u}}_{\mathrm{vh}}}\frac{E^{\mathrm{u}}_{\mathrm{v}}}{E^{\mathrm{u}}_{\mathrm{h}}} - 1\right) = u^{\mathrm{u2}}_1 + u^{\mathrm{u2}}_2 \quad 62.$$

$$q^{\mathrm{u}} = 1 = u^{\mathrm{u2}}_1 u^{\mathrm{u2}}_2 \quad 63.$$

This implies that $s^{\mathrm{u2}} - 4q^{\mathrm{u}}$ is only zero when $E^{\mathrm{u}}_{\mathrm{v}}/E^{\mathrm{u}}_{\mathrm{h}} = G_{\mathrm{vh}}/G_{\mathrm{hh}}$, which is represented by the line of equality in Figure 5(e). $s^{\mathrm{u2}} - 4q^{\mathrm{u}}$ is negative for points above the diagonal line of equality, and positive for points below it. This also confirms that undrained parameters u_i and m_i can be calculated even though the undrained compliance matrix is singular. Equation 29 reduces to

$$\text{For } i = 1, 2: \quad m^{\mathrm{u}}_i u^{\mathrm{u}}_i = 1 \quad 64.$$

Using this with $\Delta^*_2 = 0$ and with Gibson (1974) relations and Equations 33 and 37–39, and taking Equation 63 to imply $u^{\mathrm{u}}_1 u^{\mathrm{u}}_2 = 1$, gives

$$m^{\mathrm{u}}_1 = u^{\mathrm{u}}_2 \quad 65.$$

$$m^{\mathrm{u}}_2 = u^{\mathrm{u}}_1 \quad 66.$$

$$k' = \frac{1}{\sqrt{s^{\mathrm{u2}} - 4q^{\mathrm{u}}}} \quad 67.$$

$$\lambda^{\mathrm{u}}_1 = -\lambda^{\mathrm{u}}_2 = \frac{-2}{\sqrt{s^{\mathrm{u2}} - 4q^{\mathrm{u}}}} \quad 68.$$

The denominator in the last two equations is zero in the case of full isotropy, which is analysed later.

Equations 16 and 17 can be written using constant-volume parameters. In the latter, $(1 - 2\mu^{\mathrm{u}}_{\mathrm{vh}})^2$ dominates Δ^{u}_2, so that $G^{\mathrm{u}}_{\mathrm{dtx}} =$

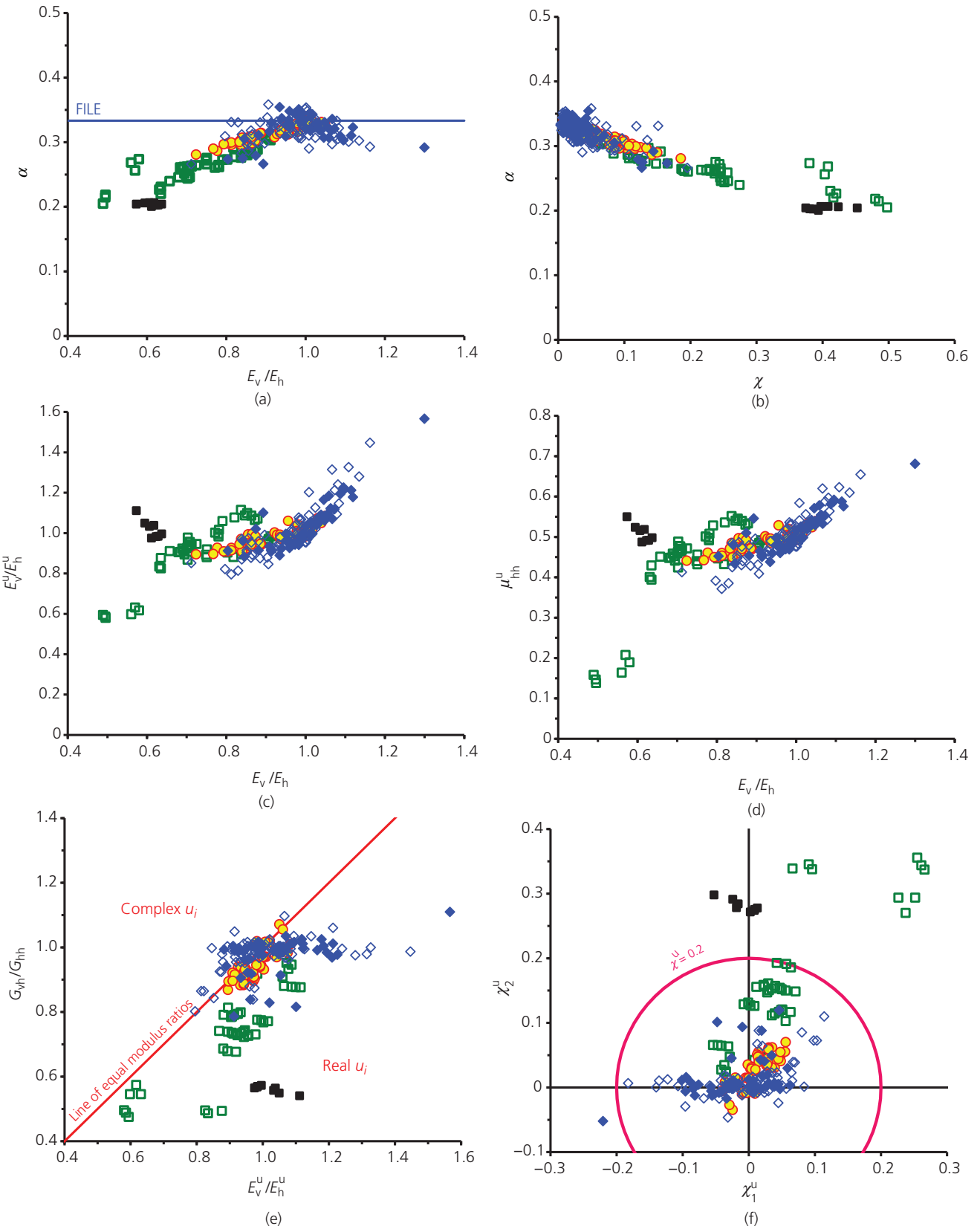

Figure 5. Undrained linear elastic properties: (a, b) α; (c–e) ratios; (f) anisotropy parameters. See Table 1 for data sources and key

$G^{u}_{utx} = E_v/3$. Hence, the triaxial aspect of anisotropy is zero for the undrained condition, Equation 20, although the shear and normal aspects are not. Figure 5(f) shows the relation between these aspects. An FILE material would plot at the origin in this diagram, and a curve of constant χ^u plots as a circle centred on the origin.

Special cases 2: full isotropy

Motivation and methodology

Barden (1963: p. 203) stated that 'isotropy is simply a special case of anisotropy'. It can therefore be useful to check that the TILE equations of Tables 2 and 3 do reduce to known solutions for the FILE materials for appropriate material constants. However, the following problem is found. For an FILE material, Young's moduli are equal, Poisson's ratios are equal and the shear moduli are equal. The solutions by Liao and Wang (1998) give $s = 2$ and $q = 1$, so $s^2 - 4q = 0$ and $u_1 = u_2 = m_1 = m_2 = 1$. This makes k and k' infinite (Equations 32 and 33) and renders λ_1 and λ_2 indeterminate (Equations 37 and 38). Special treatment is therefore needed for this material.

To find a workaround, the method by Barden (1963) of taking a limit is adapted herein. A TILE material is considered that is infinitesimally close to fully isotropic. There are several ways in which a TILE material, with five independent constants, can be close to being fully isotropic, with two. In the present paper, a material is considered with $E_v = E_h = E$ and $\mu_{vh} = \mu_{hh} = \mu$ and with the following:

$$A_{44} = G_{vh} = \frac{E}{2(1+\mu)}\left(1 - \frac{1-\mu}{2}\varepsilon^2\right) \tag{69}$$

where ε is an infinitesimally small number. This will tend to become an FILE material when ε tends to zero. Since $s^2 - 4q = 0$ for the FILE material, it will be infinitesimal for the nearly FILE material, and parameters with $(s^2 - 4q)^{1/2}$ in the denominator tend to infinity as $\varepsilon \to 0$. Details are given in sheets H1–H3 in the online supplementary material. Key results are quoted in the following.

Vertical loading

Boussinesq (1878) developed the solution for a point vertical load on the surface of an FILE half-space. The solution is explored by Westergaard (1952), Davis and Selvadurai (1996), Podio-Guidugli and Favata (2014) and others. Material displacements are given by

$$\text{Radial:} \quad U_r = \frac{P_z}{4\pi GR}\left[\frac{rz}{R^2} - (1-2\mu)\frac{r}{R+z}\right] \tag{70}$$

$$\text{Circumferential:} \quad U_\theta = 0 \tag{71}$$

$$\text{Vertical:} \quad U_z = \frac{P_z}{4\pi GR}\left[\frac{z^2}{R^2} + 2(1-\mu)\right] \tag{72}$$

where $R = (r^2 + z^2)^{1/2}$ and G is the isotropic shear modulus. Displacements for a TILE material for this case, deduced from the paper by Liao and Wang (1998), are given by the equations in (a) in Table 2. Applying results from sheets H1–H3 in the online supplementary material gives

$$\frac{\lambda_i' R_i^*}{R_i} \simeq \frac{R^*}{R}\left[\mp\frac{1}{\varepsilon} + \left(\eta - \frac{1-2\mu}{2}\right) \pm O(\varepsilon)\right] \tag{73}$$

$$\frac{\lambda_i' m_i}{R_i} \simeq \frac{1}{R}\left[\mp\frac{1}{\varepsilon} + \left(\frac{\eta}{2} + 1 - \mu\right) + O(\varepsilon)\right] \tag{74}$$

with $\eta = z^2/R^2$, where $O(\varepsilon)$ represents terms of order ε and smaller. Here and below, the $\pm$ and $\mp$ signs are such that the upper sign is for $i = 1$ and the lower for $i = 2$. Consequently, the $1/\varepsilon$ terms cancel in the summations of (a) in Table 2. Taking the limit as $\varepsilon \to 0$ then gives

$$\text{Radial:} \quad U_r = \frac{-P_z}{4\pi G_{vh}}\left[\frac{2R^*}{R}\left(\eta - \frac{1-2\mu}{2}\right)\right] \tag{75}$$

$$\text{Vertical:} \quad U_z = \frac{-P_z}{4\pi G_{vh}}\left[\frac{2}{R}\left(\frac{\eta}{2} + 1 - \mu\right)\right] \tag{76}$$

and $U_\theta = 0$. Putting $\eta = z^2/R^2$ then gives Boussinesq (1878) equations, as required.

Horizontal loading

Cerruti (1884–1885) developed the solution for a point horizontal load on the surface of an FILE half-space. The solution is explored by Westergaard (1952), Davis and Selvadurai (1996), Podio-Guidugli and Favata (2014) and others. Material displacements are given in cylindrical coordinates by

$$\text{Radial:} \quad U_r = \frac{P_x \cos\theta}{4\pi GR}\left[1 + \frac{r^2}{R^2} + (1-2\mu)\frac{z}{R+z}\right] \tag{77}$$

$$\text{Circumferential:} \quad U_\theta = \frac{-P_x \sin\theta}{4\pi GR}\left[1 + (1-2\mu)\frac{R}{R+z}\right] \tag{78}$$

79. Vertical: $$U_z = \frac{P_x \cos\theta}{4\pi G R}\left[\frac{rz}{R^2} + (1-2\mu)\frac{r}{R+z}\right]$$

Displacements for a TILE material for this case are given by the equations in (a) in Table 3. Applying results from sheets H1–H3 in the online supplementary material gives

80. $$\lambda_i \frac{R_i^*}{R_i} = \frac{R^*}{R}\left[\pm\frac{1}{\varepsilon} + \left(1-\mu-\eta\right) + O(\varepsilon)\right]$$

81. $$\frac{\lambda_i}{m_i}\frac{z_i R_i^*}{R_i} = \frac{zR^*}{R}\left[\pm\frac{1}{\varepsilon} + \left(1-\mu+\frac{1-2\eta}{2}\right) \pm O(\varepsilon)\right]$$

82. $$\frac{\lambda_i}{m_i} R_i^* = R^*\left[\pm\frac{1}{\varepsilon} + \left(1-\mu-\frac{\eta}{2}\right) + O(\varepsilon)\right]$$

The $1/\eta$ terms cancel in the summations of (a) in Table 3. Taking the limit as $\eta \to 0$ then gives

83. Radial: $$U_r = \frac{P_x}{4\pi G_{\mathrm{vh}}}\left\{\left[\frac{2zR^*}{r^2 R}\left(1-\mu+\frac{1-2\eta}{2}\right)\right] + \frac{2}{u_3}\frac{R_3^*}{r^2}\right\}$$

84. Circumferential: $$U_\theta = \frac{P_x}{4\pi G_{\mathrm{vh}}}\left\{\left[\frac{2R^*}{rR}\left(1-\mu-\frac{\eta}{2}\right)\right] - \frac{2}{u_3}\frac{R_3^*}{r^2}\right\}$$

85. Vertical: $$U_z = \frac{P_x \cos\theta}{4\pi G_{\mathrm{vh}}}\left[\frac{2R^*}{rR}(1-\mu-\eta)\right]$$

Putting $\eta = z^2/R^2$ and setting $u_3 = 1$ for the FILE material (Equation 23) then gives the solution by Cerruti (1884–1885) for this case, as required.

Serendipitous result concerning accuracy

The preceding calculations can also be interpreted as an assessment of the consequences of a small inaccuracy in the assessment of the shear modulus G_{vh}. Now ε^2 appears in Equation 69, but only terms of order ε resulted in the penultimate equations after the terms involving $1/\varepsilon$ cancel. Hence, small errors can have larger effects. For example, an error of order $\varepsilon^2 = \pm 0.01$ in G_{vh} produces an error of order $\varepsilon = \pm 0.1$ in the final displacements. This suggests that, while Barden (1963) is correct that isotropy is a special case, an FILE material may also be singular in some sense.

Compliance factors for practical applications

Motivation

Davis and Selvadurai (1996) outlined how the solution by Boussinesq (1878) for point loads on an FILE half-space can be used to calculate displacements of loaded areas of ground or stiffnesses and interface stress distributions for rigid footings. Similar techniques can evidently be used with the point load solutions listed in Tables 2 and 3 for TILE materials. The concept of 'compliance factors' proposed in the following section is intended to facilitate these calculations.

Compliance factors: theory

Equations 72 and 71 and 79 and 78 gave the displacements respectively for the solution for a point load by Boussinesq (1878) and the solution for a horizontal load by Cerruti (1884–1885), both applied to the surface of the TILE half-space. The surface has $z = 0$, implying $R = r$ (Equation 42). Hence, for combined loading, displacements (u_r, u_θ, u_z) at a point (r, θ) on the surface can be expressed as

Table 4. Compliance factors for surface displacements

Factor	Description	FILE material	TILE material	
			General	Constant volume
C_{zz}	Vertical displacement due to vertical force	$1-\mu$	$-\frac{m_1\lambda_2 + m_2\lambda_1}{2}$	$\frac{1}{u_1^{\mathrm{u}} + u_2^{\mathrm{u}}}$
C_{zx}	Vertical displacement due to horizontal force	$\frac{1-2\mu}{2}$	$\frac{\lambda_1+\lambda_2}{2}$	0
C_{rz}	Radial displacement due to vertical force	$\frac{2\mu-1}{2}$	$-\frac{\lambda_1+\lambda_2}{2}$	0
C_{rx}	Radial displacement due to horizontal force	1	$\sqrt{\frac{G_{\mathrm{vh}}}{G_{\mathrm{hh}}}}$	$\sqrt{\frac{G_{\mathrm{vh}}}{G_{\mathrm{hh}}}}$
$C_{\theta z}$	Circumferential displacement due to vertical force	0	0	0
$C_{\theta x}$	Circumferential displacement due to horizontal force	$\mu-1$	$\frac{m_1\lambda_2 + m_2\lambda_1}{2m_1 m_2}$	$\frac{-1}{u_1^{\mathrm{u}} + u_2^{\mathrm{u}}}$

86. Vertical: $$u_z = \frac{1}{2\pi G_{\mathrm{vh}} r}(C_{zz}P_z + C_{zx}P_x \cos\theta)$$

87. Radial: $$u_r = \frac{1}{2\pi G_{\mathrm{vh}} r}(C_{rz}P_z + C_{rx}P_x \cos\theta)$$

88. Circumferential: $$u_\theta = \frac{1}{2\pi G_{\mathrm{vh}} r}(C_{\theta z}P_z + C_{\theta x}P_x \sin\theta)$$

where $G_{\mathrm{vh}} = G$ for the FILE material, and the compliance factors C_{ij} are deduced directly from the displacement equations and are listed in Table 4.

For any known loads on a surface, once the compliance factors are known, the preceding equations are all that are needed to determine surface displacements, by integration over the loaded area. Also, for any given displacements of a rigid footing, these equations and the interface friction conditions are all that are needed to determine interface stresses and overall footing stiffnesses. Details of what happens inside the half-space are not needed for such determinations, as long as the half-space is known to be either an FILE or a more general TILE material. Consequently, the factors may be of particular interest in calculations using the boundary-element method described by Brebbia (1978), Banerjee and Butterfield (1981), Katsikadelis (2016), Zhou *et al*. (2109) and others.

Undrained case

Using these results with the undrained results of Equation 68 gives $C^{\mathrm{u}}_{zx} = C^{\mathrm{u}}_{rz} = 0$. This implies that there is no interaction between vertical and lateral directions at the surface, which is also the case for an FILE material with μ = 1/2. Using Equations 65–68 gives

89. $$C^{\mathrm{u}}_{zz} = -\frac{m^{\mathrm{u}}_1\lambda^{\mathrm{u}}_2 + m^{\mathrm{u}}_2\lambda^{\mathrm{u}}_1}{2} = \frac{u^{\mathrm{u}}_1 - u^{\mathrm{u}}_2}{\sqrt{s^{\mathrm{u}2} - 4q^{\mathrm{u}}}}$$

Multiplying top and bottom on the right by $u^{\mathrm{u}}_1 + u^{\mathrm{u}}_2$ and using the undrained version of Equation 26 then gives the expression for the constant volume C^{u}_{zz} in Table 4. The result for follows from $m^{\mathrm{u}}_1 m^{\mathrm{u}}_2 = u^{\mathrm{u}2}_1 u^{\mathrm{u}2}_2$ and $u^{\mathrm{u}}_1 u^{\mathrm{u}}_2 = 1$.

Compliance factors: values for materials of Table 1

Figures 6(a)–6(c) show the values of three of the compliance factors for drained conditions for the data of Table 1. While some approximate trends are visible, there are no clear correlations. The values are mostly of the same order of magnitude as would be obtained for an FILE material with μ in the range 0–0.5. Figure 6(d) shows the directional coupling factor C_{zx} plotted vertically against C_{zz}. The line marked FILE is the relationship for FILE materials, and the data tend to cluster around this line. These results may suggest that an engineering approximation of TILE materials as FILE materials may not be too inaccurate as far as surface loading is concerned, provided an accurate estimate of G_{vh} is used.

Figure 6(e) shows values of C^{u}_{zz} plotted vertically against the undrained normal modulus ratio. The data for the saturated carbonates and for the coal seem to have similar trends. Figure 6(f) shows C^{u}_{zz} plotted against the drained value. The plot shows that $C^{\mathrm{u}}_{zz} < C_{zz}$ for all of the same of Table 1, indicating stiffer vertical responses in the undrained condition compared with those in the drained condition.

Discussion and concluding remarks

Achievements of this research

It has been well established that soils are anisotropic and that the form of anisotropy known as transverse isotropy is a common form. This paper has made use of the equations by Liao and Wang (1998) for TILE materials. These equations, together with advances in soil testing, have the potential to improve significantly the accuracy of geotechnical calculations for ground movements in small-strain linear elastic contexts.

Specifically, this paper has applied the equations by Liao and Wang (1998) to the special case of point loading on the surface of a TILE half-space. Many simplifications were achieved, making the results more accessible. Equations for the special case of undrained loading were also explored, showing that this is more complex than for fully isotropic materials. The present paper has not disagreed with the suggestion by Barden (1963) that isotropy is simply a special case of anisotropy, but it has also shown that fully isotropic material is in one sense a singular material.

Anyaegbunam (2014) tried to make the equations by Liao and Wang (1998) more accessible for vertical loading at any point below the surface of a TILE half-space. The present paper has hopefully made them accessible for vertical and lateral loadings at a point on the surface. The paper has clarified the physical meanings of symbols used by Liao and Wang (1998) for lateral loads and has identified (and avoided) a suspected error in one of their equations. Details are given in sheet E2 in the online supplementary material.

Practical applications of this research

For a linear elastic material, the effects of distributed loads over a surface can be calculated by suitable integration of effects of infinitesimal point loads. The results in Tables 2 and 3, and the associated compliance factors in Table 4, can be readily applied to such calculations for settlements and other ground movements for transversely isotropic soils. In particular, the compliance factors can be convenient for the boundary-element method. Results of such calculations would need to be interpreted within limitations outlined in the following.

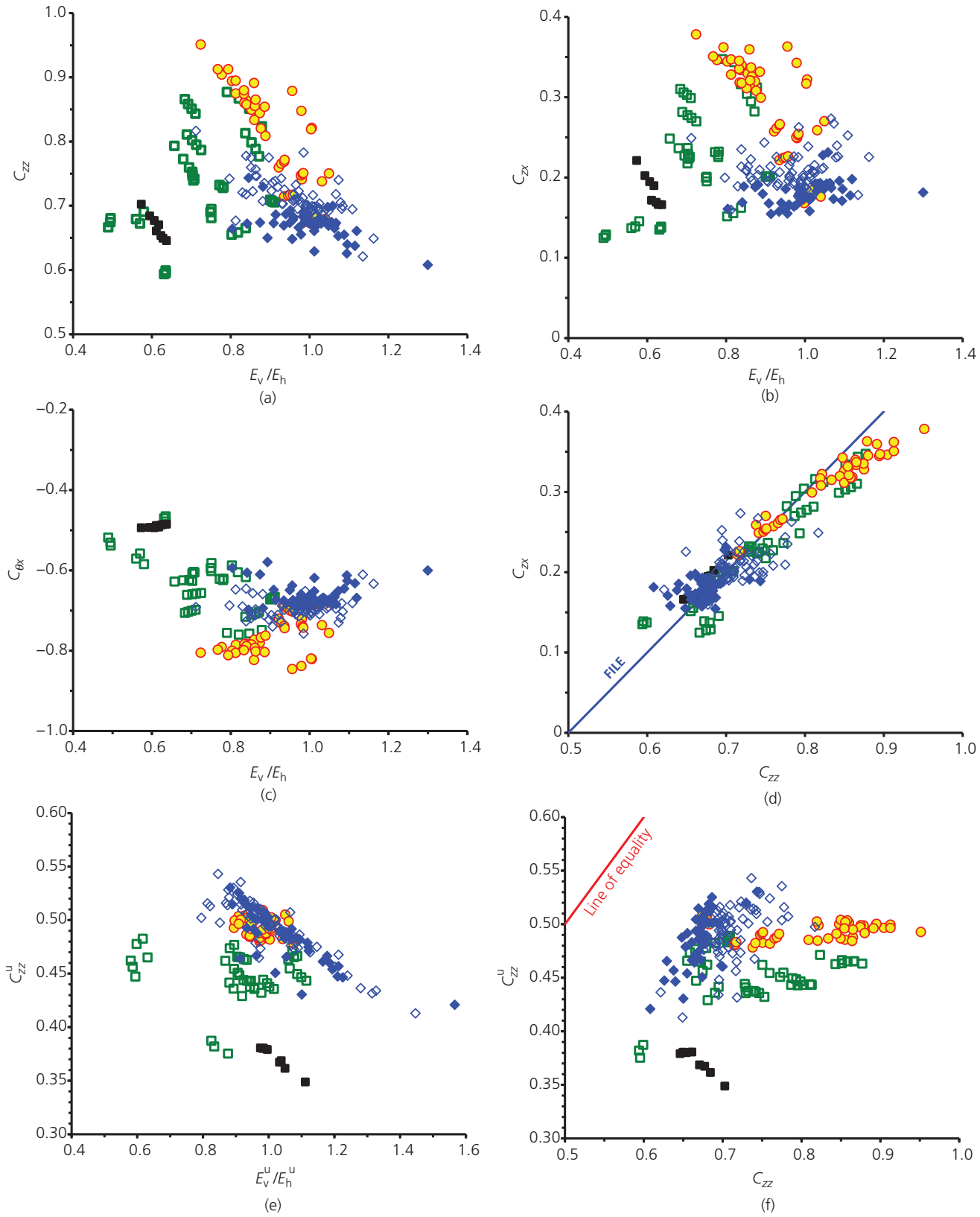

Figure 6. Compliance factors: (a–d) drained; (e) undrained; (f) compared. See Table 1 for data sources and key

It has been shown that small errors in shear modulus G_{vh} for materials close to fully isotropic can produce larger errors in displacement predictions. In agreement with Anyaegbunam (2014), the present calculations indicate that the proposed limit on G_{vh} by Raymond (1970) is invalid. This is also indicated by the data on soft rocks examined in the paper.

Limitations of this research

The primary practical limitations of the present work are that, firstly, the elastic properties of soils are not straightforward (Castellón and Ledesma, 2022; Jardine, 1992) and behaviour can be non-linear even at small strains (Atkinson, 2000; Houlsby *et al*., 2005). Consequently, elastic parameters must be selected carefully based on expected strain levels. The solutions here are limited to surface loading of a laterally and vertically uniform TILE half-space, with a flat surface and with the axis of material symmetry at right angles to the surface. More complex geometries exist, including layered soils and sloping strata. More complicated forms of anisotropy exist (Dean, 2019; Gibson, 1974).

Supplementary data availability

A supplementary file is available in PDF format as online supplementary material accompanying this article. The file presents calculations that support those in the main text and tables. All the data presented on figures in the paper are from tables in the paper by Wang (2002b). The bespoke Excel VBA software used to process the data for presentation here can be made available for research purposes by request to the author.

Appendix: shear moduli in standard triaxial tests

The purpose of this appendix is to determine the physical interpretations of the shear moduli G_{dtx} and G_{utx} of Equations 16 and 17.

The theory of the responses of TILE materials in the standard triaxial test are well documented – for example, in the papers by Barden (1963), Gibson (1974), Atkinson (1975), Graham and Houlsby (1983). If the axis of material symmetry of the sample aligned with the axial direction of the cell, then z corresponds to this direction and x and y are radial directions. Denoting changes in the axial and radial effective stresses as $\Delta\sigma_{ax}$ and $\Delta\sigma_{rad}$ and corresponding strains ε_{ax} and ε_{rad}, the compliance equation in Equation 1 for the TILE material then gives

$$90.\quad \begin{bmatrix} \varepsilon_{ax} \\ \varepsilon_{rad} \end{bmatrix} = \begin{bmatrix} \dfrac{1}{E_v} & \dfrac{-2\mu_{vh}}{E_v} \\ \dfrac{-\mu_{vh}}{E_v} & \dfrac{1-\mu_{hh}}{E_h} \end{bmatrix} \cdot \begin{bmatrix} \Delta\sigma_{ax} \\ \Delta\sigma_{rad} \end{bmatrix}$$

(e.g. Nishimura and Magalona (2020), with $\mu_{hv}/E_h = \mu_{vh}/E_v$). A change Δq in deviatoric stress, a volume strain ε_{vol} and a deviatoric strain ε_q can be defined as (e.g. Schofield and Wroth, 1968).

$$91.\quad \Delta q = \Delta\sigma_{ax} - \Delta\sigma_{rad}$$

$$92.\quad \varepsilon_{vol} = \varepsilon_{ax} + 2\varepsilon_{rad}$$

$$93.\quad \varepsilon_q = \frac{2}{3}(\varepsilon_{ax} - \varepsilon_{rad})$$

Graham and Houlsby (1983) showed that the change of deviator stress is related to strains as follows:

$$94.\quad \Delta q = J\varepsilon_{vol} + 3G^*\varepsilon_q$$

G^* can be expressed as in Equation 17. Hence, $G^* = G_{utx}$ is one-third of the slope of the plot of deviatoric stress against deviatoric strain in an undrained, constant-volume test. In a drained test with constant radial stress, volume strain occurs but $\Delta\sigma = 0$, and Equation 90 implies

$$95.\quad \varepsilon_q = \frac{\Delta q}{3G_{iso}}$$

where $G_{iso} = G_{dtx}$ is given by Equation 16. Hence, G_{dtx} is one-third of the slope of the plot of deviatoric stress against deviatoric strain in this drained (constant radial stress) type of test.

REFERENCES

Adhikari S, Mukhopadhyay T, Shaw A and Lavery NP (2020) Apparent negative values of Young's moduli of lattice materials under dynamic conditions. *International Journal of Engineering Science* **150**: article 103231, https://doi.org/10.1016/j.ijengsci.2020.103231.

Alkhalifah T and Tsvankin I (1995) Velocity analysis for transversely isotropic media. *Geophysics* **60(5)**: 1550–1566, https://doi.org/10.1190/1.1443888.

Almansi E (1899) Sull'integrazione dell'equazione differenziale $\Delta^2 n = 0$. *Annali di Matematica Pura ed Applicata* **2**: 1–51, https://doi.org/10.1007/BF02419286 (in Italian).

Anyaegbunam AJ (2014) Complete stresses and displacements in a cross-anisotropic half-space caused by a surface vertical point load. *International Journal of Geomechanics* **14(2)**: 171–181, https://doi.org/10.1061/(ASCE)GM.1943-5622.0000260.

Atkinson JH (1975) Anisotropic elastic deformation in laboratory tests on undisturbed London Clay. *Géotechnique* **25(2)**: 357–374, https://doi.org/10.1680/geot.1975.25.2.357.

Atkinson JH (2000) Non-linear soil stiffness in routine design. *Géotechnique* **50(4)**: 487–508, https://doi.org/10.1680/geot.2000.50.5.487.

Banerjee PK and Butterfield R (1981) *Boundary Element Methods in Engineering Science*. McGraw-Hill, New York, NY, USA.

Barden L (1963) Stresses and displacements in a cross-anisotropic soil. *Géotechnique* **13(3)**: 198–210, https://doi.org/10.1680/geot.1963.13.3.198.

Boussinesq J (1878) Équilibre d'élasticité d'un solide isotrope sans pesanteur, supportant différents poids. *Comptes Rendus de l'Académie des Sciences Paris* **86**: 1260–1263 (in French).

Bowles JE (1996) *Foundation Analysis and Design*. McGraw-Hill, New York, NY, USA.

Brebbia CA (1978) *The Boundary Element Method for Engineers*. Pentech Press, London, UK.

Carter J (2023) 61st Rankine Lecture: constitutive modelling in computational geomechanics. *YouTube,* 15 March. See https://www.youtube.com/watch?v=0DGS3yp3vFI (accessed 31/03/2023).

Casagrande A and Carillo N (1944) Shear failure of anisotropic materials. *Proceedings of the Boston Society of Civil Engineers* **31**: 74–87.

Cassidy MJ, Martin CM and Houlsby GT (2004) Development and application of force resultant models describing jack-up foundation behaviour. *Marine Structures* **17(3–4)**: 165–193, https://doi.org/10.1016/j.marstruc.2004.08.002.

Castellón J and Ledesma A (2022) Small strains in soil constitutive modelling. *Archive of Computational Methods in Engineering* **29(5)**: 3223–3280, https://doi.org/10.1007/s11831-021-09697-1.

Cerruti V (1884–1885) Sulla defromazione di uno strato isótropo indefinito limitado da due piani paralleli. *Atti dell'Accademia Nazionale dei Lincei Serie 4* **1**: 521–522 (in Italian).

Das BM (2009) *Shallow Foundations: Bearing Capacity and Settlement*. CRC Press, Boca Raton, FL, USA.

Davis RO and Selvadurai APS (1996) *Elasticity and Geomechanics*. Cambridge University Press, Cambridge, UK.

Dean ETR (2009) *Offshore Geotechnical Engineering: Principles and Practice*. ICE Publishing, London, UK.

Dean ETR (2019) Soil hinges: macroscopic evidence and modeling considerations. *International Journal of Geomechanics* **19(10)**, https://doi.org/10.1061/(ASCE)GM.1943-5622.0001481.

Dyvik R, Berre T, Lacasse S and Raadim B (1987) Comparison of truly undrained and constant volume direct simple shear tests. *Géotechnique* **37(1)**: 3–10, https://doi.org/10.1680/geot.1987.37.1.3.

Ferrar WL (1941) *Algebra - A Textbook Of Determinants, Matrices and Algebraic Forms*. Oxford University Press, Oxford, UK, pp. 138–141.

Fioravante V, Giretti D and Jamiolkowski M (2013) Small strain stiffness of carbonate Kenya sand. *Engineering Geology* **161**: 65–80, https://doi.org/10.1016/j.enggeo.2013.04.006.

Gazetas G (1981) Importance of soil anisotropy on foundation displacement functions. *Proceedings of the 1st International Conference on Recent Advances in Geotechnical Earthquake Engineering and Soil Dynamics, St Louis, MO, USA*, pp. 1029–1046.

Gerrard CM and Wardle IJ (1973) *Solutions for Point loads and Generalized Circular Loads Applied to a Cross Anisotropic Half-space*. Division of Applied Geomechanics, Commonwealth Scientific and Industrial Research Organisation, Sydney, Australia, Technical Paper 13.

Gibson RE (1974) The analytical method in soil mechanics. *Géotechnique* **24(2)**: 115–140, https://doi.org/10.1680/geot.1974.24.2.115.

Graham J and Houlsby GT (1983) Anisotropic elasticity of a natural clay. *Géotechnique* **33(2)**: 165–180, https://doi.org/10.1680/geot.1983.33.2.165.

Gu X, Li Y, Hu J *et al.* (2022) Elastic shear stiffness anisotropy and fabric anisotropy of natural clays. *Acta Geotechnica* **17(8)**: 3229–3243, https://doi.org/10.1007/s11440-022-01468-x.

Holl DL (1941) *Plane Strain Distribution of Stress in Elastic Media*. Iowa Engineering Department Station, Iowa State College, Ames, IA, USA. Bulletin 48.

Houlsby GT, Amorosi A and Rojas E (2005) Elastic moduli of soils dependent on pressure: a hyperelastic formulation. *Géotechnique* **55(5)**: 383–392, https://doi.org/10.1680/geot.2005.55.5.383.

Jardine RJ (1992) Some observations on the kinematic nature of soil stiffness. *Soils and Foundations* **32(2)**: 111–124, https://doi.org/10.3208/sandf1972.32.2_111.

Katsikadelis JT (2016) *The Boundary Element Method for Engineers and Scientists*. Academic Press, London, UK.

Kearey P, Brooks M and Hill I (2002) *An Introduction to Geophysical Exploration*. Blackwell Science, Chichester, UK.

Kearey P, Klepeis KA and Vine FJ (2009) *Global Tectonics*. Wiley-Blackwell, Hoboken, NJ, USA.

Knappett JA and Craig RF (2012) *Craig's Soil Mechanics*. Spon Press, London, UK.

Kramer SL (1996) *Geotechnical Earthquake Engineering*. Prentice-Hall, Upper Saddle River, NJ, USA.

Kuwano B (1999) *The Stiffness and Yielding Anisotropy of Sand*. PhD thesis, University of London, Imperial College of Science, Technology and Medicine, London, UK.

Liao JJ and Wang CD (1998) Elastic solutions for a transversely isotropic half-space subjected to a point load. *International Journal for Numerical and Analytical Methods in Geomechanics* **22(6)**: 425–447, https://doi.org/10.1002/(SICI)1096-9853(199806)22:6%3C425::AID-NAG925%3E3.0.CO;2-H.

Lings ML (2001) Drained and undrained anisotropic elastic stiffness parameters. *Géotechnique* **51(6)**: 555–565, https://doi.org/10.1680/geot.2001.51.6.555.

Lings ML, Pennington DS and Nash DFT (2000) Anisotropic stiffness parameters and their measurement in a stiff natural clay. *Géotechnique* **50(2)**: 109–125, https://doi.org/10.1680/geot.2000.50.2.109.

Liu T, Ushev ER and Jardine RJ (2020) Anisotropic stiffness and shear strength characteristics of a stiff glacial till. *Journal of Geotechnical and Geoenvironmental Engineering* **146(12)**: article 04020137, https://doi.org/10.1061/(ASCE)GT.1943-5606.0002387.

Love AEH (1927) *A Treatise on the Mathematical Theory of Elasticity*. Cambridge University Press, Cambridge, UK.

Marmo F, Sessa S, Valana N, De Gregario D and Rosati L (2020) Complete solutions of three-dimensional problems in transversely isotropic media. *Continuum Mechanics and Thermodynamics* **32(3)**: 775–802, https://doi.org/10.1007/s00161-018-0733-8.

Mašín D and Rott J (2014) Small strain stiffness anisotropy of natural sedimentary clays: review and a model. *Acta Geotechnica* **9(2)**: 299–312, https://doi.org/10.1007/s11440-013-0271-2.

Mitchell JH (1900) The stress distribution in an ælotropic solid with an infinite plane boundary. *Proceedings of the London Mathematical Society* **s1-32(1)**: 247–258, https://doi.org/10.1112/plms/s1-32.1.247.

Newmark NM (1935) *Simplified Computation of Vertical Pressures in Elastic Foundations*. Engineering Experiment Station, University of Illinois, Champaign, IL, USA, Circular 24.

Nishimura S and Magalona F (2020) An alternative method in triaxial tests to obtain cross-anisotropic elastic parameters. *Géotechnique Letters* **10(3)**: 468–477, https://doi.org/10.1680/jgele.20.00031.

Onsager L (1931) Reciprocal relations in irreversible processes. I. *Physical Review* **37(4)**: 405–426, https://doi.org/10.1103/PhysRev.37.405.

Pegah E, Liu H and Gholami A (2021) Estimating drained cross-anisotropic elastic parameters in saturated clays using undrained properties. *Engineering Geology* **293**: article 106340, https://doi.org/10.1016/jenggeo.2021.106340.

Pickering DJ (1970) Anisotropic elastic parameters for soil. *Géotechnique* **20(3)**: 271–276, https://doi.org/10.1680/geot.1970.20.3.271.

Podio-Guidugli P and Favata A (2014) *Elasticity for Geotechnicians: A Modern Exposition of Kelvin, Boussinesq, Flamant, Cerruti, Melan, and Mindlin Problems*. Springer, Cham, Switzerland.

Randolph MF and Gourvenec S (2011) *Offshore Geotechnical Engineering*. CRC Press, Boca Raton, FL, USA.

Ratananikom W, Likitlersuang S and Yimsiri S (2013) An investigation of anisotropic elastic parameters of Bangkok Clay from vertical and horizontal cut specimens. *Geomechanics and Geoengineering* **8(1)**: 15–27, https://doi.org/10.1080/17486025.2012.726746.

Raymond GP (1970) Discussion: Stresses and displacements in a cross-anisotropic soil. *Géotechnique* **20(4)**: 456–458, https://doi.org/10.1680/geot.1970.20.4.456.

Sadek T, Lings M, Dihoru L and Muir Wood D (2007) Wave transmission in Hostun sand: multiaxial experiments. *Rivista Italiana di Geotecnica* **2**: 69–84.

Schofield AN and Wroth CP (1968) *Critical State Soil Mechanics*. McGaw-Hill, New York, NY, USA.

Shi J, Haegeman W and Cnudde V (2021) Anisotropic small-strain stiffness of calcareous sand affected by sample preparation, particle characteristic and gradation. *Géotechnique* **71(4)**: 305–319, https://doi.org/10.1680/jgeot.18.P.348.

Simpson B (2017) Anisotropic linear elastic materials subject to undrained plane strain deformation. *Géotechnique* **67(6)**: 728–732, https://doi.org/10.1680/jgeot.16.P.057.

Spencer AJM (1980) *Continuum Mechanics*. Dover Publications, Garden City, NY, USA.

Srbulov M and O'Brien AS (2012) Foundations subjected to cyclic and dynamic loads. In *ICE Manual of Geotechnical Engineering* (Burland J, Chapman T, Skinner H and Brown M (eds)). ICE Publishing, London, UK, vol. 2, pp. 939–953.

Thomsen L (1986) Weak elastic anisotropy. *Geophysics* **51(10)**: 1954–1966, https://doi.org/10.1190/1.1442051.

Tsvankin I and Thomsen L (1994) Nonhyperbolic reflection moveout in anisotropic media. *Geophysics* **59(8)**: 1290–1304, https://doi.org/10.1190/1.1443686.

Wang Z (2002a) Seismic anisotropy in sedimentary rocks, part 1 a single-plug laboratory method. *Geophysics* **67(5)**: 1415–1422, https:/doi.org/10.1190/1.1512787.

Wang Z (2002b) Seismic anisotropy in sedimentary rocks, part 2 laboratory data. *Geophysics* **67(5)**: 1423–1440, https://doi.org/10.1190/1.1512743.

Wang CD (2003) Displacements and stresses due to vertical subsurface loading for a cross-anisotropic half-space. *Soils and Foundations* **43(5)**: 41–52, https://doi.org/10.3208/sandf.43.5_41.

Wang CD (2005) Lateral stress caused by horizontal and vertical surcharge strip loads on a cross-anisotropic backfill. *International Journal for Numerical and Analytical Methods in Geomechanics* **29(14)**: 1341–1361, https://doi.org/10.1002/nag.462.

Wang CD and Liao JJ (2002) Elastic solutions of displacements for a transversely isotropic half-space subjected to three-dimensional buried parabolic rectangular loads. *International Journal of Solids and Structures* **39(18)**: 4805–4824, https://doi.org/10.1016/S0020-7683(02)00370-0.

Wang CD and Pan E (2004) Stresses due to vertical subsurface loading for an inhomogeneous cross-anisotropic half-space. *Numerical and Analytical Methods in Geomechanics* **28(12)**: 1233–1255, https://doi.org/10.1002/nag.385.

Wang CD, Chen MT and Lee TC (2008) Surface displacements due to batter piles driven in cross-anisotropic media. *International Journal for Numerical and Analytical Methods in Geomechanics* **32(2)**: 121–141, https://doi.org/10.1002/nag.612.

Wang J, Zhang F and Yang Z (2019) Anisotropy in small-strain shear nodulus of permafrost at rising temperatures. *Cold Regions Science and Technology* **160**: 1–12, https://doi.org/10.1016/j.coldregions.2019.01.003.

Westergaard HM (1952) *Theory of Elasticity and Plasticity*. Harvard University Press, Cambridge, MA, USA.

Zhou W, Yue Q, Wang Q, Feng YT and Chang X (2019) The boundary element method for elasticity problems with concentrated loads based on displacement singular elements. *Engineering Analysis with Boundary Elements* **99**: 195–205, https://doi.org/10.1016/j.enganabound.2018.11.016.

Zuo L, Xu L, Baudet BA, Gao C and Huang C (2022) Small-strain shear stiffness anisotropy of a saturated clayey loess. *Géotechnique*, https://doi.org/10.1680/jgeot.21.00179.

How can you contribute?

To discuss this paper, please submit up to 500 words to the editor at journals@ice.org.uk. Your contribution will be forwarded to the author(s) for a reply and, if considered appropriate by the editorial board, it will be published as a discussion in a future issue of the journal.

Closed form solutions for a transversely isotropic linear linear elastic half-space loaded at a point on its surface

By E.T.R.Dean[1], richard.dean@caribgeo.com, November 2022

[1] Caribbean Geotechnical Design SL (Spain)

Supplement

Aim and Organization

This Supplement provides calculations that provide detailed support for results given in the main text.

The calculations are presented on Calculation sheets organized in groups as follows:

Group	Contents	No. of sheets
A	Algebra: Simplifications and useful identities	4
B	Displacements and Compliance factors	7
C	Strains	7
D	Changes of stress and surface checks	9
E	Checks on calculated changes of stress	2
F	Equilibrium in the TILE half-space	5
G	Interpretation of Point Loads	4
H	Limiting case of a FILE material	5

Reference

Liao JJ and Wang CD (1998). Elastic solutions for a transversely isotropic half-space subjected to a point load. *International Journal for Numerical and Analytical Methods in Geomechanics* 22, 425-447

Aim

The aim of the Group A calculation sheets is to provide some generally useful algebra that can simplify some of the equations used in the present paper based on Liao and Wang's (1998) general results.

Variables *k* and *T*

This sheet A1 starts by looking at a variable k defined by Liao and Wang (1998) as follows, and having units of inverse modulus:

$$k = \frac{A_{13} + A_{44}}{A_{33}A_{44}\left(u_1^2 - u_2^2\right)} \tag{A1.1}$$

Liao and Wang (1998) also defined four T values:

$$T_1 = \frac{k}{m_1}\frac{u_1 + u_2}{u_2 - u_1} \qquad T_2 = \frac{k}{m_2}\frac{2u_1\left(u_2 + m_2\right)}{\left(u_2 - u_1\right)\left(u_1 + m_1\right)} \tag{A1.2,3}$$

$$T_3 = \frac{k}{m_1}\frac{2u_2\left(u_1 + m_1\right)}{\left(u_2 - u_1\right)\left(u_2 + m_2\right)} \qquad T_4 = \frac{k}{m_2}\frac{u_1 + u_2}{u_2 - u_1} \tag{A1.4,5}$$

The general result $u_1u_2 = m_1m_2$ is derived in the main text. Using it to compare T_2 and T_3, and comparing T_1 and T_4, gives:

$$m_1T_1 = k\frac{u_1 + u_2}{u_2 - u_1} = m_2T_4 \qquad T_2 = \frac{2k}{u_2 - u_1} = T_3 \tag{A1.6,7}$$

Other useful relations include:

$$m_1T_1 - m_2T_2 + k = \frac{2k\left(u_2 - m_2\right)}{u_2 - u_1} \qquad m_1T_3 - m_2T_4 + k = \frac{-2k\left(u_1 - m_1\right)}{u_2 - u_1} \tag{A1.8,9}$$

$$T_1 - T_2 - \frac{k}{m_1} = \frac{2k\left(u_1 - m_1\right)}{m_1\left(u_2 - u_1\right)} \qquad T_3 - T_4 - \frac{k}{m_2} = \frac{-2k\left(u_2 - m_2\right)}{m_2\left(u_2 - u_1\right)} \tag{A1.10,11}$$

Further aspects of these expressions are on sheet B1.

Liao and Wang (1998) defined five adjusted depth coordinates associated with letter subscripts. These depend on the depth h at which the point loads are applied. For h=0 the definitions, which are the first expressions in each equation below, simplify as follows:

$$z_a = u_1(z+h) = u_1 z = z_1 \tag{A2.1}$$

$$z_b = u_1 z + u_2 h = u_1 z = z_1 \tag{A2.2}$$

$$z_c = u_1 h + u_2 z = u_2 z = z_2 \tag{A2.3}$$

$$z_d = u_2(z+h) = u_2 z = z_2 \tag{A2.4}$$

$$z_e = u_3(z+h) = u_3 z = z_3 \tag{A2.5}$$

There were five associated adjusted distances, which simplify as follows:

$$R_a = \sqrt{r^2 + z_a^2} = \sqrt{r^2 + z_1^2} = R_1 \tag{A2.6}$$

$$R_b = \sqrt{r^2 + z_b^2} = \sqrt{r^2 + z_1^2} = R_1 \tag{A2.7}$$

$$R_c = \sqrt{r^2 + z_c^2} = \sqrt{r^2 + z_2^2} = R_2 \tag{A2.8}$$

$$R_d = \sqrt{r^2 + z_d^2} = \sqrt{r^2 + z_2^2} = R_2 \tag{A2.9}$$

$$R_e = \sqrt{r^2 + z_e^2} = \sqrt{r^2 + z_3^2} = R_3 \tag{A2.10}$$

There were five associated modified distances, which simplify as follows:

$$R_a^* = R_a - z_a = R_1 - z_1 = R_1^* \tag{A2.11}$$

$$R_b^* = R_b - z_b = R_1 - z_1 = R_1^* \tag{A2.12}$$

$$R_c^* = R_c - z_c = R_2 - z_2 = R_2^* \tag{A2.13}$$

$$R_d^* = R_d - z_d = R_2 - z_2 = R_2^* \tag{A2.14}$$

$$R_e^* = R_e - z_e = R_3 - z_3 = R_3^* \tag{A2.15}$$

Liao and Wang (1998) defined the key geometrical variables, $z_i = u_i z$, $R_i = \sqrt{r^2 + z_i^2}$ and $R_i^* = R_i - z_i$. Differentiating these gives:

$$\frac{\partial z_i}{\partial r} = 0 \qquad \frac{\partial z_i}{\partial z} = u_i \qquad \text{(A3.1,2)}$$

$$\frac{\partial R_i}{\partial r} = \frac{r}{R_i} \qquad \frac{\partial R_i}{\partial z} = \frac{u_i z_i}{R_i} \qquad \text{(A3.3,4)}$$

$$\frac{\partial R_i^*}{\partial r} = \frac{r}{R_i} \qquad \frac{\partial R_i^*}{\partial z} = \frac{-u_i R_i^*}{R_i} \qquad \text{(A3.5,6)}$$

Other useful differentials are:

$$\frac{\partial}{\partial r}\left(\frac{R_i^*}{rR_i}\right) = \frac{z_i}{R_i^3} - \frac{R_i^*}{r^2 R_i} \qquad \frac{\partial}{\partial z}\left(\frac{R_i^*}{rR_i}\right) = \frac{-u_i r}{R_i^3} \qquad \text{(A3.7,8)}$$

$$\frac{\partial}{\partial r}\left(\frac{1}{R_i}\right) = \frac{-r}{R_i^3} \qquad \frac{\partial}{\partial z}\left(\frac{1}{R_i}\right) = \frac{-u_i z_i}{R_i^3} \qquad \text{(A3.9,10)}$$

$$\frac{\partial}{\partial r}\left(\frac{z_i R_i^*}{r^2 R_i}\right) = \frac{z_i^2}{rR_i^3} - \frac{2z_i R_i^*}{r^3 R_i} \qquad \frac{\partial}{\partial z}\left(\frac{z_i R_i^*}{r^2 R_i}\right) = \frac{u_i R_i^*}{r^2 R_i} - \frac{u_i z_i}{R_i^3} \qquad \text{(A3.11,12)}$$

$$\frac{\partial}{\partial r}\left(\frac{R_i}{r^2}\right) = \frac{1}{rR_i} - \frac{2R_i}{r^3} \qquad \frac{\partial}{\partial z}\left(\frac{R_i}{r^2}\right) = \frac{u_i z_i}{r^2 R_i} \qquad \text{(A3.13,14)}$$

$$\frac{\partial}{\partial r}\left(\frac{R_i^*}{r^2}\right) = \frac{1}{rR_i} - \frac{2R_i^*}{r^3} \qquad \frac{\partial}{\partial z}\left(\frac{R_i^*}{r^2}\right) = \frac{-u_i R_i^*}{r^2 R_i} \qquad \text{(A3.15,16)}$$

Some useful identities are:

$$\frac{R_i^*}{r^3} - \frac{z_i R_i^*}{r^3 R_i} = \frac{R_i^{*2}}{r^3 R_i} \qquad \frac{z_i R_i^*}{r^3 R_i} + \frac{R_i^*}{r^3} = \frac{1}{rR_i} \qquad \text{(A3.17,18)}$$

$$\frac{2R_i^*}{r^3} - \frac{1}{rR_i} = \frac{R_i^{*2}}{r^3 R_i} \qquad \frac{z_i R_i^*}{r^3 R_i} + \frac{R_i^*}{r^3} - \frac{z_i^2}{rR_i^3} = \frac{r}{R_i^3} \qquad \text{(A3.19,20)}$$

$$\frac{2z_i R_i^*}{r^3 R_i} - \frac{z_i^2}{rR_i^3} = \frac{r}{R_i^3} - \frac{R_i^{*2}}{r^3 R_i} \qquad \text{(A3.21,22)}$$

Liao and Wang (1998) gave the general solution of the characteristic equation for u_i^2, and they identified three cases depending on s^2-4q. The general solution is:

$$u_i^2=\frac{1}{2}\left(s\pm\sqrt{s^2-4q}\right) \tag{A4.1}$$

Case 31 is with s^2-4q positive, in which case the solutions for u_1^2 and u_2^2 are both real numbers. Three sub-cases might be imagined:

Case 1a : s is positive, in which case its magnitude will be greater than the magnitude of the positive root $\sqrt{s^2-4q}$. In this case, both u_1^2 and u_2^2 are positive real numbers

Case 1b : s is zero, or is negative with a magnitude less than $\sqrt{s^2-4q}$. In this case one of u_1^2 or u_2^2 would be positive while the other would be negative

Case 1c: s is negative and with magnitude greater than $\sqrt{s^2-4q}$, making both u_1^2 or u_2^2 negative

Cases 1b and 1c were not explicitly explored by Liao and Wang (1998), but the following argument shows that they are impossible. Using equations from the main text to calculate s^2-4q in terms of Young's and shear moduli, and using the equation for Δ_2 to substitute for μ_{vh}^2, gives

$$s^2-4q=L_1-8\frac{G_{hh}}{E_v}\left(\frac{\Delta_2 E_h}{\left(1-\mu_{hh}\right)^2}+1\right) \tag{A4.2}$$

$$L_1=\frac{2}{1-\mu_{hh}}\frac{G_{hh}}{G_{vh}}\left(2s-\frac{G_{hh}}{G_{vh}}\right) \tag{A4.3}$$

Hence if s is zero or negative, s^2-4q is also negative. This implies that there are no solution cases with one of u_i^2 is real while the other is complex. Hence Liao and Wang's (1998) three cases may be further detailed as follows:

Case 1	$s^2-4q>0$	u_1 and u_2 are both real, and positive
Case 2	$s^2-4q=0$	$u_1=u_2$. See Sheets in Group H for an example of this degenerate case
Case 3	s^2-4q	u_1 and u_2 are complex conjugates

Aim

The purpose of the Group B of Calculation sheets is to develop, starting from Liao and Wang's (1998) general equations, expressions for material displacements for the particular simple case of surface loading that is considered in the present paper. These results also allow compliance factors to be inferred.

Variables k' and λ

The following are some variables which, while possibly being of more general use, are particularly helpful for these special cases. With reference to sheet A1, it is convenient to define Liao and Wang's k in terms of a dimensionless k' as follows:

$$k = \frac{k'}{G_{vh}} \quad \text{with} \quad k' = \frac{A_{13} + A_{44}}{A_{33}\left(u_1^2 - u_2^2\right)} \tag{B1.1,2}$$

It is also convenient to define some values λ and swapped values λ' as follows:

$$\lambda_1 = \lambda_2' = \lambda_0\left(u_1 - m_1\right) \tag{B1.3}$$

$$\lambda_2 = \lambda_1' = \lambda_0\left(u_2 - m_2\right) \tag{B1.4}$$

$$\lambda_0 = \frac{2k'}{u_2 - u_1} \tag{B1.5}$$

Then the useful expressions of Sheet A1 can be re-expressed as:

$$m_1 T_1 - m_2 T_2 + k = \frac{\lambda_2}{G_{vh}} \qquad m_1 T_3 - m_2 T_4 + k = \frac{-\lambda_1}{G_{vh}} \tag{B1.6,7}$$

$$T_1 - T_2 - \frac{k}{m_1} = \frac{\lambda_1}{m_1 G_{vh}} \qquad T_3 - T_4 - \frac{k}{m_2} = \frac{-\lambda_2}{m_2 G_{vh}} \tag{B1.8,9}$$

Closed form solutions for a transversely isotropic linear elastic half-space loaded at a point on its surface	**Radial displacements due to vertical point load on the surface**	Sheet B2

Displacements

Radial displacements due to the surface vertical point load may be inferred from Liao and Wang's (1998) equations 47 and 73. Putting $P_r = P_\theta = 0$ gives:

$$U_r' = \frac{P_z}{4\pi}\left[\mp k\left(\frac{R_1^*}{rR_1} - \frac{R_2^*}{rR_2}\right)\right] \tag{B2.1}$$

$$U_r = U_r' + \frac{P_z}{4\pi}\left\{-m_1\left[T_1\frac{R_a^*}{rR_a} - T_3\frac{R_c^*}{rR_c}\right] + m_2\left[T_2\frac{R_b^*}{rR_b} - T_4\frac{R_d^*}{rR_d}\right]\right\} \tag{B2.2}$$

In the first equation, the upper sign is for $z > 0$. Using the simplification associated with surface loads (Sheet A2) to simplify the second equation gives:

$$U_r = U_r' + \frac{P_z}{4\pi}\left\{-\left(m_1T_1 - m_2T_2\right)\frac{R_1^*}{rR_1} + \left(m_1T_3 - m_2T_4\right)\frac{R_2^*}{rR_2}\right\} \tag{B2.3}$$

Using equation B2.1 to substitute for U_r' gives:

$$U_r = \frac{P_z}{4\pi}\left\{-\left(m_1T_1 - m_2T_2 + k\right)\frac{R_1^*}{rR_1} + \left(m_1T_3 - m_2T_4 + k\right)\frac{R_2^*}{rR_2}\right\} \tag{B2.4}$$

Using the simplified equations for T_i (Sheet B1) and the swapped λ-values on that sheet gives:

$$U_r = \frac{P_z}{4\pi G_{vh}}\sum_{i=1}^{2}\left(-\lambda_i'\frac{R_i^*}{rR_i}\right) \tag{B2.5}$$

Compliance factor

At the surface, $R_i^* / R_i = 1$, and the above equation implies the radial displacement is:

$$U_r\left(z=0\right) = \frac{P_z}{2\pi G_{vh}}C_{rz} \quad \text{with} \quad C_{rz} = -\left(\frac{\lambda_1 + \lambda_2}{2}\right) \tag{B2.6}$$

Done by and date	Checked by and date	Printed on
ETRD November 2022		Wednesday, 30 November 2022, 01:13

Displacements

Circumferential displacements due to the point vertical load may be inferred from Liao and Wang's (1998) equations 48 and 74. Putting $P_r = P_x$ and $P_z = P_\theta = 0$ gives:

$$U'_\theta = 0 \tag{B3.1}$$

$$U_\theta = U'_\theta + 0 \tag{B3.2}$$

This follows direction from the rotational symmetry about the vertical axis.:

Compliance factor

At the surface, the above results imply that the circumferential displacement is zero:

$$U_\theta(z=0) = \frac{P_z}{2\pi G_{vh}} C_{\theta z} \quad \text{with} \quad C_{\theta z} = 0 \tag{B3.3}$$

Closed form solutions for a transversely isotropic linear elastic half-space loaded at a point on its surface	**Vertical displacements due to vertical point load on the surface**	Sheet B4

Displacements

Vertical displacements due to the vertical point load may be inferred from Liao and Wang's (1998) equations 49 and 75. Putting $P_r = P_\theta = 0$ gives:

$$U_z' = \frac{P_z}{4\pi}\left[-k\left(\frac{m_1}{R_1} - \frac{m_2}{R_2}\right)\right] \tag{B4.1}$$

$$U_z = U_z' + \frac{P_z}{4\pi}\left\{-m_1\left[\frac{m_1 T_1}{R_a} - \frac{m_2 T_2}{R_b}\right] + m_2\left[\frac{m_1 T_3}{R_c} - \frac{m_2 T_4}{R_d}\right]\right\} \tag{B4.2}$$

In the first equation, the upper sign is for z>0 (downwards into the half-space). Using the simplification associated with surface loads (Sheet A2) to simplify the second equation gives:

$$U_z = U_z' + \frac{P_z}{4\pi}\left\{-m_1\frac{m_1 T_1 - m_2 T_2}{R_1} + m_2\frac{m_1 T_3 - m_2 T_4}{R_2}\right\} \tag{B4.3}$$

Using equation B4.1 to substitute for U_z' gives:

$$U_z = \frac{P_z}{4\pi}\left\{-m_1\frac{m_1 T_1 - m_2 T_2 + k}{R_1} + m_2\frac{m_1 T_3 - m_2 T_4 + k}{R_2}\right\} \tag{B4.4}$$

Using the simplified equations for T_i (Sheet B1) and the definitions there of swapped λ's gives:

$$U_z = \frac{P_z}{4\pi G_{vh}}\sum_{i=1}^{2}\left(-\frac{m_i \lambda_i'}{R_i}\right) \tag{B4.5}$$

Compliance factor

At the surface, $R_i = r$, and the above equation implies that the vertical displacement is:

$$U_z(z=0) = \frac{P_z}{2\pi G_{vh}} C_{zz} \quad \text{with} \quad C_{zz} = -\left(\frac{m_2\lambda_1 + m_1\lambda_2}{2}\right) \tag{B4.6}$$

Done by and date	Checked by and date	Printed on
ETRD November 2022		Wednesday, 30 November 2022, 01:15

Displacements

Radial displacements were given in Liao and Wang's (1998) equations 47 and 73. Putting $P_r = P_x$ and $P_z = P_\theta = 0$ gives:

$$U_r' = \frac{P_x \cos\theta}{4\pi}\left[k\left(\frac{z_1 R_1^*}{m_1 r^2 R_1} - \frac{z_2 R_2^*}{m_2 r^2 R_2} \right) + \frac{1}{u_3 A_{44}} \frac{R_3^*}{r^2} \right] \tag{B5.1}$$

$$U_r = U_r' + \frac{P_x \cos\theta}{4\pi}\left[-T_1 \frac{z_a R_a^*}{r^2 R_a} + T_2 \frac{z_b R_b^*}{r^2 R_b} + T_3 \frac{z_c R_c^*}{r^2 R_c} - T_4 \frac{z_d R_d^*}{r^2 R_d} + \frac{1}{u_3 A_{44}} \frac{R_e^*}{r^2} \right] \tag{B5.2}$$

Using the simplification associated with surface loads (Sheet A2) to simplify the second equation gives:

$$U_r = U_r' + \frac{P_x \cos\theta}{4\pi}\left[\left(T_2 - T_1\right) \frac{z_1 R_1^*}{r^2 R_1} + \left(T_3 - T_4\right) \frac{z_2 R_2^*}{r^2 R_2} + \frac{1}{u_3 A_{44}} \frac{R_3^*}{r^2} \right] \tag{B5.3}$$

Using equation B5.1 to substitute for U_r' gives:

$$U_r = \frac{P_x \cos\theta}{4\pi}\left[\left(T_2 - T_1 + \frac{k}{m_1} \right) \frac{z_1 R_1^*}{r^2 R_1} + \left(T_3 - T_4 - \frac{k}{m_2} \right) \frac{z_2 R_2^*}{r^2 R_2} + \frac{2}{u_3 A_{44}} \frac{R_3^*}{r^2} \right] \tag{B5.4}$$

Using the simplified equations for the T_i groups (Sheet A3) gives:

$$U_r = \frac{P_x \cos\theta}{4\pi G_{vh}}\left[\sum_{i=1}^{2} \left(-\frac{\lambda_i}{m_i} \frac{z_i R_i^*}{r^2 R_i} \right) + \frac{2}{u_3} \frac{R_3^*}{r^2} \right] \tag{B5.5}$$

Compliance factor

At the surface, $z_i = 0$, the sum term is zero, and $R_i^* / R_i = 1$, and the above equation implies that radial displacement there is:

$$U_r\left(z = 0\right) = \frac{P_x \cos\theta}{2\pi G_{vh}} C_{rz} \quad \text{with} \quad C_{rx} = \frac{1}{u_3} \tag{B5.6}$$

Displacements

Circumferential displacements due to horizontal (+x) point load may be inferred from Liao and Wang's (1998) equations 48 and 74. Putting $P_r = P_x$ and $P_z = P_\theta = 0$ gives:

$$U'_\theta = \frac{P_x \sin\theta}{4\pi}\left[-k\left(\frac{R_1^*}{m_1 r^2} - \frac{R_2^*}{m_2 r^2}\right) - \frac{1}{u_3 A_{44}}\frac{z_3 R_3^*}{r^2 R_3}\right] \tag{B6.1}$$

$$U_\theta = U'_\theta + \frac{P_x \sin\theta}{4\pi}\left[T_1\frac{R_a^*}{r^2} - T_2\frac{R_b^*}{r^2} - T_3\frac{R_c^*}{r^2} + T_4\frac{R_d^*}{r^2} - \frac{1}{u_3 A_{44}}\frac{z_e R_e^*}{r^2 R_e}\right] \tag{B6.2}$$

Using the simplification associated with surface loads (Sheet A2) to simplify the second equation gives:

$$U_\theta = U'_\theta + \frac{P_x \sin\theta}{4\pi}\left[(T_1 - T_2)\frac{R_1^*}{r^2} - (T_3 - T_4)\frac{R_2^*}{r^2} - \frac{1}{u_3 A_{44}}\frac{z_3 R_3^*}{r^2 R_3}\right] \tag{B6.3}$$

Using equation B6.1 to substitute for U'_θ gives:

$$U_\theta = \frac{P_x \sin\theta}{4\pi}\left[\left(T_1 - T_2 - \frac{k}{m_1}\right)\frac{R_1^*}{r^2} - \left(T_3 - T_4 - \frac{k}{m_2}\right)\frac{R_2^*}{r^2} - \frac{2}{u_3 A_{44}}\frac{z_3 R_3^*}{r^2 R_3}\right] \tag{B6.4}$$

Using the simplified equations for T_i (Sheet B1) gives:

$$U_\theta = \frac{P_x \sin\theta}{4\pi G_{vh}}\left[\sum_{i=1}^{2}\left(\frac{\lambda_i}{m_i}\frac{R_i^*}{r^2}\right) - \frac{2}{u_3}\frac{z_3 R_3^*}{r^2 R_3}\right] \tag{B6.5}$$

Compliance factor

At the surface, the summation is zero, and $R_i^* / R_i = 1$, and the above equation implies that the circumferential displacement is:

$$U_\theta(z=0) = \frac{P_x \sin\theta}{2\pi G_{vh}} C_{\theta r} \quad \text{with} \quad C_{\theta x} = \frac{1}{2}\left(\frac{\lambda_1}{m_1} + \frac{\lambda_2}{m_2}\right) \tag{B6.6}$$

Vertical displacements due to horizontal (+x) point load are inferred from Liao and Wang's (1998) equations 49 and 75. Putting $P_r = P_x$ and $P_z = P_\theta = 0$ gives:

$$U_z' = \frac{P_x \cos\theta}{4\pi}\left[\mp k\left(\frac{R_1^*}{rR_1} - \frac{R_2^*}{rR_2}\right)\right] \tag{B7.1}$$

$$U_z = U_z' + \frac{P_x \cos\theta}{4\pi}\left\{m_1\left[T_1\frac{R_a^*}{rR_a} - T_2\frac{R_b^*}{rR_b}\right] - m_2\left[T_3\frac{R_c^*}{rR_c} - T_4\frac{R_d^*}{rR_d}\right]\right\} \tag{B7.2}$$

In the first equation, the upper sign is for z>0 (downwards into the half-space). Using the simplification associated with surface loads (Sheet A2) to simplify the second equation gives:

$$U_z = U_z' + \frac{P_x \cos\theta}{4\pi}\left\{m_1\left(T_1 - T_2\right)\frac{R_1^*}{rR_1} - m_2\left(T_3 - T_4\right)\frac{R_2^*}{rR_2}\right\} \tag{B7.3}$$

Using equation B7.1 to substitute for U_z' gives:

$$U_z = \frac{P_x \cos\theta}{4\pi}\left\{\left[m_1\left(T_1 - T_2\right) - k\right]\frac{R_1^*}{rR_1} - \left[m_2\left(T_3 - T_4\right) - k\right]\frac{R_2^*}{rR_2}\right\} \tag{B7.4}$$

Using the simplified equations for the T_i groups (Sheet B1) gives:

$$U_z = \frac{P_x \cos\theta}{4\pi G_{vh}}\sum_{i=1}^{2}\left(\lambda_i \frac{R_i^*}{rR_i}\right) \tag{B7.5}$$

Compliance factor

At the surface, the summation is zero, and $R_i^* / R_i = 1$, and the above equation implies that the vertical displacement is:

$$U_z\left(z=0\right) = \frac{P_x \cos\theta}{2\pi G_{vh}} C_{zx} \quad \text{with} \quad C_{zx} = \frac{\lambda_1 + \lambda_2}{2} \tag{B7.6}$$

Aim

The purpose of this group C of Calculation sheets is to calculate the strains that are implied by the displacement equations of group B.

Compatibility Equations

The compatibility relations between displacements and strains in cylindrical coordinates are well known, and were quoted by Liao and Wang (1998). The normal strains can be expressed as:

$$\varepsilon_{rr} = -\frac{\partial U_r}{\partial r} \tag{C1.1}$$

$$\varepsilon_{\theta\theta} = -\frac{U_r}{r} - \frac{\partial U_\theta}{r\partial\theta} \tag{C1.2}$$

$$\varepsilon_{zz} = \frac{-\partial U_{zz}}{\partial z} \tag{C1.3}$$

It is convenient to represent shear strains using engineering shear strain parameters:

$$\gamma_{\theta z} = \gamma_{z\theta} = -\frac{\partial U_\theta}{\partial z} - \frac{\partial U_z}{r\partial\theta} \tag{C1.4}$$

$$\gamma_{zr} = \gamma_{rz} = -\frac{\partial U_z}{\partial r} - \frac{\partial U_r}{\partial z} \tag{C1.5}$$

$$\gamma_{r\theta} = \gamma_{\theta r} = \frac{U_\theta}{r} - \frac{\partial U_\theta}{\partial r} - \frac{\partial U_r}{r\partial\theta} \tag{C1.6}$$

Vertical loading

Radial displacements for vertical loading were calculated in sheet B2. Applying the equation for radial strain in sheet C1 to the result gives:

$$\varepsilon_{rr} = -\frac{\partial}{\partial r}\left\{\frac{P_z}{4\pi G_{vh}}\sum_{i=1}^{2}\left(-\lambda_i'\frac{R_i^*}{rR_i}\right)\right\} \tag{C2.1}$$

Evaluating the differential gives

$$\varepsilon_{rr} = \frac{P_z}{4\pi G_{vh}}\sum_{i=1}^{2}\left[\lambda_i'\left(\frac{z_i}{R_i^3}-\frac{R_i^*}{r^2R_i}\right)\right] \tag{C2.2}$$

Lateral (+x) loading

Radial displacements were calculated for horizontal (+x) loading in sheet B5. Applying the equation for radial strain in sheet C1 to the result gives:

$$\varepsilon_{rr} = -\frac{\partial}{\partial r}\left\{\frac{P_x\cos\theta}{4\pi G_{vh}}\left[\sum_{i=1}^{2}\left(-\frac{\lambda_i}{m_i}\frac{z_iR_i^*}{r^2R_i}\right)+\frac{2}{u_3}\frac{R_3^*}{r^2}\right]\right\} \tag{C2.3}$$

Using sheet A3 to differentiate gives:

$$\varepsilon_{rr} = \frac{P_x\cos\theta}{4\pi G_{vh}}\left[\sum_{i=1}^{2}\left(\frac{\lambda_i}{m_i}\left(\frac{z_i^2}{rR_i^3}-\frac{2z_iR_i^*}{r^3R_i}\right)\right)-\frac{2}{u_3}\left(\frac{1}{rR_i}-\frac{2R_i}{r^3}\right)\right] \tag{C2.4}$$

Using equation A3.19 to re-express the sum and equation A3.21 to simplify the last term gives:

$$\varepsilon_{rr} = \frac{P_x\cos\theta}{4\pi G_{vh}}\left[\sum_{i=1}^{2}\left(\frac{\lambda_i}{m_i}\left(\frac{R_i^{*2}}{r^3R_i}-\frac{r}{R_i^3}\right)\right)+\frac{2}{u_3}\frac{R_3^{*2}}{r^3R_3}\right] \tag{C2.5}$$

Vertical loading

Circumferential displacements due to vertical loading are zero by symmetry (sheet B3). However, the circumferential strain equation of sheet C1 also involves radial displacements which were calculated on sheet B2.

$$\varepsilon_{\theta\theta} = -\frac{1}{r}\left\{\frac{P_z}{4\pi G_{vh}}\sum_{i=1}^{2}\left(-\lambda_i'\frac{R_i^*}{rR_i}\right)\right\} - \frac{\partial}{r\partial\theta}\{0\} \tag{C3.1}$$

The result for circumferential strain is:

$$\varepsilon_{\theta\theta} = \frac{P_z}{4\pi G_{vh}}\sum_{i=1}^{2}\left(\lambda_i'\frac{R_i^*}{r^2R_i}\right) \tag{C3.2}$$

Lateral (+x) loading

Circumferential displacements due to horizontal (+x) loading were calculated in sheet B6. The equation for circumferential strain in sheet C1 also involves the radial displacements which were calculated on sheet B5, and gives:

$$\begin{aligned}\varepsilon_{\theta\theta} = &-\frac{1}{r}\left\{\frac{P_x\cos\theta}{4\pi G_{vh}}\left[\sum_{i=1}^{2}\left(-\frac{\lambda_i}{m_i}\frac{z_iR_i^*}{r^2R_i}\right)+\frac{2}{u_3}\frac{R_3^*}{r^2}\right]\right\}\\ &-\frac{\partial}{r\partial\theta}\left\{\frac{P_x\sin\theta}{4\pi G_{vh}}\left[\sum_{i=1}^{2}\left(\frac{\lambda_i}{m_i}\frac{R_i^*}{r^2}\right)-\frac{2}{u_3}\frac{z_3R_3^*}{r^2R_3}\right]\right\}\end{aligned} \tag{C3.3}$$

Evaluating this, and using equation A3.17 to simplify the last term, gives:

$$\varepsilon_{\theta\theta} = \frac{P_x\cos\theta}{4\pi G_{vh}}\left\{\sum_{i=1}^{2}\left[\frac{\lambda_i}{m_i}\left(\frac{z_iR_i^*}{r^2R_i}-\frac{R_i^*}{r^2}\right)\right]-\frac{2}{u_3}\frac{R_3^{*2}}{r^3R_3}\right\} \tag{C3.4}$$

Using equation A3.17 to simplify the sum, gives:

$$\varepsilon_{\theta\theta} = \frac{P_x\cos\theta}{4\pi G_{vh}}\left\{\sum_{i=1}^{2}\left(-\frac{\lambda_i}{m_i}\frac{R_i^{*2}}{r^3R_i}\right)-\frac{2}{u_3}\frac{R_3^{*2}}{r^3R_3}\right\} \tag{C3.5}$$

Vertical loading

Vertical displacements due to vertical loading were calculated in sheet B4. Applying the equation for radial strain in sheet C1 to the result gives:

$$\varepsilon_{zz} = \frac{-\partial}{\partial z}\left\{\frac{P_x \cos\theta}{4\pi G_{vh}} \sum_{i=1}^{2}\left(-\frac{m_i \lambda_i'}{R_i}\right)\right\} \tag{C4.1}$$

Evaluating the differential gives

$$\varepsilon_{zz} = \frac{P_z}{4\pi G_{vh}} \sum_{i=1}^{2}\left(-m_i u_i \lambda_i' \frac{z_i}{R_i^3}\right) \tag{C4.2}$$

Lateral (+x) loading

Vertical displacements due to horizontal (+x) loading were calculated in sheet B7. Applying the equation for radial strain in sheet C1 to the result gives:

$$\varepsilon_{zz} = -\frac{\partial}{\partial z}\left\{\frac{P_x \cos\theta}{4\pi G_{vh}} \sum_{i=1}^{2}\left(\lambda_i \frac{R_i^*}{rR_i}\right)\right\} \tag{C4.3}$$

Using sheet A3 to evaluate the result gives:

$$\varepsilon_{zz} = \frac{P_x \cos\theta}{4\pi G_{vh}} \sum_{i=1}^{2}\left[\lambda_i u_i \frac{r}{R_i^3}\right] \tag{C4.4}$$

Vertical loading

The equation for shear strain in the $z\theta$ plane in sheet C1 involves both the circumferential displacement and vertical displacement. The first is zero for vertical loading (sheet B3). The second is given on sheet B4. Applying the equation for $\gamma_{z\theta}$ on sheet C1 and evaluating the differential gives:

$$\gamma_{\theta z} = -\frac{\partial}{\partial z}(0) - \frac{\partial}{r\partial\theta}\left\{\frac{P_z}{4\pi G_{vh}}\sum_{i=1}^{2}\left(-\frac{m_i\lambda_i'}{R_i}\right)\right\} = 0 \qquad \text{(C5.1)}$$

Lateral (+x) loading

Using sheet B6 for the circumferential displacements due to a horizontal (+x) surface point load and sheet B7 for the vertical displacements, and applying the equation for $\gamma_{z\theta}$ on sheet C1 gives:

$$\gamma_{\theta z} - \frac{\partial}{\partial z}\left\{\frac{P_x\sin\theta}{4\pi G_{vh}}\left[\sum_{i=1}^{2}\left(\frac{\lambda_i}{m_i}\frac{R_i^*}{r^2}\right) - \frac{2}{u_3}\frac{z_3R_3^*}{r^2R_3}\right]\right\} - \frac{\partial}{r\partial\theta}\left\{\frac{P_x\cos\theta}{4\pi G_{vh}}\sum_{i=1}^{2}\left(\lambda_i\frac{R_i^*}{rR_i}\right)\right\} \qquad \text{(C5.2)}$$

Using sheet A3 to evaluate the result gives:

$$\gamma_{\theta z} = \frac{P_x\sin\theta}{4\pi G_{vh}}\left[\sum_{i=1}^{2}\left(\frac{\lambda_i}{m_i}\left(\frac{u_iR_i^*}{r^2R_i}\right)\right) + \frac{2}{u_3}\left(\frac{u_3R_3^*}{r^2R_3} - \frac{u_3z_3}{R_3^3}\right)\right] + \frac{P_x\sin\theta}{4\pi G_{vh}}\sum_{i=1}^{2}\left(\lambda_i\frac{R_i^*}{r^2R_i}\right) \qquad \text{(C5.3)}$$

Collecting terms gives:

$$\gamma_{\theta z} = \frac{P_x\sin\theta}{4\pi G_{vh}}\left[\sum_{i=1}^{2}\left(\frac{\lambda_i}{m_i}(u_i+m_i)\frac{R_i^*}{r^2R_i}\right) + 2\left(\frac{R_3^*}{r^2R_3} - \frac{z_3}{R_3^3}\right)\right] \qquad \text{(C5.4)}$$

Vertical loading

The equation for shear strain in the rz plane in sheet C1 involves both the radial displacement and vertical displacement. These are on sheets B2 and B4 respectively. Applying the equation for γ_{rz} on sheet C1 and evaluating the differential gives:

$$\gamma_{rz} = -\frac{\partial}{\partial r}\left\{\frac{P_z}{4\pi G_{vh}}\sum_{i=1}^{2}\left(-\frac{m_i\lambda_i'}{R_i}\right)\right\} - \frac{\partial}{\partial z}\left\{\frac{P_z}{4\pi G_{vh}}\sum_{i=1}^{2}\left(-\lambda_i'\frac{R_i^*}{rR_i}\right)\right\} \tag{C6.1}$$

Evaluating the differentials gives:

$$\gamma_{rz} = \frac{P_z}{4\pi G_{vh}}\sum_{i=1}^{2}\left(-\lambda_i'(u_i+m_i)\frac{r}{R_i^3}\right) \tag{C6.2}$$

Lateral (+x) loading

Using sheet B5 for the radial displacements due to a horizontal (+x) surface point load and sheet B7 for the vertical displacements, and applying the equation for $\gamma_{z\theta}$ on sheet C1 gives:

$$\gamma_{rz} = -\frac{\partial}{\partial r}\left\{\frac{P_z\cos\theta}{4\pi G_{vh}}\sum_{i=1}^{2}\left(\lambda_i\frac{R_i^*}{rR_i}\right)\right\} - \frac{\partial}{\partial z}\left\{\frac{P_x\cos\theta}{4\pi G_{vh}}\left[\sum_{i=1}^{2}\left(-\frac{\lambda_i}{m_i}\frac{z_iR_i^*}{r^2R_i}\right)+\frac{2}{u_3}\frac{R_3^*}{r^2}\right]\right\} \tag{C6.3}$$

Using sheet A3 to evaluate the result gives:

$$\gamma_{rz} = \frac{P_z\cos\theta}{4\pi G_{vh}}\left\{\sum_{i=1}^{2}\left[\lambda_i\left(\frac{R_i^*}{r^2R_i}-\frac{z_i}{R_i^3}\right)\right]+\left[\sum_{i=1}^{2}\left(\frac{\lambda_iu_i}{m_i}\left(\frac{R_i^*}{r^2R_i}-\frac{z_i}{R_i^3}\right)\right)+\frac{2}{u_3}\frac{u_3R_3^*}{r^2R_3}\right]\right\} \tag{C6.4}$$

Collecting terms gives:

$$\gamma_{rz} = \frac{P_z\cos\theta}{4\pi G_{vh}}\left\{\sum_{i=1}^{2}\left[\frac{\lambda_i}{m_i}(u_i+m_i)\left(\frac{R_i^*}{r^2R_i}-\frac{z_i}{R_i^3}\right)\right]+2\frac{R_3^*}{r^2R_3}\right\} \tag{C6.5}$$

Vertical loading

The equation for shear strain in the $z\theta$ plane in sheet C1 involves both the circumferential displacement and vertical displacement. The first is zero for vertical loading (sheet B3). The second is given on sheet B4. Applying the equation for $\gamma_{z\theta}$ on sheet C1 and evaluating the differential gives:

$$\gamma_{r\theta} = \frac{1}{r}\{0\} - \frac{\partial}{\partial r}\{0\} - \frac{\partial}{r\partial\theta}\left\{\frac{P_z}{4\pi G_{vh}}\sum_{i=1}^{2}\left(-\lambda_i'\frac{R_i^*}{rR_i}\right)\right\} = 0 \tag{C7.1}$$

Lateral (+x) loading

Using sheet B6 for the circumferential displacements due to a horizontal (+x) surface point load and sheet B7 for the vertical displacements, and applying the equation for $\gamma_{z\theta}$ on sheet C1 gives:

$$\begin{aligned}\gamma_{r\theta} = {} & \frac{1}{r}\left\{\frac{P_x\sin\theta}{4\pi G_{vh}}\left[\sum_{i=1}^{2}\left(\frac{\lambda_i}{m_i}\frac{R_i^*}{r^2}\right) - \frac{2}{u_3}\frac{z_3R_3^*}{r^2R_3}\right]\right\} \\ & -\frac{\partial}{\partial r}\left\{\frac{P_x\sin\theta}{4\pi G_{vh}}\left[\sum_{i=1}^{2}\left(\frac{\lambda_i}{m_i}\frac{R_i^*}{r^2}\right) - \frac{2}{u_3}\frac{z_3R_3^*}{r^2R_3}\right]\right\} \\ & -\frac{\partial}{r\partial\theta}\left\{\frac{P_x\cos\theta}{4\pi G_{vh}}\left[\sum_{i=1}^{2}\left(-\frac{\lambda_i}{m_i}\frac{z_iR_i^*}{r^2R_i}\right) + \frac{2}{u_3}\frac{R_3^*}{r^2}\right]\right\}\end{aligned} \tag{C7.2}$$

Using sheet A3 to evaluate the result gives:

$$\gamma_{r\theta} = \frac{P_x\sin\theta}{4\pi G_{vh}}\left\{\begin{aligned}&\left[\sum_{i=1}^{2}\left(\frac{\lambda_i}{m_i}\frac{R_i^*}{r^3}\right) - \frac{2}{u_3}\frac{z_3R_3^*}{r^3R_3}\right] + \\ &\left[\sum_{i=1}^{2}\left(\frac{\lambda_i}{m_i}\left(\frac{2R_i^*}{r^3} - \frac{1}{rR_i}\right)\right) + \frac{2}{u_3}\left(\frac{z_3^2}{rR_i^3} - \frac{2z_3R_3^*}{r^3R_3}\right)\right] + \\ &\left[\sum_{i=1}^{2}\left(-\frac{\lambda_i}{m_i}\frac{z_iR_i^*}{r^3R_i}\right) + \frac{2}{u_3}\frac{R_3^*}{r^3}\right]\end{aligned}\right\} \tag{C7.3}$$

Collecting terms gives:

$$\gamma_{r\theta} = \frac{P_x\sin\theta}{4\pi G_{vh}}\left\{\sum_{i=1}^{2}\left(\frac{\lambda_i}{m_i}\frac{2R_i^{*2}}{r^3R_i}\right) + \frac{2}{u_3}\left(\frac{R_3^*}{r^3} + \frac{z_3^2}{rR_i^3} - \frac{3z_3R_3^*}{r^3R_3}\right)\right\} \tag{C7.4}$$

Aims

The purpose of this group D of Calculation sheets is to calculate the changes of stresses that are implied by the strain equations of group C. Checks are also made that the stresses are zero at the centre, except at the origin of the cylindrical coordinates where the load are applied.

Constitutive Equations

The constitutive relations of a transversely isotropic linear elastic material in cylindrical coordinates are well known, and were quoted by Liao and Wang (1998) using the Aij notation for constrained moduli. The changes of normal stresses can be expressed as:

$$\begin{bmatrix} \sigma_{rr} \\ \sigma_{\theta\theta} \\ \sigma_{zz} \end{bmatrix} = \begin{bmatrix} A_{11} & A_{11}-2A_{66} & A_{13} \\ A_{12}-2A_{66} & A_{11} & A_{13} \\ A_{13} & A_{13} & A_{33} \end{bmatrix} \begin{bmatrix} \varepsilon_{rr} \\ \varepsilon_{\theta\theta} \\ \varepsilon_{zz} \end{bmatrix} \quad \text{(D1.1)}$$

The shear stresses are given by:

$$\gamma_{zr} = \frac{\tau_{zr}}{A_{44}} \qquad \gamma_{z\theta} = \frac{\tau_{z\theta}}{A_{44}} \qquad \gamma_{r\theta} = \frac{\tau_{r\theta}}{A_{66}} \quad \text{(D1.2,3,4)}$$

with: $$A_{44} = G_{vh} \qquad A_{66} = G_{hh} = \frac{E_h}{2(1+\mu_{hh})} \quad \text{(D1.5,6)}$$

Useful expressions

The characteristic equation was given in the main text in the form provided by Liao and Wang (1998). It gives two expressions for m_i. The following useful identities are deduced from these expressions:

$$A_{11} - m_i u_i A_{13} = u_i \left(u_i + m_i\right) A_{44} \quad \text{(D1.7)}$$

$$A_{13} - m_i u_i A_{33} = -\frac{u_i + m_i}{u_i} A_{44} \quad \text{(D1.8)}$$

Closed form solutions for a transversely isotropic linear elastic half-space loaded at a point on its surface	**Sum of the radial and circumferential strains**	Sheet D2

Rationale

The constitutive equation for normal stresses on Sheet D1 can be conveniently written in terms of the sum of the radial and circumferential strains as follows:

$$\sigma_{rr} = A_{11}\left(\varepsilon_{rr} + \varepsilon_{\theta\theta}\right) - 2A_{66}\varepsilon_{\theta\theta} + A_{13}\varepsilon_{zz} \tag{D2.1}$$

$$\sigma_{\theta\theta} = A_{11}\left(\varepsilon_{rr} + \varepsilon_{\theta\theta}\right) - 2A_{66}\varepsilon_{rr} + A_{13}\varepsilon_{zz} \tag{D2.2}$$

$$\sigma_{zz} = A_{13}\left(\varepsilon_{rr} + \varepsilon_{\theta\theta}\right) + A_{33}\varepsilon_{zz} \tag{D2.3}$$

Vertical point load

The sum of the two strains can be calculated using the first sets of results from Sheets C2 and C3, giving:

$$\varepsilon_{rr} + \varepsilon_{\theta\theta} = \frac{P_z}{4\pi G_{vh}} \sum_{i=1}^{2} \left[\lambda_i' \left(\frac{z_i}{R_i^3} - \frac{R_i^*}{r^2 R_i} \right) \right] + \frac{P_z}{4\pi G_{vh}} \sum_{i=1}^{2} \left(\lambda_i' \frac{R_i^*}{r^2 R_i} \right) \tag{D2.4}$$

Simplifying gives:

$$\varepsilon_{rr} + \varepsilon_{\theta\theta} = \frac{P_z}{4\pi G_{vh}} \sum_{i=1}^{2} \left[\lambda_i' \frac{z_i}{R_i^3} \right] \tag{D2.5}$$

Horizontal (+x) point load

The sum of the two strains can be calculated using the second sets of results from Sheets C2 and C3, the latter with equation C3.4, giving:

$$\varepsilon_{rr} + \varepsilon_{\theta\theta} = \frac{P_x \cos\theta}{4\pi G_{vh}} \left\{ \begin{array}{l} \displaystyle\sum_{i=1}^{2} \left[\frac{\lambda_i}{m_i} \left(\frac{z_i^2}{r R_i^3} - \frac{2 z_i R_i^*}{r^3 R_i} \right) \right] + \frac{2}{u_3} \frac{R_3^{*2}}{r^3 R_3} \\ \displaystyle + \sum_{i=1}^{2} \left[\frac{\lambda_i}{m_i} \left(\frac{z_i R_i^*}{r^3 R_i} - \frac{R_i^*}{r^3} \right) \right] - \frac{2}{u_3} \frac{R_3^{*2}}{r^3 R_3} \end{array} \right\} \tag{D2.6}$$

Simplifying using equation A3.18 gives:

$$\varepsilon_{rr} + \varepsilon_{\theta\theta} = \frac{P_x \cos\theta}{4\pi G_{vh}} \sum_{i=1}^{2} \left(-\frac{\lambda_i}{m_i} \frac{r}{R_i^3} \right) \tag{D2.7}$$

Done by and date	Checked by and date	Printed on
ETRD November 2022		Wednesday, 30 November 2022, 11:06

The normal stresses due to the vertical point load can be calculated in accordance with the strains on sheets C2 to C4, the constitutive equations of Sheet D1, and the sum of the radial and circumferential strains for this loading on sheet D2:

$$\frac{4\pi G_{vh}}{P_z}\sigma_{rr} = A_{11}\left\{\sum_{i=1}^{2}\left[\lambda_i'\frac{z_i}{R_i^3}\right]\right\} - 2A_{66}\left\{\sum_{i=1}^{2}\left(\lambda_i'\frac{R_i^*}{r^2R_i}\right)\right\} + A_{13}\left\{\sum_{i=1}^{2}\left(-m_iu_i\lambda_i'\frac{z_i}{R_i^3}\right)\right\} \tag{D3.1}$$

$$\frac{4\pi G_{vh}}{P_z}\sigma_{\theta\theta} = A_{11}\left\{\sum_{i=1}^{2}\left[\lambda_i'\frac{z_i}{R_i^3}\right]\right\} - 2A_{66}\left\{\sum_{i=1}^{2}\left[\lambda_i'\left(\frac{z_i}{R_i^3}-\frac{R_i^*}{r^2R_i}\right)\right]\right\} + A_{13}\left\{\sum_{i=1}^{2}\left(-m_iu_i\lambda_i'\frac{z_i}{R_i^3}\right)\right\} \tag{D3.2}$$

$$\frac{4\pi G_{vh}}{P_z}\sigma_{zz} = A_{13}\left\{\sum_{i=1}^{2}\left[\lambda_i'\frac{z_i}{R_i^3}\right]\right\} + A_{33}\left\{\sum_{i=1}^{2}\left(-m_iu_i\lambda_i'\frac{z_i}{R_i^3}\right)\right\} \tag{D3.3}$$

Collecting terms gives:

$$\sigma_{rr} = \frac{P_z}{4\pi G_{vh}}\left\{\sum_{i=1}^{2}\left[\lambda_i'\left(A_{11}-m_iu_iA_{13}\right)\frac{z_i}{R_i^3}\right] + 2A_{66}\sum_{i=1}^{2}\left[-\lambda_i'\frac{R_i^*}{r^2R_i}\right]\right\} \tag{D3.4}$$

$$\sigma_{\theta\theta} = \frac{P_z}{4\pi G_{vh}}\left\{\sum_{i=1}^{2}\left[\lambda_i'\left(A_{11}-m_iu_iA_{13}\right)\frac{z_i}{R_i^3}\right] - 2A_{66}\left\{\sum_{i=1}^{2}\left[\lambda_i'\left(\frac{z_i}{R_i^3}-\frac{R_i^*}{r^2R_i}\right)\right]\right\}\right\} \tag{D3.5}$$

$$\sigma_{zz} = \frac{P_z}{4\pi G_{vh}}\sum_{i=1}^{2}\left[\lambda_i'\left(A_{13}-m_iu_iA_{33}\right)\frac{z_i}{R_i^3}\right] \tag{D3.6}$$

Using equations D1.7 and D1.8, and recalling that $A_{44} = G_{vh}$ and $A_{66} = G_{hh}$, gives:

$$\sigma_{rr} = \frac{P_z}{4\pi}\left\{\sum_{i=1}^{2}\left[\lambda_i'u_i\left(u_i+m_i\right)\frac{z_i}{R_i^3}\right] + 2\frac{G_{hh}}{G_{vh}}\sum_{i=1}^{2}\left[-\lambda_i'\frac{R_i^*}{r^2R_i}\right]\right\} \tag{D3.7}$$

$$\sigma_{\theta\theta} = \frac{P_z}{4\pi}\left\{\sum_{i=1}^{2}\left[\lambda_i'u_i\left(u_i+m_i\right)\frac{z_i}{R_i^3}\right] - 2\frac{G_{hh}}{G_{vh}}\sum_{i=1}^{2}\left[\lambda_i'\left(\frac{z_i}{R_i^3}-\frac{R_i^*}{r^2R_i}\right)\right]\right\} \tag{D3.8}$$

$$\sigma_{zz} = \frac{P_z}{4\pi}\sum_{i=1}^{2}\left[-\frac{\lambda_i'}{u_i}\left(u_i+m_i\right)\frac{z_i}{R_i^3}\right] \tag{D3.9}$$

The shear stresses ae the products of the engineering shear strains by the relevant shear moduli. Hence using Sheets C5, C6, and C7 for the case of a vertical point load:

$$\tau_{z\theta} = 0 \tag{D4.1}$$

$$\tau_{rz} = \frac{P_z}{4\pi}\sum_{i=1}^{2}\left(-\lambda_i'\left(u_i + m_i\right)\frac{r}{R_i^3}\right) \tag{D4.2}$$

$$\tau_{\theta r} = 0 \tag{D4.3}$$

Normal stresses

The normal stress on the free surface of the half-space is required to be zero except at the singular load point. This stress is given by equation D3.9, which contains two components that are zero when $z = 0$. Hence the condition is satisfied.

Shear stresses

The shear stresses on the free surface are also required to be zero except at the singular load point. The relevant stresses are given in equations D3.1 (which gives $\tau_{z\theta} = 0$) and D3.2. The latter reduces to the following when $z = 0$ and $r \neq 0$:

$$\tau_{rz} = \frac{P_z \cos\theta}{4\pi r^2} \sum_{i=1}^{2} -\lambda_i' \left(u_i + m_i \right) \tag{D5.1}$$

Using equations B1.3 and B1.4 together with the relation $m_1 m_2 = u_1 u_2$ (proved in the main text), it is found that the sum in this equation is zero. Hence the condition is satisfied.

The normal stresses due to the horizontal (+x) point load can be calculated in accordance with the strains on sheets C2 to C4, the constitutive equations of Sheet D1, and the sum of the radial and circumferential strains for this loading on sheet D2:

$$\frac{4\pi G_{vh}}{P_x\cos\theta}\sigma_{rr} = A_{11}\left\{\sum_{i=1}^{2}\left(-\frac{\lambda_i}{m_i}\frac{r}{R_i^3}\right)\right\} - 2A_{66}\left\{\sum_{i=1}^{2}\left(-\frac{\lambda_i}{m_i}\frac{R_i^{*2}}{r^3R_i}\right) - \frac{2}{u_3}\frac{R_3^{*2}}{r^3R_3}\right\} + A_{13}\left\{\sum_{i=1}^{2}\left(\lambda_i u_i\frac{r}{R_i^3}\right)\right\} \quad \text{(D6.1)}$$

$$\frac{4\pi G_{vh}}{P_x\cos\theta}\sigma_{\theta\theta} = A_{11}\left\{\sum_{i=1}^{2}\left(-\frac{\lambda_i}{m_i}\frac{r}{R_i^3}\right)\right\} - 2A_{66}\left\{\sum_{i=1}^{2}\left(\frac{\lambda_i}{m_i}\left(\frac{R_i^{*2}}{r^3R_i} - \frac{r}{R_i^3}\right)\right) + \frac{2}{u_3}\frac{R_3^{*2}}{r^3R_3}\right\} + A_{13}\left\{\sum_{i=1}^{2}\left(\lambda_i u_i\frac{r}{R_i^3}\right)\right\} \quad \text{(D6.2)}$$

$$\frac{4\pi G_{vh}}{P_x\cos\theta}\sigma_{zz} = A_{13}\sum_{i=1}^{2}\left(-\frac{\lambda_i}{m_i}\frac{r}{R_i^3}\right) + A_{33}\left\{\sum_{i=1}^{2}\left(\lambda_i u_i\frac{r}{R_i^3}\right)\right\} \quad \text{(D6.3)}$$

Collecting terms, and using the identities in equations D1.7 and D1.8, gives:

$$\sigma_{rr} = \frac{P_x\cos\theta}{4\pi}\left\{\sum_{i=1}^{2}\left(-\frac{\lambda_i}{m_i}u_i\left(u_i+m_i\right)\frac{r}{R_i^3}\right) - \frac{2G_{hh}}{G_{vh}}\left[\sum_{i=1}^{2}\left(-\frac{\lambda_i}{m_i}\frac{R_i^{*2}}{r^3R_i}\right) - \frac{2}{u_3}\frac{R_3^{*2}}{r^3R_3}\right]\right\} \quad \text{(D6.4)}$$

$$\sigma_{\theta\theta} = \frac{P_x\cos\theta}{4\pi}\left\{\sum_{i=1}^{2}\left(-\frac{\lambda_i}{m_i}u_i\left(u_i+m_i\right)\frac{r}{R_i^3}\right) - \frac{2G_{hh}}{G_{vh}}\left\{\sum_{i=1}^{2}\left[\frac{\lambda_i}{m_i}\left(\frac{R_i^{*2}}{r^3R_i} - \frac{r}{R_i^3}\right)\right] + \frac{2}{u_3}\frac{R_3^{*2}}{r^3R_3}\right\}\right\} \quad \text{(D6.5)}$$

$$\sigma_{zz} = \frac{P_x\cos\theta}{4\pi}\sum_{i=1}^{2}\left(\frac{\lambda_i}{m_i u_i}\left(u_i+m_i\right)\frac{r}{R_i^3}\right) \quad \text{(D6.6)}$$

The shear stresses are the products of the engineering shear strains by the relevant shear moduli. Hence using Sheets C5, C6, and C7 for the case of a horizontal (+x) point load:

$$\tau_{\theta z} = \frac{P_x \sin\theta}{4\pi}\left\{\sum_{i=1}^{2}\left[\frac{\lambda_i}{m_i}(u_i + m_i)\frac{R_i^*}{r^2 R_i}\right] + 2\left(\frac{R_3^*}{r^2 R_3} - \frac{z_3}{R_3^3}\right)\right\} \tag{D7.1}$$

$$\tau_{rz} = \frac{P_x \cos\theta}{4\pi}\left\{\sum_{i=1}^{2}\left[\frac{\lambda_i}{m_i}(u_i + m_i)\left(\frac{R_i^*}{r^2 R_i} - \frac{z_i}{R_i^3}\right)\right] + 2\frac{R_3^*}{r^2 R_3}\right\} \tag{D7.2}$$

$$\tau_{r\theta} = \frac{P_x \sin\theta}{4\pi}\frac{G_{hh}}{G_{vh}}\left\{\sum_{i=1}^{2}\left(\frac{\lambda_i}{m_i}\frac{2R_i^{*2}}{r^3 R_i}\right) + \frac{2}{u_3}\left(\frac{3z_3 R_3^*}{r^3 R_3} - \frac{R_3^*}{r^3} - \frac{z_3^2}{r R_i^3}\right)\right\} \tag{D7.3}$$

This sheet derives some expressions involving sums that will be useful in assessing equilibrium on sheet D9 and in group F. Using the expressions for λ_i in equations B1.3 and B1.4 gives:

$$\sum_{i=1}^{2}\left(\frac{\lambda_i}{m_i u_i}\left(u_i+m_i\right)\right)=\lambda_o\left(\frac{u_1}{m_1}-\frac{m_1}{u_1}+\frac{u_2}{m_2}-\frac{m_2}{u_2}\right)=0 \tag{D8.1}$$

Using $u_1u_2=m_1m_2$ which was derived in the main text, the first fraction cancels the fourth and the second cancels the third, making the sum zero. Substituting for λ_i' in the following gives:

$$\sum_{i=1}^{2}\left[\lambda_i'\left(u_i+m_i\right)\right]=\lambda_0\left\{\left(u_2-m_2\right)\left(u_1+m_1\right)+\left(u_1-m_1\right)\left(u_2+m_2\right)\right\}=0 \tag{D8.2}$$

Multiplying out the brackets reveals terms that cancel to give the result zero. Substituting for λ_i' in the following gives

$$\sum_{i=1}^{2}\left\{\lambda_i'\left(\frac{u_i+m_i}{u_i}\right)\right\}=\lambda_0\left\{\frac{\left(u_2-m_2\right)\left(u_1+m_1\right)}{u_1}+\frac{\left(u_1-m_1\right)\left(u_2+m_2\right)}{u_2}\right\} \tag{D8.3}$$

$$\sum_{i=1}^{2}\left[\frac{\lambda_i}{m_i}\left(u_i+m_i\right)\right]=\lambda_0\left\{\frac{u_1^2-m_1^2}{m_1}+\frac{u_2^2-m_2^2}{m_2}\right\} \tag{D8.4}$$

Multiplying out, and using $u_1u_2=m_1m_2$, gives:

$$\sum_{i=1}^{2}\left\{\lambda_i'\left(\frac{u_i+m_i}{u_i}\right)\right\}=\lambda_0\frac{\left(m_1u_2-m_2u_1\right)\left(u_2-u_1\right)}{u_1u_2} \tag{D8.5}$$

$$\sum_{i=1}^{2}\left[\frac{\lambda_i}{m_i}\left(u_i+m_i\right)\right]=-\lambda_0\frac{\left(m_1u_2-m_2u_1\right)\left(u_2-u_1\right)}{u_1u_2} \tag{D8.6}$$

Using equation B1.5 for λ_0, and then using equation B1.2 to substitute for k', and the characteristic equation to substitute for m_i, gives:

$$\sum_{i=1}^{2}\left\{\lambda_i'\left(\frac{u_i+m_i}{u_i}\right)\right\}=2 \tag{D8.7}$$

$$\sum_{i=1}^{2}\left[\frac{\lambda_i}{m_i}\left(u_i+m_i\right)\right]=-2 \tag{D8.8}$$

Normal stresses

The normal stress on the free surface of the half-space is required to be zero at al points except the load point which is at the origin. For horizontal (+x) loading, this stress is given by equation D6.6, which reduces to the following when $z = 0$ and $r \neq 0$:

$$\sigma_{zz} = \frac{P_x \cos\theta}{4\pi r^2} \sum_{i=1}^{2} \left(\frac{\lambda_i}{m_i u_i} (u_i + m_i) \right) \tag{D9.1}$$

Using equation D8.1 shows that this is zero. Hence the required condition is satisfied.

Shear stresses

The shear stresses on the free surface are also required to be zero except at the load point. The relevant stresses are given in equations D7.1 and D7.2. These reduce to the following when $z = 0$ and $r \neq 0$:

$$\tau_{\theta z} = \frac{P_x \sin\theta}{4\pi r^2} \left\{ \sum_{i=1}^{2} \left[\frac{\lambda_i}{m_i} (u_i + m_i) \right] + 2 \right\} \tag{D9.2}$$

$$\tau_{rz} = \frac{P_x \cos\theta}{4\pi r^2} \left\{ \sum_{i=1}^{2} \left[\frac{\lambda_i}{m_i} (u_i + m_i) \right] + 2 \right\} \tag{D9.3}$$

Using equation D8.6 shows that the right sides are zero. Hence the required condition is satisfied.

Closed form solutions for a transversely isotropic linear elastic half-space loaded at a point on its surface	**Group Aim and Implementation**	Sheet E1

Aims

Previously in this Supplement, displacement equations were developed in group B by applying the condition $h=0$ (representing surface loading) to the displacement equations given by Liao and Wang (1998). These were differentiate group C to determine strains, and Group C then applied the material constitutive relations to get the final results in group D.

Liao and Wang (1998) also provided stress equations. They occupy about 3 A4 pages in that paper. The purpose of this group E of Calculation sheets is to check that the stresses calculated in group D agree with the result of applying the condition $h=0$ to the stress equations..

Implementation

Preliminary checks were done by inspection. The table below lists the parameter being checked, the equation number in these calculation sheets, the equation numbers in Kiao and Wang (1998), and the result of the checks.

Stress	Eqn No's in Liao and Wang (1998)	Vertical load		Horizontal (+x) load	
		Eqn No's here	Result	Eqn No's here	Result
σ_{rr}	50 and 76	D3.7	agree	D6.4	agree
$\sigma_{\theta\theta}$	51 and 77	D3.8	agree	D6.5	agree
σ_{zz}	52 and 78	D3.9	agree	D6.6	agree
$\tau_{z\theta}$	54 and 80	D4.1	agree	D7.1	agree
τ_{rz}	55 and 81	D4.2	agree	D7.2	disagree
$\tau_{r\theta}$	53 and 79	D4.3	agree	D7.3	agree

Action

Sheet E2 details the problem. To resolve it, Group F of the Calculations sheets carries out a detailed check that the equations derived in Group D satisfy equilibrium within the half-space. Group G checks that the stress system within the half-space is in equilibrium with the applied loads.

Done by and date	Checked by and date	Printed on
ETRD November 2022		Wednesday, 30 November 2022, 11:24

Liao and Wang (1998)'s equations 55 and 81 include contributions from three point loads. Putting $P_z = P_\theta = 0$ and $P_r = P_x$, they reduce respectively to:

$$\tau'_{rz} = \frac{P_z \cos\theta}{4\pi}\left[\frac{k\left(u_1+m_1\right)A_{44}}{m_1}\left(\frac{z_1}{R_1^3}-\frac{R_1^*}{r^2R_1}\right)-\frac{k\left(u_1+m_1\right)A_{44}}{m_1}\left(\frac{z_2}{R_2^3}-\frac{R_2^*}{r^2R_2}\right)+\frac{R_3^*}{r^2R_3}\right] \quad \text{(E2.1)}$$

$$\tau_{rz} = \tau'_{rz} + \frac{P_z \cos\theta}{4\pi r^2}\left\{\begin{array}{l}\left(u_1+m_1\right)A_{44}\left[T_1\left(\frac{z_a}{R_a^3}-\frac{R_a^*}{r^2R_a}\right)-T_2\left(\frac{z_b}{R_b^3}-\frac{R_b^*}{r^2R_b}\right)\right] \\ -\left(u_2+m_2\right)A_{44}\left[T_3\left(\frac{z_c}{R_c^3}-\frac{R_c^*}{r^2R_c}\right)-T_4\left(\frac{z_d}{R_d^3}-\frac{R_d^*}{r^2R_d}\right)\right]-\frac{R_e^*}{r^2R_e}\end{array}\right\} \quad \text{(E2.2)}$$

Using Sheet A2 to substitute for the subscripted variables in the second equation gives:

$$\tau_{rz} = \tau'_{rz} + \frac{P_z \cos\theta}{4\pi r^2}\left\{\begin{array}{l}\left(u_1+m_1\right)A_{44}\left[\left(T_1-T_2\right)\left(\frac{z_1}{R_1^3}-\frac{R_1^*}{r^2R_1}\right)\right] \\ -\left(u_2+m_2\right)A_{44}\left[\left(T_3-T_4\right)\left(\frac{z_2}{R_2^3}-\frac{R_2^*}{r^2R_2}\right)\right]-\frac{R_3^*}{r^2R_3}\end{array}\right\} \quad \text{(E2.3)}$$

Using the first equation to substitute for τ'_{rz} then gives:

$$\tau_{rz} = \frac{P_z \cos\theta}{4\pi}\left\{\begin{array}{l}\left(u_1+m_1\right)A_{44}\left[\left(T_1-T_2+\frac{k}{m_1}\right)\left(\frac{z_1}{R_1^3}-\frac{R_1^*}{r^2R_1}\right)\right] \\ -\left(u_2+m_2\right)A_{44}\left[\left(T_3-T_4+\frac{k}{m_2}\right)\left(\frac{z_2}{R_2^3}-\frac{R_2^*}{r^2R_2}\right)\right]\end{array}\right\} \quad \text{(E2.4)}$$

This result does not agree with the calculations in group D for two reasons. First, the signs of the k / m_i factors in the inner brackets do not match those in equations B1.8 and B1.9. The shear stresses in the Group D calculation sheets were obtained by multiplying the shear strains from Group C by the appropriate shear moduli. Hence using equation C6.5:

$$\tau_{rz} = \frac{P_z \cos\theta}{4\pi}\left\{\sum_{i=1}^{2}\left[\frac{\lambda_i}{m_i}\left(u_i+m_i\right)\left(\frac{z_i}{R_i^3}-\frac{R_i^*}{r^2R_i}\right)\right]+2\frac{R_3^*}{r^2R_3}\right\} \quad \text{(E2.5)}$$

The second reason is that equation E2.4 does not include the term involving R_3^* However, E2.5 is indeed obtained from E2.1 and E2.3 if the first negative sign in equations E2.2 and E2.3 is changed to a positive sign.

Aims

The purpose of this group F of Calculation sheets is to check that the changes of stresses that were calculated in group D satisfy equilibrium.

Equilibrium equations

The equilibrium equations of a material in cylindrical coordinates are well known, and were quoted by Liao and Wang (1998). For the present context there are no body forces within the half-space, and the equations simplify as follows:

radial: $$\frac{\partial \sigma_{rr}}{\partial r}+\frac{\partial \tau_{r\theta}}{r\partial \theta}+\frac{\partial \tau_{rz}}{\partial z}+\frac{\sigma_{rr}-\sigma_{\theta\theta}}{r}=0 \quad \text{(F1.1)}$$

circumferential: $$\frac{\partial \tau_{r\theta}}{\partial r}+\frac{\partial \sigma_{\theta\theta}}{r\partial \theta}+\frac{\partial \tau_{\theta z}}{\partial z}+\frac{2\tau_{r\theta}}{r}=0 \quad \text{(F1.2)}$$

vertical: $$\frac{\partial \tau_{rz}}{\partial r}+\frac{\partial \tau_{\theta z}}{r\partial \theta}+\frac{\partial \sigma_{zz}}{\partial z}+\frac{\tau_{rz}}{r}=0 \quad \text{(F1.3)}$$

Radial equilibrium

The stresses caused by a vertical point load are given on sheets D3 and D4. Radial equilibrium is described by equation F1.1. Differentiating appropriately, the terms are:

$$\frac{\partial \sigma_{rr}}{\partial r} = \frac{P_z}{4\pi G_{vh}} \sum_{i=1}^{2} \left[\lambda_i' \left(u_i + m_i \right) A_{44} \frac{-3u_i z_i r}{R_i^5} - 2A_{66} \left(\frac{z_i}{r R_i^3} - \frac{2R_i^*}{r^3 R_i} \right) \right] \tag{F2.1}$$

$$\frac{\partial \tau_{r\theta}}{r \partial \theta} = 0 \tag{F2.2}$$

$$\frac{\partial \tau_{rz}}{\partial z} = \frac{P_z}{4\pi G_{vh}} \sum_{i=1}^{2} \left[\lambda_i' u_i \left(u_i + m_i \right) A_{44} \frac{3z_i r}{R_i^5} \right] \tag{F2.3}$$

$$\frac{\sigma_{rr} - \sigma_{\theta\theta}}{r} = \frac{P_z}{4\pi G_{vh}} \sum_{i=1}^{2} \left[\lambda_i' A_{66} \left(\frac{2z_i}{r R_i^3} - \frac{4R_i^*}{r^3 R_i} \right) \right] \tag{F2.4}$$

Inspection shows that these sum to zero, confirming that radial equilibrium is satisfied.

Circumferential equilibrium

The symmetry of the vertical load and half-space geometry means that all terms in the circumferential equilibrium equation (F1.2) are zero.

Vertical equilibrium

For vertical equilibrium, equation F1.3:

$$\frac{\partial \tau_{rz}}{\partial r} = \frac{P_z}{4\pi G_{vh}} \sum_{i=1}^{2} \left[\lambda_i' \left(u_i + m_i \right) A_{44} \left(\frac{3r^2}{R_i^5} - \frac{1}{R_i^3} \right) \right] \tag{F2.5}$$

$$\frac{\partial \tau_{\theta z}}{r \partial \theta} = 0 \tag{F2.6}$$

$$\frac{\partial \sigma_{zz}}{\partial z} = \frac{P_z}{4\pi G_{vh}} \sum_{i=1}^{2} \left[\lambda_i' \left(u_i + m_i \right) A_{44} \left(\frac{3z_i^2}{R_i^5} - \frac{1}{R_i^3} \right) \right] \tag{F2.7}$$

$$\frac{\tau_{rz}}{r} = \frac{P_z}{4\pi G_{vh}} \sum_{i=1}^{2} \left[-\lambda_i' \left(u_i + m_i \right) A_{44} \frac{1}{R_i^3} \right] \tag{F2.8}$$

Since $3r^2 + 3z_i^2 = 3R_i^2$, the right sides sum to zero, confirming that vertical equilibrium is satisfied.

The stresses caused by a horizontal (+x) point load are given on sheets D6 and D7, and in Table 4 of the main text. Radial equilibrium is described by equation F1.1. Its terms are as follows, where $A_{44} = G_{vh}$ and $A_{66} = G_{hh}$:

$$\frac{\partial \sigma_{rr}}{\partial r} = \frac{P_x \cos\theta}{4\pi G_{vh}} \left\{ \sum_{i=1}^{2} \left[-\frac{\lambda_i u_i}{m_i}\left(u_i + m_i\right) A_{44} \left(\frac{1}{R_i^3} - \frac{3r^2}{R_i^5} \right) + 2A_{66} \frac{\lambda_i}{m_i} \left(\frac{1}{R_i^3} - \frac{3R_i^{*2}}{r^4 R_i} \right) \right] + \frac{4A_{66}}{u_3} \left(\frac{1}{R_3^3} - \frac{3R_3^{*2}}{r^4 R_3} \right) \right\} \tag{F3.1}$$

$$\frac{\partial \tau_{r\theta}}{r\partial \theta} = \frac{P_x \cos\theta}{4\pi G_{vh}} \left\{ \left(\sum_{i=1}^{2} \left[\frac{\lambda_i}{m_i} 2A_{66} \left(\frac{R_i^{*2}}{r^4 R_i} \right) \right] \right) - \frac{2A_{66}}{u_3} \left(\frac{3z_3 R_3^*}{r^4 R_3} - \frac{z_3^2}{r^2 R_3^3} - \frac{R_3^*}{r^4} \right) \right\} \tag{F3.2}$$

$$\frac{\partial \tau_{rz}}{\partial z} = \frac{P_x \cos\theta}{4\pi G_{vh}} \left\{ \left(\sum_{i=1}^{2} \left[A_{44} \frac{\lambda_i u_i}{m_i} \left(u_i + m_i\right) \left(\frac{3z_i^2}{R_i^5} - \frac{2}{R_i^3} \right) \right] \right) - 2A_{44} \frac{u_3}{R_3^3} \right\} \tag{F3.3}$$

$$\frac{\sigma_{rr} - \sigma_{\theta\theta}}{r} = \frac{P_x \cos\theta}{4\pi G_{vh}} \sum_{i=1}^{2} \left[\frac{\lambda_i}{m_i} 2A_{66} \left(\frac{R_i^{*2}}{r^4 R_i} + \frac{z_i^2}{r^2 R_i^3} - \frac{2z_i R_i^*}{r^4 R_i} \right) \right] + \frac{2A_{66}}{u_3} \frac{4R_3^{*2}}{r^4 R_3} \tag{F3.4}$$

Collecting like terms, the following algebraic identities are found to be useful:

$$-\left(\frac{1}{R_i^3} - \frac{3r^2}{R_i^5} \right) + \left(\frac{3z_i^2}{R_i^5} - \frac{2}{R_i^3} \right) = 0 \tag{F3.5}$$

$$\left(\frac{1}{R_i^3} - \frac{3R_i^{*2}}{r^4 R_i} \right) + \left(\frac{R_i^{*2}}{r^4 R_i} \right) + \left(\frac{R_i^{*2}}{r^4 R_i} + \frac{z_i^2}{r^2 R_i^3} - \frac{2z_i R_i^*}{r^4 R_i} \right) = 0 \tag{F3.6}$$

$$\left(\frac{2}{R_3^3} - \frac{6R_i^{*2}}{r^4 R_3} \right) - \left(\frac{3z_3 R_3^*}{r^4 R_3} - \frac{z_3^2}{r^2 R_3^3} - \frac{R_3^*}{r^4} \right) - \frac{1}{R_3^3} + \frac{4R_3^{*2}}{r^4 R_3} = 0 \tag{F3.7}$$

Using these, it is confirmed that the terms of the radial equilibrium equation sum to zero, confirming that radial equilibrium is satisfied.

The stresses caused by a horizontal (+x) point load are given on sheets D6 and D7, and in Table 4 of the main text. Azimuthal (circumferential) equilibrium is described by equation F1.2. Its terms are as follows, where $A_{44} = G_{vh}$ and $A_{66} = G_{hh}$:

$$\frac{\partial \tau_{r\theta}}{\partial r} = \frac{P_x \sin\theta}{4\pi G_{vh}} \left\{ \left(\sum_{i=1}^{2} \left[\frac{\lambda_i}{m_i} 2A_{66} \left(\frac{1}{R_i^3} - \frac{3R_i^{*2}}{r^4 R_i} \right) \right] \right) - \frac{2A_{66}}{u_3} \left(\frac{6R_3^{*2}}{r^4 R_i} - \frac{1}{R_3^3} - \frac{3r^2}{R_3^5} \right) \right\} \tag{F4.1}$$

$$\frac{\partial \sigma_{\theta\theta}}{r\partial \theta} = \frac{P_x \sin\theta}{4\pi G_{vh}} \left\{ \begin{array}{c} \sum_{i=1}^{2} \left[\frac{\lambda_i u_i}{m_i} \left(u_i + m_i \right) A_{44} \frac{1}{R_i^3} + 2A_{66} \frac{\lambda_i}{m_i} \left(\frac{z_i^2}{r^2 R_i^3} - \frac{2z_i R_i^*}{r^4 R_i} \right) \right] \\ + \frac{4A_{66}}{u_3} \left(\frac{2R_3^*}{r^4} - \frac{1}{r^2 R_3} \right) \end{array} \right\} \tag{F4.2}$$

$$\frac{\partial \tau_{\theta z}}{\partial z} = \frac{P_x \sin\theta}{4\pi G_{vh}} \left\{ \left(\sum_{i=1}^{2} \left[-\frac{\lambda_i}{m_i} A_{44} u_i \left(u_i + m_i \right) \frac{1}{R_i^3} \right] \right) - 2A_{44} u_3 \left(\frac{2}{R_3^3} - \frac{3z_3^2}{r^2 R_3^5} \right) \right\} \tag{F4.3}$$

$$\frac{2\tau_{r\theta}}{r} = \frac{P_x \sin\theta}{4\pi G_{vh}} \left\{ \left(\sum_{i=1}^{2} \left[\frac{\lambda_i A_{66}}{m_i} \left(\frac{4R_i^{*2}}{r^4 R_i} \right) \right] \right) - \frac{2A_{66}}{u_3} \left(\frac{6z_3 R_3^*}{r^4 R_3} - \frac{2z_3^2}{r^2 R_3^3} - \frac{2R_3^*}{r^4} \right) \right\} \tag{F4.4}$$

Collecting like terms, the following algebraic identities are found to be useful:

$$\left(\frac{1}{R_i^3} - \frac{3R_i^{*2}}{r^4 R_i} \right) + \left(\frac{z_i^2}{r^2 R_i^3} - \frac{2z_i R_i^*}{r^4 R_i} \right) + \left(\frac{2R_i^{*2}}{r^4 R_i} \right) = 0 \tag{F4.5}$$

$$-\left(\frac{6R_3^{*2}}{r^4 R_i} - \frac{1}{R_3^3} - \frac{3r^2}{R_3^5} \right) + \left(\frac{4R_3^*}{r^4} - \frac{2}{r^2 R_3} \right) - \left(\frac{2}{R_3^3} - \frac{3z_3^2}{r^2 R_3^5} \right) - \left(\frac{6z_3 R_3^*}{r^4 R_3} - \frac{2z_3^2}{r^2 R_3^3} - \frac{2R_3^*}{r^4} \right) = 0 \tag{F4.6}$$

Using these, it is confirmed that the terms of the circumferential equilibrium equation sum to zero, confirming that circumferential equilibrium is satisfied.

The stresses caused by a horizontal (+x) point load are given on sheets D6 and D7, and in Table 4 of the main text. Vertical equilibrium is described by equation F1.3. Its terms are as follows, where $A_{44} = G_{vh}$ and $A_{66} = G_{hh}$:

$$\frac{\partial \tau_{rz}}{\partial r} = \frac{P_x \cos\theta}{4\pi G_{vh}} \left\{ \left(\sum_{i=1}^{2} \left[A_{44} \frac{\lambda_i}{m_i} (u_i + m_i) \left(\frac{z_i}{r R_i^3} - \frac{2R_i^*}{r^3 R_i} + \frac{3 z_i r}{R_i^5} \right) \right] \right) + 2A_{44} \left(\frac{z_3}{r R_3^3} - \frac{2R_3^*}{r^3 R_3} \right) \right\} \quad \text{(F5.1)}$$

$$\frac{\partial \tau_{\theta z}}{r \partial \theta} = \frac{P_x \cos\theta}{4\pi G_{vh}} \left\{ \left(\sum_{i=1}^{2} \left[\frac{\lambda_i}{m_i} A_{44} (u_i + m_i) \left(\frac{R_i^*}{r^3 R_i} \right) \right] \right) - 2A_{44} \left(\frac{z_3}{r R_3^3} - \frac{R_3^*}{r^3 R_3} \right) \right\} \quad \text{(F5.2)}$$

$$\frac{\partial \sigma_{zz}}{\partial z} = \frac{P_x \cos\theta}{4\pi G_{vh}} \sum_{i=1}^{2} \left[\frac{\lambda_i}{m_i} (u_i + m_i) A_{44} \frac{-3 z_i r}{R_i^5} \right] \quad \text{(F5.3)}$$

$$\frac{\tau_{rz}}{r} = \frac{P_x \cos\theta}{4\pi G_{vh}} \left\{ \left(\sum_{i=1}^{2} \left[A_{44} \frac{\lambda_i}{m_i} (u_i + m_i) \left(\frac{R_i^*}{r^3 R_i} - \frac{z_i}{r R_i^3} \right) \right] \right) + 2A_{44} \frac{R_3^*}{r^3 R_3} \right\} \quad \text{(F5.4)}$$

Collecting like terms confirms that the terms of the vertical equilibrium equation sum to zero, confirming that vertical equilibrium is satisfied.

Aims

The purpose of this group G of Calculation sheets is to check that the changes of stresses that were calculated in group D are in equilibrium with the applied loads. A calculation is also presented for the horizontal point load P_y in the +y direction.

Method

A cylindrical disc-shaped part of the TILE half-space is considered between $z=0$ and $z=D$, centred on the load point and with radius J. Its upper surface carries the point loads at the origin of coordinates, but is otherwise unstressed.

The vertical point load P_x is equilibrated by a force V_{eq} that comes in part from the vertical stress on the base and in part from the shear stress on the sides:

$$V_{eq}=\int_{r=0}^{J}\int_{\theta=0}^{2\pi}\sigma_{zz}\,r\,dr\,d\theta+\int_{z=0}^{h}\int_{\theta=0}^{2\pi}\tau_{rz}\,J\,d\theta\,dz \qquad \text{(G1.1)}$$

Calculations Sheets D3 and D4 show that the relevant stresses due to P_x vary with the cosine of the azimuth. Hence their azimuthal integrals will be zero, and P_x does not affect the vertical load.

The horizontal force P_x is equilibrated by shear stress on the base of the disc and by shear and normal stresses on its sides. Resolving appropriately, the force $H_{eq,x}$ in the +x direction due to these stresses is found to be:

$$H_{eq,x}=\int_{r=0}^{J}\int_{\theta=0}^{2\pi}\left(\tau_{rz}\cos\theta-\tau_{\theta z}\sin\theta\right)r\,dr\,d\theta-\int_{z=0}^{h}\int_{\theta=0}^{2\pi}\left(\sigma_{rr}\cos\theta-\tau_{r\theta}\sin\theta\right)J\,d\theta\,dz \qquad \text{(G1.2)}$$

Calculations Sheets D6 and D7 show that the relevant stresses due to P_z are independent of azimuth, implying the integrals for this load will be zero. Hence P_z does not represent horizontal loads. τ_{rz} and σ_{rr} vary with $\cos\theta$ while the other two stresses vary with $\sin\theta$. Hence the azimuthal variations in the integrands for the y-direction are $\cos\theta\sin\theta$, which integrates to zero over 2π radians. This implies P_x does not apply a net load in the y direction. Hence P_x will relate to $H_{eq,x}$ only.

Using Sheets D3 and D4 to substitute for the stresses in equation G1.1, doing the azimuthal integrals, and noting that $G_{vh} = A_{44}$, gives:

$$V_{eq} = \frac{P_z}{2}\sum_{i=1}^{2}\left\{-\lambda_i'\left(\frac{u_i+m_i}{u_i}\right)\int_{r=0}^{J}\frac{z_i}{R_i^3}\,r\,dr\right\} + \frac{P_z}{2}\sum_{i=1}^{2}\left\{-\lambda_i'\left(u_i+m_i\right)\int_{z=0}^{h}\frac{r}{R_i^3}\,J\,dz\right\} \tag{G2.1}$$

where the first integral is to be evaluated at $z = D$ and the second at $r = J$. Doing the integrals gives:

$$V_{eq} = \frac{P_z}{2}\sum_{i=1}^{2}\left\{\lambda_i'\left(\frac{u_i+m_i}{u_i}\right)\left[\frac{z_i}{R_i}\right]_{r=0}^{J}\right\} + \frac{P_z}{2}\sum_{i=1}^{2}\left\{\lambda_i'\left(\frac{u_i+m_i}{u_i}\right)\left[J\,\frac{R_i^*}{rR_i}\right]_{z=0}^{h}\right\} \tag{G2.2}$$

Putting $z = h$ and $r = J$. and evaluating gives:

$$\left[\frac{z_i}{R_i}\right]_{r=0}^{J} = \left[\frac{u_i h}{R_i}\right]_{r=0}^{J} = \frac{u_i h}{\sqrt{J^2+u_i^2h^2}} - 1 \tag{G2.3}$$

$$\left[J\,\frac{R_i^*}{rR_i}\right]_{z=0}^{h} = \left[\frac{R_i^*}{R_i}\right]_{z=0}^{h} = \left[1-\frac{z_i}{R_i}\right]_{z=0}^{h} = \frac{-u_i h}{\sqrt{J^2+u_i^2h^2}} \tag{G2.4}$$

Substituting into the previous equation, simplifying, and using equation D8.5, gives:

$$V_{eq} = \frac{P_z}{2}\sum_{i=1}^{2}\left\{-\lambda_i'\left(\frac{u_i+m_i}{u_i}\right)\right\} = P_z \tag{G2.5}$$

This confirms that P_z can be interpreted as the vertical point load.

Using Sheets D3 and D4 to substitute for the stresses in equation G1.2, doing the azimuthal integrals, and noting that $G_{vh} = A_{44}$, gives $H_{eq,x} = H_1 + H_2$ with

$$H_1 = \frac{P_x}{4}\int_{r=0}^{J}\left\{\begin{array}{l}\left\{\left(\sum_{i=1}^{2}\left[\frac{\lambda_i}{m_i}(u_i+m_i)\left(\frac{R_i^*}{r^2R_i}-\frac{z_i}{R_i^3}\right)\right]\right)+2\frac{R_3^*}{r^2R_3}\right\}\\ -\left\{\left(\sum_{i=1}^{2}\left[\frac{\lambda_i}{m_i}(u_i+m_i)\frac{R_i^*}{r^2R_i}\right]\right)-2\left(\frac{z_3}{R_3^3}-\frac{R_3^*}{r^2R_3}\right)\right\}\end{array}\right\}rdr \qquad \text{(G3.1)}$$

$$H_2 = -\frac{P_x}{4}\int_{z=0}^{h}\left\{\begin{array}{l}\left\{\sum_{i=1}^{2}\left[-\frac{\lambda_i u_i}{m_i}(u_i+m_i)\frac{r}{R_i^3}+2\frac{A_{66}}{A_{44}}\frac{\lambda_i}{m_i}\frac{R_i^{*2}}{r^3R_i}\right]+4\frac{u_3R_3^{*2}}{r^3R_3}\right.\\ \left.-\left\{\left(\sum_{i=1}^{2}\left[2\frac{A_{66}}{A_{44}}\frac{\lambda_i}{m_i}\frac{R_i^{*2}}{r^3R_i}\right]\right)-2u_3\left(\frac{3z_3R_3^*}{r^3R_3}-\frac{z_3^2}{rR_3^3}-\frac{R_3^*}{r^3}\right)\right\}\end{array}\right\}Jdz \qquad \text{(G3.2)}$$

Collecting like terms gives:

$$H_1 = \frac{P_x}{4}\int_{r=0}^{J}\left\{\left(\sum_{i=1}^{2}\left[-\frac{\lambda_i}{m_i}(u_i+m_i)\frac{z_i}{R_i^3}\right]\right)+2\frac{z_3}{R_3^3}\right\}rdr \qquad \text{(G3.3)}$$

$$H_2 = \frac{P_x}{4}\int_{z=0}^{h}\left(\sum_{i=1}^{2}\left[\frac{\lambda_i u_i}{m_i}(u_i+m_i)\frac{Jr}{R_i^3}\right]+2u_3\frac{Jr}{R_3^3}\right)dz \qquad \text{(G3.4)}$$

Doing the integrations gives:

$$H_1 = \frac{P_x}{4}\left\{\left(\sum_{i=1}^{2}\left\{\frac{\lambda_i}{m_i}(u_i+m_i)\left[-\frac{z_i}{R_i}\right]_{r=0}^{J}\right\}\right)+2\left[-\frac{z_3}{R_3}\right]_{r=0}^{J}\right\} \qquad \text{(G3.5)}$$

$$H_2 = \frac{P_x}{4}\left\{\left(\sum_{i=1}^{2}\frac{\lambda_i}{m_i}(u_i+m_i)\left[-J\frac{R_i^*}{rR_i}\right]_{z=0}^{h}\right)+2\left[-J\frac{R_3^*}{rR_3}\right]_{z=0}^{h}\right\} \qquad \text{(G3.6)}$$

Evaluating the bounds, adding, and using equation D8.6, gives:

$$H_{eq} = H_1 + H_2 = \frac{P_x}{4}\left\{\left(\sum_{i=1}^{2}\left\{\frac{\lambda_i}{m_i}(u_i+m_i)\right\}\right)+2\right\} = P_x \qquad \text{(G3.7)}$$

This confirms that P_x can be interpreted as the point load in the horizontal +x direction.

Closed form solutions for a transversely isotropic linear elastic half-space loaded at a point on its surface	**Group Aim and Method**	Sheet H1

Aims

The purpose of this group H of Calculation sheets demonstrates that the displacement equations derived in Group B from Liao and Wang's (1998) results simplify correctly to the known solutions for a FIEL material when the material constants simplify to those of a FILE material.

Method: A Nearly FILE material

For a FILE material, the Young's moduli are equal to each other, the Poisson's ratios are equal to each other and the shear moduli are equal to each other. Liao and Wang's (1998) then solutions give $s=2$ and $q=1$, so $s^2-4q=0$ and $u_1=u_2=m_1=m_2=1$. This makes k and k' infinite (Sheet A1), and renders λ_1 and λ_2 indeterminate (Sheet B1).

To resolve this, a material is considered that is infinitesimally close to fully isotropic. A TILE material has five independent material parameters while a FILE material has two, so there are several ways in which a TILE material can be close to being fully isotropic. In the present paper, a material is considered with $E_v=E_h=E$ and $\mu_{vh}=\mu_{hh}=\mu$, and with the following:

$$A_{44}=G_{vh}=\frac{E}{2(1+\mu)}\left(1-\frac{1-\mu}{2}\varepsilon^2\right) \qquad \text{(H1.1)}$$

where ε is an infinitesimally small number. This material will tend to become a FILE material when ε tends to zero. This particular choice means that the following apply, and are amongst the variables that are unaffected by ε:

$$\Delta_1=\frac{1+\mu}{E} \qquad \Delta_2=\frac{(1+\mu)(1-2\mu)}{E} \qquad \text{(H1.2,3)}$$

$$A_{11}=A_{33}=\frac{(1-\mu)E}{(1+\mu)(1-2\mu)} \qquad A_{11}=A_{33}=\frac{(1-\mu)E}{(1+\mu)(1-2\mu)} \qquad \text{(H1.4,5)}$$

The following are also found be useful:

$$E^*=\frac{E}{2(1+\mu)(1-2\mu)} \qquad A_{11}-A_{44}u_i^2=E^*\left\{1-(1-2\mu)\left(\frac{\mu}{2}\varepsilon^2\pm\varepsilon\right)\right\} \qquad \text{(H1.6,7)}$$

$$A_{13}+A_{44}=E^*\left(1-\frac{(1-\mu)(1-2\mu)}{2}\varepsilon^2\right) \qquad \frac{A_{13}+A_{44}}{A_{33}}\simeq\frac{1}{2(1-\mu)}-(1-2\mu)\frac{\varepsilon^2}{4} \qquad \text{(H1.8,9)}$$

Done by and date	Checked by and date	Printed on
ETRD November 2022		Wednesday, 30 November 2022, 16:27

Closed form solutions for a transversely isotropic linear elastic half-space loaded at a point on its surface	**Solving the characteristic equation**	Sheet H2

Using equations from sheet H1, Liao and Wang (1998) parameters s and q are obtained as follows, where $O\left(\varepsilon^n\right)$ means terms of order ε^n and smaller:

$$s = 2\left(1+\frac{\varepsilon^2}{2}\right)+O\left(\varepsilon^4\right) \qquad q = 1 \qquad \text{(H2.1,2)}$$

These results lead to the following, where the approximately equals signs indicate that terms of higher order in ε than those retained have been ignored :

$$s^2-4q \simeq 4\varepsilon^2\left(1+\frac{\varepsilon^2}{4}\right) \qquad \sqrt{s^2-4q} \simeq 2\varepsilon\left(1+\frac{\varepsilon^2}{8}\right) \qquad \text{(H2.3,4)}$$

$$u_1^2 \simeq 1+\varepsilon+\frac{\varepsilon^2}{2} \qquad u_2^2 = 1-\varepsilon+\frac{\varepsilon^2}{2} \qquad \text{(H2.5,6)}$$

Using standard Taylor's approximations to order ε^2 :

$$u_i \simeq 1\pm\frac{\varepsilon}{2}+\frac{\varepsilon^2}{8} \qquad \frac{1}{u_i} \simeq 1\mp\frac{\varepsilon}{2}+\frac{\varepsilon^2}{8} \qquad \text{(H2.7,8)}$$

where here and later, the symbols $\pm$ and $\mp$ are such that the upper sign is for *i*=1, the lower for *i*=2. The following results are found to be useful:

$$E^* = \frac{E}{2(1+\mu)(1-2\mu)} \qquad A_{11}-A_{44}u_i^2 = E^*\left\{1-(1-2\mu)\left(\frac{\mu}{2}\varepsilon^2\pm\varepsilon\right)\right\} \qquad \text{(H2.9,10)}$$

$$A_{13}+A_{44} = E^*\left(1-\frac{(1-\mu)(1-2\mu)}{2}\varepsilon^2\right) \qquad \frac{A_{13}+A_{44}}{A_{33}} \simeq \frac{1}{2(1-\mu)}-(1-2\mu)\frac{\varepsilon^2}{4} \qquad \text{(H2.11,12)}$$

The following then follow by applying the characteristic equation and following through:

$$m_i u_i \simeq 1\mp(1-2\mu)\varepsilon+\frac{(1-2\mu)^2}{2}\varepsilon^2 \qquad \text{(H2.13)}$$

$$m_i \simeq 1\mp\frac{3-4\mu}{2}\varepsilon+\frac{(3-4\mu)^2}{8}\varepsilon^2 \qquad \text{(H2.14)}$$

$$\frac{1}{m_i} \simeq 1\pm\frac{3-4\mu}{2}\varepsilon+\frac{(3-4\mu)^2}{8}\varepsilon^2 \qquad \text{(H2.15)}$$

Done by and date	Checked by and date	Printed on
ETRD November 2022		Wednesday, 30 November 2022, 16:31

Closed form solutions for a transversely isotropic linear elastic half-space loaded at a point on its surface	**Other useful parameters**	Sheet H3

Material parameters

The following useful results can be deduced by combining results from sheet H2 with equations from sheet B1:

$$\lambda_0 \simeq \frac{1}{2(1-\mu)}\left\{\frac{1}{\varepsilon^2}-\left[1+(3-4\mu)^2\right]\right\} \tag{H3.1}$$

$$u_i - m_i = 2(1-\mu)\left\{\pm\varepsilon - \frac{1-2\mu}{2}\varepsilon^2\right\} \tag{H3.2}$$

$$\lambda_i \simeq \pm\frac{1}{\varepsilon} - \left(\frac{1-2\mu}{2}\right) \tag{H3.3}$$

$$\frac{\lambda_i}{m_i} \simeq \pm\frac{1}{\varepsilon} + (1-\mu) \pm \varepsilon(3-4\mu)^2 \tag{H3.4}$$

$$\lambda_i' m_i \simeq \mp\frac{1}{\varepsilon} + (1-\mu)\left\{1 \mp \frac{3-4\mu}{4}\varepsilon\right\} \tag{H3.5}$$

The result for λ_i confirms that this parameter will tend to infinity when ε tends to zero, but that combinations of parameters such as $\lambda_1 + \lambda_2$ can remain finite.

Geometric variables

Approximations for Liao and Wang's 81998) parameters z_i and R_i (for i=1 and 2)can readily be developed using the results from sheet H2:

$$z_i \simeq z\left(1 \pm \frac{\varepsilon}{2}\right) \tag{H3.6}$$

$$R_i \simeq R\left\{1 \pm \frac{\eta\varepsilon}{2}\right\} \quad \text{with} \quad \eta = \frac{z^2}{R^2} \tag{H3.7, 8}$$

The following may then be inferred:

$$\frac{1}{R_i} \simeq \frac{1}{R}\left\{1 \mp \frac{\eta\varepsilon}{2}\right\} \qquad R_i^* \simeq R^*\left\{1 \mp \frac{\eta\varepsilon}{2}\right\} \tag{H3.9, 10}$$

$$\frac{R_i^*}{R_i} \simeq \frac{R^*}{R}(1 \mp \eta\varepsilon) \qquad \frac{z_i R_i^*}{R_i} \simeq \left\{1 \pm (1-2\eta)\frac{\varepsilon}{2}\right\} \tag{H3.11, 12}$$

Done by and date	Checked by and date	Printed on
ETRD November 2022		Wednesday, 30 November 2022, 16:30

Boussinesq's (1878) solution

Boussinesq (1878) developed the solution for a point vertical load on the surface of a FILE half-space. The solution is explored by Westergaard (1952), Davis and Selvadurai (1996), Podio-Guidugli and Favata (2014) and others. The material displacements are given by:

radial: $$U_r = \frac{P_z}{4\pi GR}\left\{\frac{rz}{R^2} - (1-2\mu)\frac{r}{R+z}\right\} \quad \text{(H4.1)}$$

vertical: $$U_z = \frac{P_z}{4\pi GR}\left\{\frac{z^2}{R^2} + 2(1-\mu)\right\} \quad \text{(H4.2)}$$

and $U_\theta = 0$, where $R = \sqrt{r^2 + z^2}$ and G is the isotropic shear modulus.

The limit of the nearly FILE material

Displacements for a TILE material for this case, deduced from Liao and Wang (1998), are given on Sheets B2 to B4. Applying results from Sheets B3 to the parameters in these equations gives:

radial: $$\frac{\lambda_i' R_i^*}{R_i} \simeq \lambda_i \simeq \frac{R^*}{R}\left[\mp\frac{1}{\varepsilon} + \left(\eta - \frac{1-2\mu}{2}\right) \pm O(\varepsilon)\right] \quad \text{(H4.3)}$$

vertical: $$\frac{\lambda_i' m_i}{R_i} \simeq \lambda_i' m_i \simeq \frac{1}{R}\left[\mp\frac{1}{\varepsilon} + \left(\frac{\eta}{2} + 1 - \mu\right) + O(\varepsilon)\right] \quad \text{(H4.4)}$$

where $O(\varepsilon)$ represents terms of order ε and smaller. Substituting for the terms in each summation in the relevant equations of Sheets B2 to B4, the terms with sign switches cancel, including the terms with denominator ε. Taking the limit as $\varepsilon \to 0$ then gives:

vertical: $$U_z = \frac{-P_z}{4\pi G_{vh}}\left[\frac{2}{R}\left(\frac{\eta}{2} + 1 - \mu\right)\right] \quad \text{(H4.5)}$$

radial: $$U_r = \frac{-P_z}{4\pi G_{vh}}\left[\frac{2R^*}{R}\left(\eta - \frac{1-2\mu}{2}\right)\right] \quad \text{(H4.6)}$$

Putting $\eta = z^2 / R^2$, from Sheet H3, gives Boussinesq's (1878) equations, as required.

References for this Sheet

See list of references in main text

Cerruti's (1882) solution

Cerruti (1882) developed the solution for a point horizontal load on the surface of a FILE half-space. The solution is explored by Westergaard (1952), Davis and Selvadurai (1996), Podio-Guidugli and Favata (2014) and others. The material displacements are given in cylindrical coordinates by:

radial: $$U_r = \frac{P_x \cos\theta}{4\pi GR}\left\{1+\frac{r^2}{R^2}+(1-2\mu)\frac{z}{R+z}\right\} \quad \text{(H5.1)}$$

circumferential: $$U_\theta = \frac{-P_x \sin\theta}{4\pi GR}\left\{1+(1-2\mu)\frac{R}{R+z}\right\} \quad \text{(H5.2)}$$

vertical: $$U_z = \frac{P_x \cos\theta}{4\pi GR}\left\{\frac{rz}{R^2}+(1-2\mu)\frac{r}{R+z}\right\} \quad \text{(H5.3)}$$

where $R=\sqrt{r^2+z^2}$ and G is the isotropic shear modulus.

The limit of the nearly FILE material

Displacements for a TILE material for this case, deduced from Liao and Wang (1998), are given on Sheets B5 to B7. Applying equations H3.4 and H3.12, H4.4 and H3.4 and H3.9, and H3.3 and H3.11 respectively gives;

$$U_r = \frac{P_x \cos\theta}{4\pi G_{vh}}\left[\sum_{i=1}^{2}\left(-\frac{zR^*}{r^2R}\left(\pm\frac{1}{\varepsilon}+\left(1-\mu+\frac{1-2\eta}{2}\right)\pm O(\varepsilon)\right)\right)+\frac{2}{u_3}\frac{R_3^*}{r^2}\right] \quad \text{(H5.4)}$$

$$U_\theta = \frac{P_x \sin\theta}{4\pi G_{vh}}\left[\sum_{i=1}^{2}\left(\frac{R^*}{r^2}\left(\pm\frac{1}{\varepsilon}+\left(1-\mu-\frac{\eta}{2}\right)+O(\varepsilon)\right)\right)-\frac{2}{u_3}\frac{z_3R_3^*}{r^2R_3}\right] \quad \text{(H5.5)}$$

$$U_z = \frac{P_x \cos\theta}{4\pi G_{vh}}\sum_{i=1}^{2}\left(\frac{R^*}{rR}\left[\pm\frac{1}{\varepsilon}+\left(1-\mu-\eta\right)+O(\varepsilon)\right]\right) \quad \text{(H5.6)}$$

The s terms cancel in the summations, and the $O(\varepsilon)$ terms tend to zero as ε tends to zero. Putting $\eta = z^2/R^2$ (equation H3.8) setting $u_3 = 1$ for the FILE material (equation H2.2, then gives Cerruti's (18782) solution for this case, as required.

References for this Sheet

See list of references in main text